Comparison of industrial wastes as binder in the agglomeration of coal fines

CN Henning

orcid.org/ 0000-0001-7235-7875

Dissertation accepted in fulfilment of the requirements for the degree *Master of Engineering in Chemical Engineering* at the North West University

Supervisor:	Prof JR Bunt
Co-supervisor:	Miss NT Leokaoke
Co-supervisor:	Prof HWJP Neomagus
Assistant-supervisor:	Prof LJ Grobler

Graduation:	August 2021
Student number:	24217646

DECLARATION OF AUTHORSHIP

I, Chantalé Nadine Henning, declare that this report is a presentation of my own original work.

Whenever contributions of others are involved, every effort was made to indicate this clearly, with due reference to the literature.

No part of this work has been submitted in the past, or is being submitted, for a degree or examination at any other university or course.

Signed on this, 20th day of February 2021 in Potchefstroom.

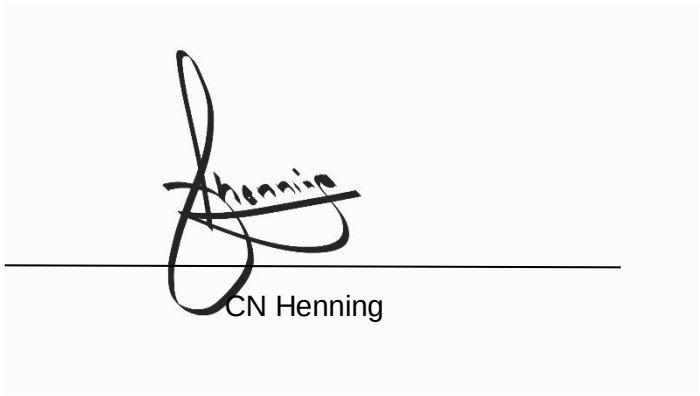

CN Henning

ACKNOWLEDGEMENTS

First and foremost I give thanks to our Heavenly Father who gave me strength and determination even when I couldn't see the light at the end.

The following persons/ institutions are acknowledged for their involvement during the course of the study:

- Prof John Bunt, Nthabiseng Leokaoke and Prof Hein Neomagus, thank you for your guidance and support – your advice has been invaluable in the course of this study.
- The chemistry personnel: Prof Christien Strydom and Romanus Uwaoma, your technical assistance was appreciated.
- The laboratory staff: Clement Mgano and Ms René Bekker, for training and advice on the laboratory equipment and procedures.
- The workshop staff: Mr Jan Kroeze, Mr Adrian Brock, Mr Elias Mofokeng and Warren Brauns, for assisting with any and all technical issues that occurred.
- The administrative staff: Ms Sanet Botes and Tanya Fouche, for always ensuring that the required paperwork was in order.
- Andrei Koekemoer, for your assistance in procuring samples and analysing results.
- Nicolaas Engelbrecht, for your expertise with gas analysis.
- Callie Marais, for your help with experimental work.
- Danél Bartlett, Naldo Meyer, Coen Mouton and Rainer Greyling, thank you for preserving my sanity.
- Donne-Lee Henning, I could not have done it without you.
- My parents, Deon and Nandia, and sisters, Donna and Cheri, thank you for your unconditional love and support through the course of my studies.

The information presented in this dissertation is based on the research financially supported by the National Research Foundation (NRF) and South African Research Chairs Initiatives (SARChI) of the Department of Science and Technology (Coal Research chair Grant No. 86880). Any opinions, conclusions or recommendations expressed are that of the author(s) and no liability is accepted on the NRF's regard.

ABSTRACT

The industries that consumed the most coal in South Africa, in 2015, were electricity generation, 53%, basic iron and steel manufacturing, 20%, and synthetic fuel and chemical industries, 10%, with the rest being used in various other smaller industries, 17%. Coal fines (-1 mm) that are discarded due to handling issues provide an alternate source of fuel, which can be utilised through agglomeration. Briquetting is a large-scale agglomeration method where coal fines, with or without a binder, can be used to produce fuel briquettes. Binders are usually needed to produce briquettes that are strong and water resistant and should therefore also increase the briquette reactivity, be environmentally friendly and be cost effective. Hazardous wastes are expensive to dispose of and harmful to the environment, which is why they should be evaluated as binders for coal briquetting.

The binding properties of five industrial wastes were evaluated to determine their efficacy in the agglomeration of Highveld inertinite-rich coal fines: (A) waterworks bio-sludge from a petrochemical industry, (B) acrylic acid containing a hydrocarbon by-product from a petrochemical industry, (C) pitch from a petrochemical industry, (D) wax emulsion from a petrochemical industry, and (E) recycled low-density polyethylene (LDPE) from a North-West plastic recycling company.

The compressive strength, CS (MPa), impact resistance index, IRI (-), friability index, FR (%), abrasion resistance, AR (%), and water resistance index, WRI (%) of the briquettes were determined to evaluate the mechanical strength of the briquettes. The binderless briquettes had a maximum CS of 3.4 MPa, which is higher than the minimum CS of bituminous coal (2.1 MPa). The addition of Binders A–E was therefore investigated to use the briquettes as carriers for the reduction of hazardous wastes. The optimal concentration for each binder, based on mechanical strength (CS, IRI, FR, AR), was determined as 15% Binder A (4.1 MPa; 68; 80%; 99.3%), 20% Binder B (2.3 MPa, 87, 71%, 99.5%), 20% Binder C (8.2 MPa, 1000, 100%, 99.2%), 5% Binder D (2.4 MPa, 21, 46%, 95.3%) and 5% Binder E (5.3 MPa, 97, 52%, 98.3%). Briquettes bound with 20% Binder B, and 5–10% Binder E were water resistant.

The reactivity of the optimal briquettes during pyrolysis (900°C), combustion (850, 875 and 900°C) and gasification (1000 and 1025°C) were tested to evaluate the effect of the binders. The binders had a small effect on the pyrolysis yields and no observable effect on the combustion and gasification reactivity of the briquettes due to the binders decomposing below 500°C.

The briquettes were matched with suitable industrial processes based on the mechanical strength and reactivity results that were obtained. The binderless as well as the Binder B and D bound briquettes may be suitable for use in PCC boilers due to their strength being high enough to

enable transportation and low enough not to inhibit pulverising. Binders B, C and E bound briquettes may be more suited for use in a Lurgi-gasifier. None of the binders are recommended for use in blast furnaces due to the high ash yield, low volatile matter content and lack of swelling properties.

Keywords

Coal briquetting, binders, hazardous waste, compressive strength, impact resistance, water resistance, pyrolysis, combustion, gasification

TABLE OF CONTENTS

DECLARATION OF AUTHORSHIP ..... **I**

ACKNOWLEDGEMENTS ..... **II**

ABSTRACT ..... **III**

LIST OF EQUATIONS ..... **IX**

LIST OF FIGURES ..... **X**

LIST OF TABLES ..... **XIV**

LIST OF ABBREVIATIONS ..... **XVII**

LIST OF SYMBOLS ..... **XIX**

CHAPTER 1: INTRODUCTION **1**

1.1 Overview **1**
1.2 Background and motivation **1**
1.3 Problem statement **3**
1.4 Aim and objectives **3**
1.5 Scope of investigation **3**
1.6 Study outline **4**

CHAPTER 2: LITERATURE REVIEW **5**

2.1 Overview **5**
2.2 Coal **5**
2.2.1 Highveld coalfields 6
2.2.2 Coal fines 8
2.3 Coal agglomeration **9**
2.3.1 Methods 9
2.3.1.1 Spherical agglomeration 10
2.3.1.2 Pelletising 10
2.3.1.3 Briquetting 11
2.3.2 Briquetting variables 12
2.3.2.1 Coal classification 12
2.3.2.2 Particle size distribution 17
2.3.2.3 Binding mechanisms 17
2.3.2.4 Binders 22

2.3.2.5 Pressure and temperature 25

2.4 Physical properties of briquettes 26

2.4.1 Compressive strength 26

2.4.2 Impact resistance 28

2.4.3 Abrasion resistance 30

2.4.4 Water resistance 31

2.4.5 Thermal degradation 32

2.5 Reactivity of coal 34

2.6 Industrial applications of coal 35

2.6.1 Electricity generation 36

2.6.1.1 Pulverised coal combustion 37

2.6.1.2 Fluidised bed combustion 39

2.6.2 Liquid fuels and chemicals production 41

2.6.3 Metallurgical use 44

2.6.3.1 Blast furnace method 45

2.6.3.2 Direct reduction method 47

CHAPTER 3: METHODOLOGY 50

3.1 Overview 50

3.2 Materials 50

3.2.1 Coal 50

3.2.2 Binders 50

3.2.3 Liquids 51

3.2.4 Gases 52

3.3 Coal preparation and sampling 52

3.4 Coal and briquette characterisation 53

3.4.1 Particle size distribution 53

3.4.2 Coal and briquette composition 53

3.4.3 Gross calorific value 53

3.5 Laboratory-scale briquetting 54

3.5.1 Binder preparation 54

3.5.2 Batch briquetting process 55

3.5.3 Curing 56

3.6 Pilot-scale briquetting 56

3.6.1 Binder preparation 56

3.6.2 Continuous briquetting process 57
3.6.3 Curing 57

3.7 Mechanical strength tests 57
3.7.1 Compressive strength test 57
3.7.2 Drop shatter test 58
3.7.3 Tumbler test 58
3.7.4 Water-immersion test 59

3.8 Reactivity tests 59
3.8.1 Free swelling index 60
3.8.2 Thermal degradation 60
3.8.3 Pyrolysis 60
3.8.4 Thermogravimetric analysis 60
3.8.5 Fischer assay 61

3.9 Coal characterisation results 63

CHAPTER 4: MECHANICAL STRENGTH RESULTS 67

4.1 Overview 67
4.2 Phase 1: Laboratory-scale briquetting 67
4.2.1 Compressive strength results 67
4.2.2 Water resistance results 73
4.2.3 Summary of lab-scale briquettes 74

4.3 Phase 2: Pilot-scale briquetting 75
4.3.1 Compressive strength results 75
4.3.2 Impact resistance results 78
4.3.3 Durability results 79
4.3.4 Water resistance results 80
4.3.5 Optimisation of binder concentrations for pilot-scale briquettes 82

CHAPTER 5: REACTIVITY RESULTS 83

5.1 Overview 83
5.2 Proximate analysis and calorific value results 83
5.3 Pyrolysis results 84
5.3.1 Thermal fragmentation results 84
5.3.2 Fischer assay results 85

5.4 Combustion results 87
5.5 Gasification results 89

5.6 Matching with industrial processes 90

CHAPTER 6: CONCLUSION AND RECOMMENDATIONS 93

6.1 Overview 93
6.2 Conclusions 93
6.3 Contribution to the scientific field 95
6.4 Recommendations 95

LIST OF REFERENCES 96

APPENDIX A: SUMMARY OF THE MATERIAL SAFETY DATA SHEETS FOR THE WASTE BINDERS 113

APPENDIX B: MOISTURE EVAPORATION/ADSORPTION OF LAB-SCALE BRIQUETTES 114

APPENDIX C: DROP SHATTER TEST RESULTS FOR THE PILOT-SCALE BRIQUETTES 116

APPENDIX D: WATER RESISTANCE TEST RESULTS FOR THE PILOT-SCALE BRIQUETTES 120

APPENDIX E: OPTIMISATION OF THE PILOT-SCALE BINDER CONCENTRATIONS 128

APPENDIX F: THERMAL FRAGMENTATION TEST 131

APPENDIX G: FREE SWELLING INDEX RESULTS 132

APPENDIX H: COMBUSTION RESULTS 134

APPENDIX I: REPEATIBILITY OF EXPERIMENTS 138

LIST OF EQUATIONS

Equation 2-1: Parr formula 13
Equation 2-2: Gates-Gaudin-Schumann distribution model 17
Equation 2-3: Compressive strength (CS) 27
Equation 2-4: Impact resistance index (IRI_A) 28
Equation 2-5: Impact resistance index (IRI_B) 29
Equation 2-6: Shatter index (SI) 29
Equation 2-7: Friability index (FR) 29
Equation 2-8: Abrasion resistance (AR) 30
Equation 2-9: Water resistance index (WRI) 31
Equation 2-10: Ergun index 33
Equation 2-11: Thermal fragmentation 33
Equation 2-12: Free swelling index (FSI – calculated) 33
Equation 3-1: Binder mass (m_{binder}) 54
Equation 4-1: Binder optimisation 82
Equation 5-1: Conversion (X) 87
Equation 5-2: Conversion rate (dX/dt) 87

LIST OF FIGURES

Figure 1-1: Layout of the chapters in the study 4

Figure 2-1: Global primary energy consumption by fuel type adapted from BP·(2019) 5

Figure 2-2: South African primary energy consumption by fuel type adapted from BP·(2019) 6

Figure 2-3: Illustration of extrusion with (a) a roller and die and (b) a die with cylindrical openings adapted from Conkle·and·Ragavan·(1992) 11

Figure 2-4: Illustration of briquetting with a roll press adapted from Conkle·and·Ragavan·(1992) 12

Figure 2-5: The effect of coalification on the grade, type and rank of coal adapted from Laj·and·Barnikel·(2016) 13

Figure 2-6: Illustrations of the liquid states in briquettes based on the liquid saturation for (a) dry, (b) adsorption layers, (c) liquid bridges – pendular sate, (d) transitional – funicular state, (e) fully saturated – capillary state, and (f) droplet, adapted from Pietsch·(2004) 20

Figure 2-7: Forces briquettes encounter during storage, handling and transportation: (a) compressive force, (b) impact force and (c) attrition force, adapted from Dohm·*et·al.*·(2012) 26

Figure 2-8: The different types of coal and their respective uses retrieved from Speight·(2008) 36

Figure 2-9: Simplified diagram of a coal-fired electricity generation process adapted from Speight·(2008) 37

Figure 2-10: Simplified diagram of an ICL gasification process adapted from Mahinpey·and·Gomez·(2016) 42

Figure 2-11: Simplified diagram of the blast furnace iron making process adapted from Carpenter·(2006) and SEAISI·(2016) 46

Figure 2-12: Simplified diagram of the direct reduction iron making process adapted from Carpenter·(2006) and SEAISI·(2016) 47

Figure 3-1: Coal preparation – coning and quartering, adapted from Crosby·and·Patel·(1995) 52

Figure 3-2: Briquetting process: (a) before and (b) after 55

Figure 3-3: Schematic of the (a) axially vertical and (b) flat-horizontal positions for testing compressive strength 58

Figure 3-4: Schematic of the in-house testing rig setup for thermogravimetric analysis 61

Figure 3-5: Cumulative density particle size distribution of the coal fines (-1 mm) 66

Figure 4-1: Compressive strength results over a period of 21 days for the lab-scale binderless briquettes 68

Figure 4-2: Compressive strength results over a period of 21 days for the lab-scale briquettes manufactured with Binder A 69

Figure 4-3: Compressive strength results over a period of 21 days of the lab-scale briquettes manufactured with Binder B 70

Figure 4-4: Compressive strength results over a period of 21 days of the lab-scale briquettes manufactured with Binder C 71

Figure 4-5: Compressive strength results over a period of 21 days of the lab-scale briquettes manufactured with Binder D 72

Figure 4-6: Compressive strength results of the lab-scale briquettes manufactured with Binder E 73

Figure 4-7: Wet compressive strength results of the lab-scale briquettes bound with 10 and 15% Binder E 74

Figure 4-8: Compressive strength results over a period of 21 days of the pilot-scale binderless briquettes manufactured with a moisture addition of 2.5, 5.0 and 10.0% 76

Figure 4-9: Compressive strength results over a period of 21 days of the pilot-scale briquettes manufactured with Binders A–E 77

Figure 4-10: Average impact resistance index results of the pilot-scale binderless briquettes and briquettes bound with Binders A–E 78

Figure 4-11: Average friability index results of the pilot-scale binderless briquettes and briquettes bound with Binders A–E 79

Figure 4-12: Average abrasion resistance results of the pilot-scale binderless briquettes and briquettes bound with Binders A–E 80

Figure 5-1: Thermal fragmentation pre-test images of the optimal concentration briquettes with (a) 5% moisture, (b) 15% Binder A, (c) 20% Binder B, (d) 20% Binder C, (e) 5% Binder D, and (f) 5% Binder E 84

Figure 5-2: Thermal fragmentation post-test images of the optimal concentration briquettes with (a) 5% moisture, (b) 15% Binder A, (c) 20% Binder B, (d) 20% Binder C, (e) 5% Binder D, and (f) 5% Binder E 85

Figure 5-3: Pyrolysis gas composition (H_2, CH_4, CO, CO_2) of the optimal concentration briquettes 87

Figure 5-4: Graphs of the conversion rate versus conversion for the binderless and Binder A–E bound briquettes during combustion at (a) 850°C, (b) 875°C, and (c) 900°C..... 88

Figure 5-5: Graphs of the conversion rate versus conversion for the binderless and Binder A–E bound briquettes during gasification at (a) 1000°C and (b) 1025°C 90

Figure B-1: Weight change (%) over 21 days of the Phase 1 lab-scale briquettes that were manufactured with Binders A–D (5–15%) at maximum moisture addition (17%) 115

Figure C-1: Example of the impact resistance index dependence on the number of pieces the briquette breaks into, $N_{pieces} < 10$, and number of drops before it breaks, $N_{drops} < 10$..... 116

Figure C-2: Example of the friability index dependence on the weight of the largest piece of briquette, m_f, after it breaks for a briquette with an initial weight, m_0, of 4 g 118

Figure F-1: Thermal fragmentation post-test images of the optimal concentration briquettes with (a) 5% moisture, (b) 15% Binder A, (c) 20% Binder B, (d) 20% Binder C, (e) 5% Binder D, and (f) 5% Binder E that were manually broken in half..... 131

Figure G-1: Images of the optimal concentration briquettes with (a) 5% moisture, (b) 15% Binder A, (c) 20% Binder B, (d) 20% Binder C, (e) 5% Binder D, and (f) 5% Binder E after the free swelling index test..... 132

Figure H-1: Graph of the weight loss, *m* (g), over time, *t* (min), for the isothermal combustion of the binderless briquette with 5% moisture addition at 900°C 134

Figure H-2: Images of the binderless briquette with 5% moisture addition (a) after isothermal combustion at 900°C and (b) after force was applied 134

Figure H-3: Combustion (850°C) graphs of the fractional conversion over time for the (a) binderless and optimal briquettes bound with binder (b) A, (c) B, (d) C, (e) D, and (f) E..... 135

Figure H-4: Combustion (875°C) graphs of the fractional conversion over time for the (a) binderless and optimal briquettes bound with binder (b) A, (c) B, (d) C, (e) D, and (f) E..... 136

Figure H-5: Combustion (900°C) graphs of the fractional conversion over time for the (a) binderless and optimal briquettes bound with binder (b) A, (c) B, (d) C, (e) D, and (f) E..... 137

Figure I-1: Particle size distribution, PSD, results of the coal fines (-1 mm) for three runs 138

Figure I-2: Repeatability of the combustion results for 20% Binder C bound briquettes at 900°C..... 139

Figure I-3: Repeatability of the gasification results for binderless briquettes at 1000°C 139

LIST OF TABLES

Table 2-1: Summary of the Highveld Coalfield seams adapted from Cairncross·(2001) and Hancox·and·Götz·(2014) 7

Table 2-2: Quality of coal fines dumped in discard dumps and slurry dams adapted from the Department of Minerals and Energy·(2001) 9

Table 2-3: Ash yield class categories retrieved from ISO·(2005) 14

Table 2-4: Vitrinite content class categories retrieved from ISO·(2005) 15

Table 2-5: Summary of coal ranks and their approximate properties adapted from Arnold·(2013), Bowen·and·Irwin·(2008), Laj·and·Barnikel·(2016), Speight·(2008), and Woodruff·*et·al.*·(2017) 16

Table 2-6: Agglomeration binding mechanisms and their respective bond types adapted from Rumpf (cited by Pietsch, 2004) 18

Table 2-7: Pyrolysis reactions and products at low, medium, high and plasma temperature ranges adapted from Speight·(2012) 35

Table 2-8: Summary of some coal properties and their desired values and effects on pulverised coal combustion adapted from de Korte·and·Jeffrey·(2016), Skorupska·(1993), and Wu·(2005) 38

Table 2-9: Summary of some coal properties and their desired values and effects on fluidised bed combustion adapted from Aziz·and·Dittus·(2011), Belaid·(2017), Fernando·(2004), Henderson·(2003), Hotta·(2009), Jin·*et·al.*·(2003), and Wu·(2006) 40

Table 2-10: Summary of some coal properties and their desired values and effects on coal gasification adapted from Couch·(2008), Vamvuka·(1999), van Dyk·*et·al.*·(2001), van Dyk·*et·al.*·(2006), and Weiss·and·Turna·(2009) 43

Table 2-11: Summary of some coal properties and their desired values and effects on blast furnace and direct reduction iron making adapted from Carpenter·(2004) and Chatterjee·(2010) 48

Table 3-1: Overview of the binder properties which may be beneficial in briquetting coal fines 51

Table 3-2: Standards for proximate analysis, ultimate analysis, XRD and XRF 53

Table 3-3: Comparison of the proximate analysis, ultimate analysis and gross calorific value of the coal fines and ROM coal from the same area adapted from Leokaoke·*et·al.*·(2019) 63

Table 3-4: Mineralogical composition from the XRD analysis results for the coal fines 64

Table 3-5: Ash composition from the XRF analysis results for the coal fines 65

Table 4-1: Water resistance index, WRI (%), of lab-scale briquettes with Binder E at 30, 60, 120 and 180 min..... 73

Table 4-2: Summary of the lab-scale briquettes manufactured with Binders A–E 74

Table 4-3: Water resistance of the pilot-scale briquettes manufactured with water and Binders A–E based on their condition..... 81

Table 4-4: Water resistance index and wet compressive strength of the briquettes bound with Binders B (10, 15, 20%) and E (5, 10%) that were intact after 30 min 82

Table 4-5: Optimal concentrations for the pilot-scale briquettes manufactured with water and Binders A–E and their mechanical strength and water resistance 82

Table 5-1: Proximate analysis and calorific value results of the optimal concentration briquettes compared to ROM coal adapted from Leokaoke·*et·al.*·(2019)..... 83

Table 5-2: Fischer assay results of the optimal briquettes 86

Table 5-3: Properties of coal feedstock used in PCC and CFBC boilers 91

Table 5-4: Properties of coal feedstock used in CTL gasifiers 92

Table A-1: Physical and chemical properties of Binders A–E adapted from the material safety data sheets (MSDS)..... 113

Table C-1: Impact resistance index results for binderless and Binders A–E bound pilot-scale briquettes, over a 21-day period..... 117

Table C-2: Friability index results for binderless and Binders A–E bound pilot-scale briquettes, over a 21-day period..... 119

Table D-1: Water resistance test images of the pilot-scale binderless briquettes with 2.5, 5 and 10% moisture addition..... 120

Table D-2: Water resistance test images of the pilot-scale binderless briquettes bound with 5, 10 and 15% Binder A 122

Table D-3: Water resistance test images of the pilot-scale binderless briquettes bound with 5, 10, 15 and 20% Binder B..... 123

Table D-4: Water resistance test images of the pilot-scale binderless briquettes bound with 5, 10, 15 and 20% Binder C 124

Table D-5: Water resistance test images of the pilot-scale binderless briquettes bound with 2.5 and 5.0% Binder D 126

Table D-6: Water resistance test images of the pilot-scale binderless briquettes bound with 5 and 10% Binder E 127

Table E-1: Summary of the mechanical strength and water resistance results for the pilot-scale briquettes 128

Table E-2: Mechanical strength results, water resistance index, handling, binder cost and hazardous nature of the briquettes as fractions for the optimisation of the binder concentrations 129

Table E-3: Optimisation of the binder concentrations based on mechanical strength results, water resistance index, handling, binder cost and hazardous nature of the briquettes as weighted fractions 130

Table G-1: Free swelling index calculated with the pore resistance number of the optimal briquettes 133

Table I-1: Comparison of the char yields obtained from the proximate analysis, Fischer assay and pyrolysis experiments of the optimal pilot-scale briquettes 138

LIST OF ABBREVIATIONS

adb	Air-dried basis
AFT	Ash fusion temperature
AI	Alkaline index
ar	As-received basis
AR	Abrasion resistance
ASAE	American Society of Agricultural Engineers
ASTM	American Society for Testing and Materials
BF	Blast furnace
BGR	Federal Institute for Geosciences and Natural Resources
BVT	Bureau Veritas Testing and Inspection
CFPB	Circulating fluidised bed combustion
CMSA	Colleges of Mines of South Africa
CS	Compressive strength
CS_{wet}	Wet compressive strength
CTL	Coal-to-liquids
CV	Calorific value
dafb	Dry, ash free basis
db	Dry basis
DCL	Direct coal liquefaction
dmmfb	Dry, mineral matter-free basis
DRI	Direct reduced iron
FBC	Fluidised bed combustion
FBDB	Fixed bed dry bottom
FFF	Fossil Fuel Foundation
FR	Friability index
FSI	Free swelling index
FT	Fischer-Tropsch
GC	Gas chromatograph

ICL	Indirect coal liquefaction
IDT	Initial deformation temperature
IGCC	Integrated gasification combined cycle
IRI	Impact resistance index
ISO	International Organization for Standardization
JIS	Japanese Industrial Standards
LDPE	Low-density polyethylene
MS	Mass spectrometry
MSDS	Material safety datasheet
MSW	Municipal solid waste
mmfb	Mineral matter-free basis
mmmfb	Moist, mineral matter-free basis
PCC	Pulverised coal combustion
PCI	Pulverised coal injection
PEC	Primary energy consumption
PRN	Pore resistance number
PSD	Particle size distribution
PVA	Polyvinyl alcohol
RDF	Refuse derived fuel
ROM	Run-of-mine
SDS	Safety data sheets
SEAISI	South East Asia Iron and Steel Institute
SI	Shatter index
TCD	Thermal conductivity detector
TG	Thermogravimetric
TGA	Thermogravimetric analysis
WCA	World Coal Association
WRI	Water resistance index
XRD	X-ray diffraction
XRF	X-ray fluorescence

LIST OF SYMBOLS

A	Area	(m^2)
D	Density	(g/cm^3)
d	Diameter	(mm)
d_i	Internal diameter	(mm)
F	Fracture load	(N)
h	Height	(mm or cm)
l	Length	(mm)
m	Mass	(g)
m_0	Initial mass	(g)
m_{ash}	Mass of ash yield	(g)
m_i	Mass at interval i	(g)
m_f	Final mass	(g)
m_w	Mass of absorbed water	(g)
N	Number	(-)
r	Radius	(mm)
t	Time	(min)
t_i	Time at interval i	
V	Volume	(cm^3)
w	Width	(mm)
x	Mass fraction	(-)
X	Carbon conversion	(-)

CHAPTER 1: INTRODUCTION

1.1 Overview

In Chapter 1 a basic introduction is given on what fine coal is, why, and how it should be agglomerated for use in industrial processes. Section 1.2 gives a brief background on fine coal and industrial waste pollution and motivates the utilisation of these wastes. The problem statement is described in Section 1.3 and the objectives that need to be met to achieve the aim of this study are defined in Section 1.4. The scope of the study is set out in Section 1.5 and outlines the criteria that will be considered to evaluate the binding efficacy of the industrial waste materials. Section 1.6 shows the outline of the study to make navigating the concepts investigated in the dissertation easier.

1.2 Background and motivation

Coal is defined as “a black or brownish-black solid combustible substance formed by the partial decomposition of vegetable matter without free access of air and under the influence of moisture and often increased pressure and temperature that is widely used as a natural fuel” (Merriam-Webster Inc., 2019). It supplies approximately 27% of the world’s energy and 71% of the energy in South Africa (BP, 2019). The country also uses coal for steel manufacturing, coke and refined petroleum production, cement manufacturing, pulp and paper manufacturing, as well as sugar mills (CMSA, 2018; FFF, 2011). It is therefore important to ensure that no useful coal goes to waste.

Coal with a small particle size can be classified as fine (-1 mm) and ultra-fine (-0.15 mm) (Hardman & Lind, 2003). In South Africa approximately 4% of the run-of-mine (ROM) coal is classified as ultra-fine, which means that almost 11 Mtpa of coal is being dumped due to particle size (BP, 2019; Reddick *et al.*, 2007). The 29 active discard dumps and 17 active slurry ponds in South Africa have a combined content of more than 361 Mt (Muzenda, 2014). The coal in these dump sites can spontaneously combust or contaminate the surrounding area by means of gaseous pollutants or acid mine drainage (Lewitt, 2011; WCA, 2019b). The legislation regarding these dumps have therefore become stricter, hence expensive methods of covering the dumps have become a necessity (Lewitt, 2011). The small particle size of the coal fines also causes handling issues due to the propensity of the coal to block equipment and transportation mechanisms (Holuszko & Laskowski, 2004).

Coal agglomeration methods can be used to decrease the volume of hazardous coal fines by making them useful. The quality of discarded coal fines is usually very low, but it can still be used industrially, *e.g.* to generate electricity (Lloyd, 2000). Agglomeration methods include pelletising, briquetting and spherical agglomeration (England, 2000). The quality of agglomerates can be

described by the following characteristics: water resistance, mechanical strength and reactivity (Mills, 1908; Waters, 1969). Binderless briquettes are mainly produced with lignite and a binder is usually needed to improve the quality of the briquettes (Komarek, 1967; Zhang *et al.*, 2018). Binders can affect the properties of the produced agglomerates and should therefore comply with the following list of contributions (England, 2000):

- increase the mechanical strength of the agglomerates by creating stronger bonds between coal particles;
- increase the water resistance of the agglomerates to allow them to be stored outside or used in systems where they may become wet without disintegrating;
- increase or meet the ROM "parent" coal properties with regards to reactivity;
- be environmentally friendly through reducing pollution by utilising wastes and/ or not giving off additional harmful components when used in industrial processes; and
- be financially feasible.

In the past both inorganic (*e.g.,* clay, lime, cement) and organic (*e.g.,* wood products, sugar-factory residues, starch) binders have been used during coal agglomeration (Mills, 1908). Waste materials have also been evaluated as binders to reduce environmental pollution and the costs involved in agglomeration (Dec, 2005; Engelleitner, 2001). South Africa generated roughly 67 Mtpa of hazardous waste in 2017 and some of these wastes should therefore be investigated to determine their binding capabilities (Department of Environmental Affairs, 2018). Hazardous waste is defined as "any waste that contains organic or inorganic elements or compounds that may, owing to the inherent physical, chemical or toxicological characteristics of that waste, have a detrimental impact on health and the environment and includes hazardous substances, materials or objects within the business waste, residue deposits and residue stockpiles" (Department of Environmental Affairs, 2013). Agglomerating coal fines by using hazardous wastes can decrease the size of the dumping sites of these components while also creating a useable product.

There are four primary industries where coal is utilised: electricity generation (boilers), cement production (high temperature kilns), transportation fuel development (gasifiers) and steel manufacturing (coke ovens) (WCA, 2019c). The processes that the coal goes through varies in these industries and it is therefore important to research the characteristics of the coal used in each of the industrial applications to determine the suitability of hazardous wastes as binders in these processes.

1.3 Problem statement

Based on the background provided, fine coal and industrial hazardous waste dump sites pose an environmental and physical hazard and should therefore be reduced. The briquetting of coal fines and various waste materials should be tested to determine if viable agglomerates can be produced for use in industrial processes.

1.4 Aim and objectives

The aim of this study is to evaluate industrial waste streams as potential binders to agglomerate inertinite-rich, high ash coal fines and to classify these agglomerates for use in various industrial processes.

The following objectives are established to achieve this aim:

- prepare and characterise the discard coal and waste materials (*i.e.* potential binders);
- assess the effect of different waste materials at various concentrations on the mechanical strength and water resistance of briquettes produced on laboratory-scale;
- quantify the effect of the waste materials on the mechanical strength of briquettes produced on pilot-scale;
- assess the effect of different waste materials on the water resistance of the pilot-scale briquettes; and
- conduct reactivity tests to determine the appropriate industrial processes where the briquettes could be utilised.

1.5 Scope of investigation

The five industrial wastes that will be considered in this study are: A: waterworks bio-sludge, B: acrylic acid containing a hydrocarbon by-product, C: pitch, D: wax emulsion, and E: recycled low-density polyethylene. The study will be divided into three phases to achieve the objectives set out in Section 1.4:

- Phase 1: Laboratory-scale batch briquetting

  During this phase, the maximum amount of industrial waste material that can be added to inertinite-rich coal fines during laboratory-scale briquetting will be determined. To do this, cylindrical briquettes are produced using the Lloyd LRX Press, and the compressive strength and water resistance of these briquettes will be tested and compared. The effect of moisture addition will also be evaluated. Only the binders that do not negatively impact the compressive strength and water resistance of the briquettes will be used in the following phase of the study.

- Phase 2: Pilot-scale continuous briquetting

In this phase the viability of the various binders will be evaluated based on the compressive strength, impact resistance, durability (*i.e.,* friability and abrasion resistance) and water resistance of the briquettes. The information gathered during phase 1 will be utilised to produce roller-pressed briquettes in a continuous process to determine the optimal concentration for each binder.

- Phase 3: Matching with industrial processes

The heating value, reactivity (*i.e.,* pyrolysis, combustion and gasification), proximate analysis and thermal fragmentation of the optimal briquettes manufactured in phase 2 will be evaluated and matched to industrial processes. The main processes that will be investigated are electricity generation (boilers), transportation fuel development (gasifiers), and steel manufacturing (coke ovens).

1.6 Study outline

The outline of this study is illustrated in Figure 1-1. Chapter 1 introduces the study and gives some background on coal fines and the need for fine coal agglomeration. In Chapter 2 the available information on coal, binders, agglomeration methods and the uses of coal/ agglomerates are reviewed and summarised. The materials and methods that are used during the study are described in Chapter 3 and the results are reported and discussed in Chapters 4 and 5. The conclusions that can be reached from the results obtained are given in Chapter 6 along with all recommendations for future studies.

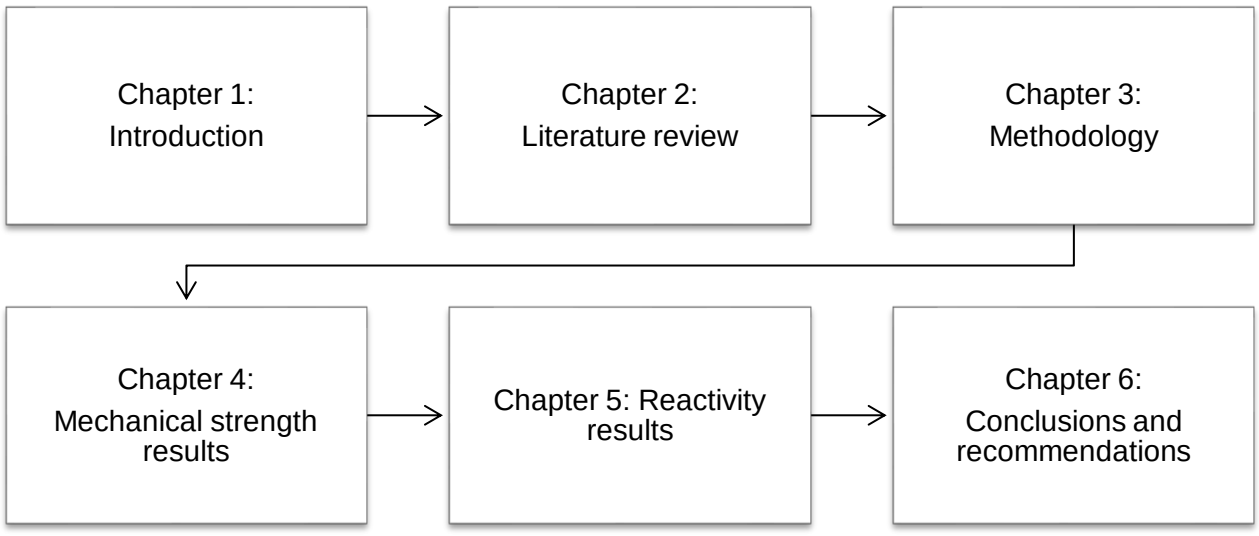

Figure 1-1: Layout of the chapters in the study

CHAPTER 2: LITERATURE REVIEW

2.1 Overview

The topics that are discussed in this chapter will provide a relevant understanding of what coal is, why it is important to agglomerate fine coal, and how these agglomerates can be used in industrial applications. The coal that will be used in this study is from the Highveld coalfields and Section 2.2 therefore describes the characteristics of Highveld coal specifically. Furthermore, the effect of coal fines and how they can be agglomerated are also discussed. Section 2.3 provides a description of the different variables that play a role during coal briquetting and why these variables are important. The properties of industrially viable briquettes are defined in Section 2.4 and the tests to determine these properties are also described. Section 2.6 provides a summary of the industrial processes in which the briquettes can be used, *i.e.* electricity generation, petrochemical industry and steel manufacturing.

2.2 Coal

In 2018, the global amount of economically recoverable coal reserves was approximately 1 054 782 Mt, which can last nearly 132 years at the current production rate of 8 013 Mtpa (BP, 2019). This timeline is based on the reserves-to-production ratio, which is calculated by dividing the remaining proved reserves by the production in that year and refers to the amount of time that the reserves would last if the production continued at that rate (BP, 2019). The coal reserves can be divided into two groups: (1) anthracite and bituminous coal, and (2) sub-bituminous and lignite coal. Group 1 coal accounts for almost 70% of the global coal reserves (BP, 2019). The global primary energy consumption (PEC) is 13 865 Mtoe and the breakdown based on fuel type is shown in Figure 2-1 (BP, 2019).

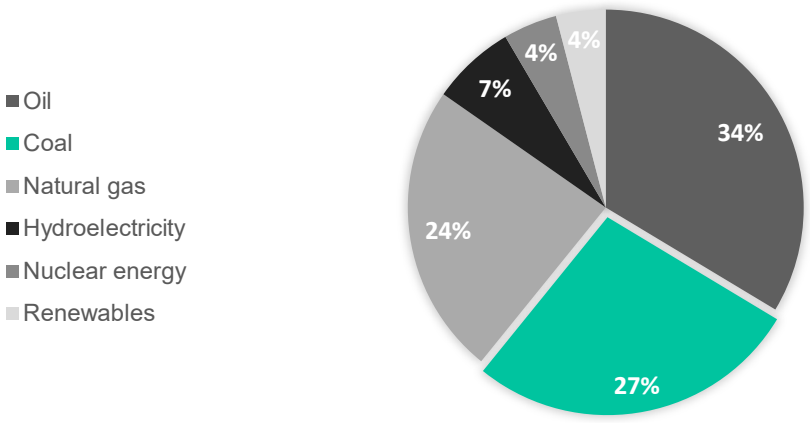

Figure 2-1: Global primary energy consumption by fuel type adapted from BP (2019)

Based on the coal consumption of 7 717 Mtpa equating to 27% of the global PEC, even though strides are being made to increase the use of renewable fuels, coal is clearly still a widely used

resource (BP, 2019). Notably, even though coal reserves are spread over numerous countries compared to other energy sources, it also has the highest specific CO_2 emissions (BGR, 2019).

The coal in South Africa is classified as mainly Group 1 coal and the economically recoverable coal reserves contain approximately 9 893 Mt, which accounts for almost 1% of the global coal reserves (BP, 2019). South Africa is the seventh largest coal producer and with the current rate of production being 253 Mtpa, the reserves-to-production ratio is 39 years (BP, 2019). Figure 2-2 depicts the division of South African primary energy consumption of 152 Mtpa, with regards to the various fuel sources that are used (BP, 2019). Fossil fuels make up almost the whole sector, with coal being the most used fuel source at 71% of the PEC.

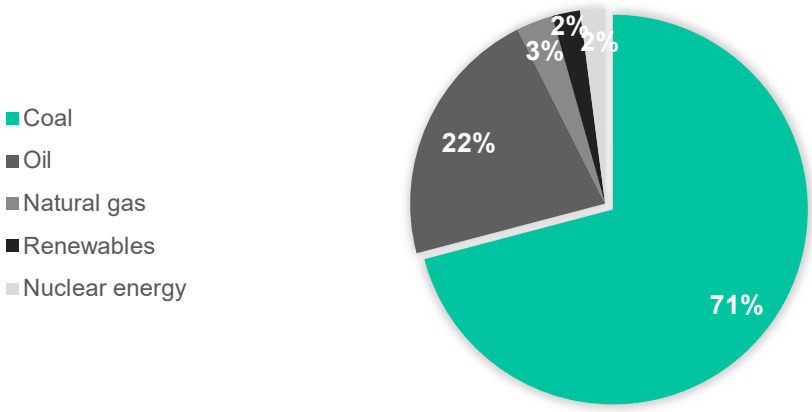

Figure 2-2: South African primary energy consumption by fuel type adapted from BP (2019)

There are 19 coalfields in South Africa, but more than 70% of the country's reserves are in the central basin: Highveld, Witbank, Waterberg and Ermelo (FFF, 2013).

2.2.1 Highveld coalfields

The Highveld Coalfield accounts for nearly 29% of the coal reserves in South Africa and is integral to the long-term running of Sasol's Synthetic Fuels as well as power stations in the area, *e.g.* Eskom's Kriel, Matla and Tutuka power stations (Hancox & Götz, 2014; Jeffrey *et al.*, 2015). The coalfield extends over an area of approximately 700 000 ha in south-eastern Gauteng and Mpumalanga and a summary of the coal seams is shown in Table 2-1 (Hancox & Götz, 2014). The No. 2 Seam is low-grade bituminous coal, but the quality can increase to 27 MJ/kg in some areas (Jeffrey, 2005). Most of the coal resources are contained in the No. 4 Seam, which is divided into the No. 4 Lower (4L) and No. 4 Upper (4U) Seam (Hancox & Götz, 2014). The coal that is mined from this section is usually low-grade bituminous coal, but the coal quality may vary depending on the depth of the seam (Jeffrey, 2005). The coal quality decreases in the upper 1 m of the seam (ash yield: 40%, calorific value: 15 MJ/kg) and increases at the thicker seam areas

in the lower 3–4 m (ash yield: 21%, calorific value: 23 MJ/kg) (Jordaan, 1986). This coal can be used for electricity generation (Hancox & Götz, 2014). Coal from the No. 5 Seam can be used in metallurgical processes due the ash yield, volatile matter and calorific values being 19%, 32% and >25 MJ/kg, respectively (Barker, cited by Hancox & Götz, 2014).

Table 2-1: Summary of the Highveld Coalfield seams adapted from Cairncross (2001) and Hancox and Götz (2014)

Seam		Depth[a]	Thickness[a]	Qualities[a,b]
1		-	-	-
2		30–240 m	<1–10 m	Moisture content: ±4% Ash yield: 22–35% Volatile matter: ±20% Calorific value: 20–23 MJ/kg
3		-	<0.5–1.0 m	Calorific value: ±28 MJ/kg
4	**4L**	15–300 m	<1–12 m	Moisture content: ±2.5% Ash yield: 20–35% Volatile matter: ±20% Calorific value: 18–25 MJ/kg
	4U		1.5–3.4 m	
5		15–150 m	0.3–3.0 m	Moisture content: ±3% Ash yield: ±17% Volatile matter: ±33% Calorific value: ±26 MJ/kg

Source: [a] Hancox and Götz (2014) and [b] Cairncross (2001)

In South Africa there are two main types of coal mining techniques: underground mining and surface mining (FFF, 2011). Approximately 51% of mining is done underground and 49% is done on the surface (Department of Energy, 2018). Underground mining is mainly done by bord-and-pillar mining where coal is mined from between pillars, which are left to support the overlying rocks (Lloyd, 2002). Another underground mining technique that is used to mine a small amount of coal is longwall mining, which entails removing all the minable coal and leaving the rock ceiling to collapse into the hollow area (Lloyd, 2002). Conveyor belts, shuttle cars and continuous miners are used to remove the mined coal for both methods (Jeffrey *et al.*, 2015). Surface mining techniques include opencast mining and strip mining. During opencast mining coal deposits are exposed by removing a large area of topsoil and surface rocks, also known as the overburden, and moving it to another location (Lloyd, 2002). The coal can be extracted with trucks and mechanised shovels or bucket-wheel excavators (FFF, 2011). To rehabilitate the area, the overburden can be returned to the mined area at a later stage and covered with the topsoil (Lloyd, 2002). Strip mining entails removing the overburden one strips at a time to expose and

extract the coal deposits and then dumping the overburden of the new strip into the previously mined area (Lloyd, 2002). Dragline equipment is used for excavation (FFF, 2011). The use of underground/ surface mining methods depends on geological factors (Lloyd, 2002).

Coal that is newly mined is referred to as ROM (run-of-mine) coal and contains impurities such as rocks, wood, ash-forming minerals and moisture (FFF, 2011). These impurities can negatively impact the value of the coal by reducing the heating value and increasing the volume of material that is handled, the impact of the material on end-use equipment and the hazardous emissions that form during end-use processes (FFF, 2011). Coal preparation involves the removal of the impurities and can be divided into two stages: (1) screening and (2) washing. In stage 1 the large impurities, *e.g.* rocks and wood, are removed before the ROM coal is crushed and separated into various size fractions through screening (FFF, 2011). The coal can then be sold or sent to stage 2 for washing where the ash-forming minerals are removed with density separating techniques (FFF, 2011).

2.2.2 Coal fines

Coal breakage occurs systematically throughout the whole coal chain due to both deliberate, *e.g.* crushing, and inadvertent, *e.g.* transportation, causes (Hardman & Lind, 2003). The breakage leads to the formation of fine (-1.0 mm) and ultra-fine (-0.15 mm) coal, which relates to a loss of profits if the coal does not meet end-use specifications (de Korte, 2016; Hardman & Lind, 2003). During coal mining the production of coal fines is primarily caused by mechanical equipment and transportation (Hardman & Lind, 2003). If these coal fines are not handled appropriately in underground mines, they could become airborne (at -0.1 mm) and cause dust explosions or are respirable (at -0.007 mm) and cause damage to workers' health (Hardman & Lind, 2003). The small particle size of coal fines also causes handling issues due to the propensity of the coal to block equipment and transportation mechanisms (Holuszko & Laskowski, 2004). The moisture retention capacity of coal increases with a decrease in coal size, and the calorific value of the coal will therefore be reduced (Hardman & Lind, 2003).

In South Africa, studies have been done to find ways of reducing the formation of coal fines during mining and preparation or altering end-use processes to accommodate coal fines, however, they are usually expensive and not highly effective (Hand, 2000; Mjonono *et al.*, 2018; Muzenda, 2014; Reddick *et al.*, 2007). The annual discard and slurry production, consisting of mainly bituminous coal, is estimated to be more than 42.5 Mtpa and 11.3 Mtpa, respectively (Department of Minerals and Energy, 2001). The 29 active discard dumps and 17 active slurry ponds in South Africa have a combined content of more than 361 Mt (Muzenda, 2014). The coal in these disposal sites can spontaneously combust or contaminate the surrounding area by

means of gaseous pollutants or acid mine drainage (Lewitt, 2011; WCA, 2019c). The legislation regarding these dumps have therefore become stricter and expensive methods of covering the disposal sites have become a necessity (Lewitt, 2011). However, the quality of the coal fines, shown in Table 2-2, is usually very poor and the end-use industrial option for re-using these fines are limited (Department of Minerals and Energy, 2001). With economically recoverable coal resources in South Africa only dwindling and the disposal sites being an economic and environmental burden, it is essential to explore methods of utilising coal fines as a resource.

Table 2-2: Quality of coal fines dumped in discard dumps and slurry dams adapted from the Department of Minerals and Energy (2001)

Property	Discard dumps	Slurry ponds
Calorific value (MJ/kg)	Most: 10–15 Some: 15–20	20–25
Volatile matter content (%)	16–20	17–27
Fixed carbon content (%)	20–40	40–55
Ash yield (%)	40–50	20–30
Sulphur (%)	1–3	0–2

2.3 Coal agglomeration

Coal agglomeration methods can be utilised to make coal fines useable through grouping the coal particles together to form a larger mass with similar characteristics as the ROM “parent” coal (England, 2000). The three traditional coal agglomeration methods are: briquetting, pelletising and spherical agglomeration (England, 2000). Briquetting and pelletising methods are usually used to agglomerate coal fines, but large-scale applications have been limited due to the costs involved (Couch, 1998). Binders can be used during briquetting and pelletising to enhance the binding mechanism of the coal particles; however, they also contribute substantially to the cost of the process (Couch, 1998; England, 2000; Mehta & Parekh, 1996).

2.3.1 Methods

The choice of coal agglomeration method that should be used depends on the properties of the coal fines, the required product characteristics (*e.g.,* handleability and strength), the difference between coal cost and product value, and the binder availability and cost (Whitehead, cited by Couch, 2002). The variables that affect coal briquetting and pelletising are discussed in further detail in Section 2.3.2.

2.3.1.1 Spherical agglomeration

Spherical agglomeration, *i.e.* oil agglomeration, depends on the lipophilic and hydrophobic nature of coal (England, 2000). During the process, a bridging agent, *e.g.* oil, is added to a fine coal slurry under high shear conditions where the coal particles become coated in the agent and draw closer together until the maximum amount of water is repulsed (England, 2000). The mineral matter impurities are left in the water (England, 2000). However, oil agglomeration is only possible if the coal particles are hydrophobic enough (Özer *et al.*, 2017). Surface-modification agents can be added to increase the agglomeration of the coal particles and decrease the amount of bridging agent that is needed (Özer *et al.*, 2017). The spherical agglomerates that are formed can be recovered by skimming, screening or by using a sink/ tank density separator (Özer *et al.*, 2017). The agglomerates can then be dewatered by stockpiling or screening and pelletised or added to the coarse coal product (England, 2000; Özer *et al.*, 2017).

2.3.1.2 Pelletising

There are two types of coal pelletising methods: (1) pelleting by agglomeration, and (2) pelletising by extrusion (Conkle & Ragavan, 1992; Lewitt, 2011). To differentiate between the two types of methods the products from method 1 and 2 will be referred to as pellets and extrudates, respectively. During method 1 coal fines are shaped into spherical pellets with a disk or drum pelletiser, and during method 2 extrudates are formed by extruding coal fines through one or more dies or a ring die (Couch, 1998; Lewitt, 2011).

Disk pelletising involves the formation of spherical pellets by rolling the coal fines on a rotating, inclined pan (Couch, 1998; Lewitt, 2011). The coal fines and binder are mixed and fed to the disk where a nucleating spray initiates and promotes the formation of pellets by clumping the coal particles together, and once the pellets are heavy enough, they are thrown off the disk edge (Couch, 1998). The moisture content of the coal affects the size and strength of the pellet and should be high: >20% for fine coal and >40% for ultra-fine coal (unless the ash content is high) (Couch, 1998; England, 2000). A binder is always added, and the relation of moisture content and binder is extremely important and should be carefully controlled (England, 2000). The angle of the disk and the speed of its rotation can be adjusted to control the size of the pellets (Couch, 1998). The pellets should be treated after being formed and the type of treatment depends on the binder that was used (Couch, 1998; England, 2000). Drum pelletising is like disk pelletising and entails the formation of spherical pellets by rotating coal fines in a rotating, inclined drum (England, 2000). However, the length of the drum is important as it affects the size of the pellets and there are usually more unprocessed coal fines at the end of the drum (England, 2000). Both disk and drum pelletising are simple and cheap methods that can be used to produce

relatively weak pellets with a diameter of 5-80 mm (England, 2002; Whitehead, cited by Couch, 2002).

Extruder pelletising entails the formation of cylindrical extrudates by applying compressive strength to coal fines with a die (Couch, 1998; England, 2000; Lewitt, 2011) (Conkle & Ragavan, 1992). During extrusion with a roller and die, a mixture of coal fines and binder is fed to a screw-feeder that pushes it into a chamber where a rotating roller forces the mixture through a die and an external blade cuts the extrudates into the required size, as shown in Figure 2-3(a) (Couch, 1998; England, 2000) (Conkle & Ragavan, 1992). The coal fines should have a moisture content below 12% (Couch, 1998). Extrusion with one or more cylindrical dies at the end of the screw-feeder chamber, depicted in Figure 2-3(b), creates a cylindrical rod that can be cut into the required size by a rotating blade (Couch, 1998). The extrudates should be treated after the process (Couch, 1998; England, 2000). Extrusion pelletising is a relatively expensive process, and the operating costs of the equipment is considerably high due to wear (Whitehead, cited by Couch, 2002).

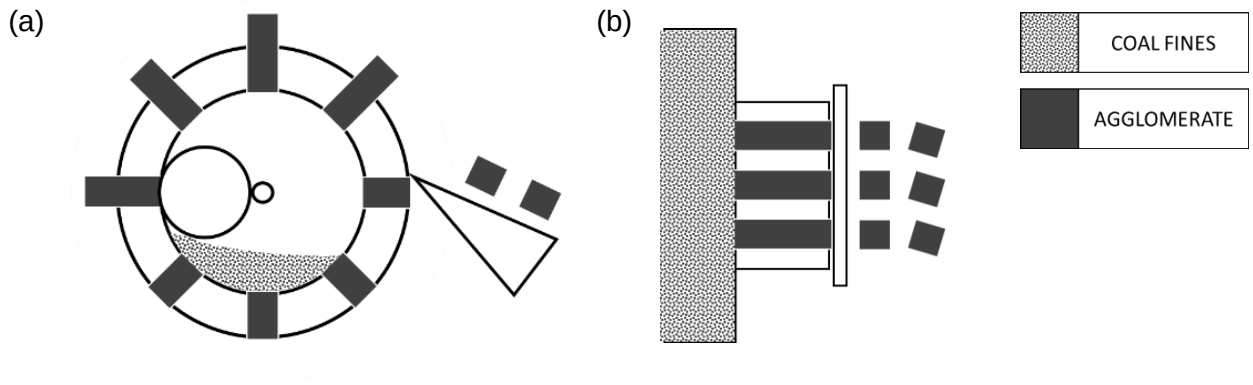

Figure 2-3: Illustration of extrusion with (a) a roller and die and (b) a die with cylindrical openings adapted from Conkle and Ragavan (1992)

2.3.1.3 Briquetting

Briquette manufacturing, *i.e.* briquetting, entails the agglomeration of coal fines into usually ovoid-shaped briquettes using compressive force (Conkle & Ragavan, 1992). The coal fines are dried to the required moisture content and then mixed with a binder, if necessary, before being fed by a screw-feeder to a roll press with twin opposing rolls containing one or more rows of compartments, as illustrated in Figure 2-4 (Conkle & Ragavan, 1992; Couch, 1998; England, 2000).

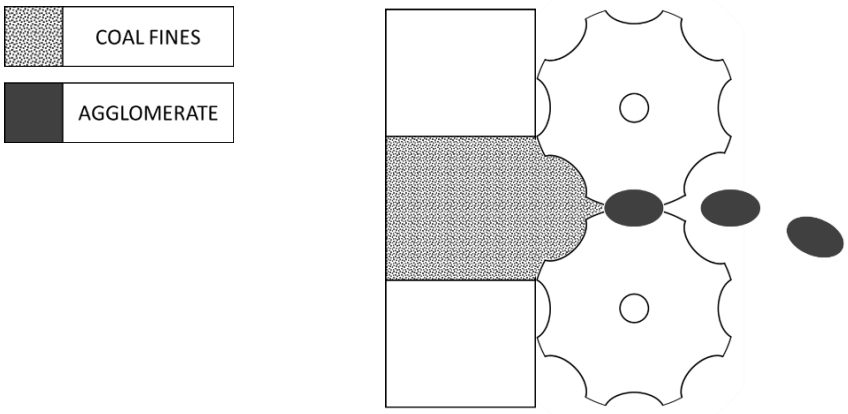

Figure 2-4: Illustration of briquetting with a roll press adapted from Conkle and Ragavan (1992)

Briquetting is used to agglomerate coal fines with a relatively low moisture content (<35%), which can be achieved through thermal drying, *e.g.* rotary drier, fluidised bed or flash dryer (England, 2000; Komarek, 1991). A binder is typically necessary to create mechanically strong briquettes with bituminous coal, but some soft brown coals can be briquetted without a binder (Couch, 1998). Anthracite coal, however, is usually too hard to be briquetted (Jones, 1963). The speed of the screw-feeder generally affects the strength of bituminous coal briquettes due to the added energy causing high shear deformation (England, 2000; Komarek, 1991). The unprocessed coal fines that pass through the roll press by being caught between the roll, but outside of the compartments, can be separated from the briquettes using a screen and recycled back to the feed (England, 2000). A ring-type roll press is preferred for coals that are difficult to agglomerate (Couch, 2002). Treatment of the briquettes with heat or cold after manufacturing depends on the binder that was used since some binders require heat to spread between the coal particles or to activate, while other binders decompose at higher temperatures (England, 2000; Kaliyan & Morey, 2009). Briquetting is a relatively expensive process (Whitehead cited by Couch, 2002).

2.3.2 Briquetting variables

In this section the characteristics of the coal fines that need to be agglomerated, *e.g.* particle size distribution, type, rank and grade, as well as the process variables of the agglomeration method, *e.g.* binding mechanisms, binder, temperature and pressure will be reviewed.

2.3.2.1 Coal classification

Coal is formed during the process of coalification, where pressure, heat and microbial activity between other rock strata shapes a combustible, organic rock from ancient vegetation (peat) over a lengthy period (Arnold, 2013; O'Keefe *et al.*, 2013). The type of plant material, degree of

metamorphism and range of impurities during the coalification process determines the type, rank and grade of coal that is formed, respectively (Arnold, 2013; O'Keefe *et al.*, 2013).

Figure 2-5 illustrates the three variables of coalification, as well as the main ranks of coal that can form: peat, lignite, bituminous and anthracite (Laj & Barnikel, 2016). These variables each play a role during the agglomeration of coal fines. Another important variable is the particle size distribution of the coal fines.

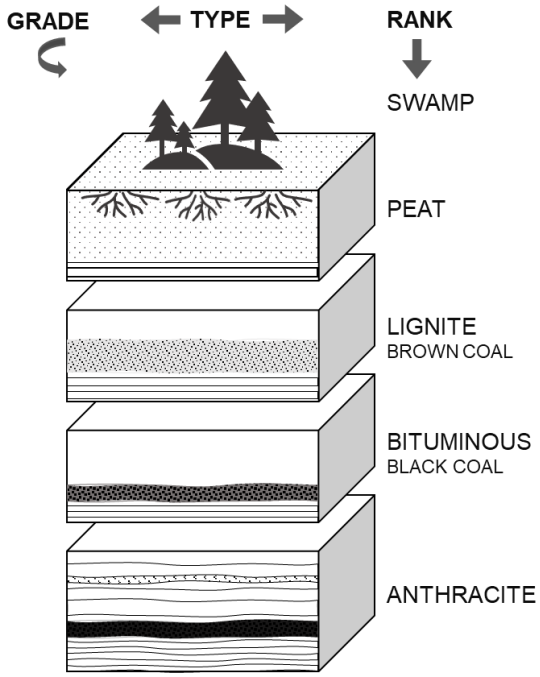

Figure 2-5: The effect of coalification on the grade, type and rank of coal adapted from Laj and Barnikel (2016)

a. Coal grade

Coal grade describes the purity of the peat, *i.e.* the extent to which mineral matter has been kept out of the coal, during accumulation (syngenetic), after burial (epigenetic) and during rank advance (O'Keefe *et al.*, 2013). Mineral matter, *e.g.* quartz, pyrite, marcasite, clay and carbonaceous minerals, therefore, determines coal grade (Falcon, 2013; Woodruff *et al.*, 2017). Ash and sulphur result from the mineral matter of the coal after combustion and the Parr formula, Equation 2-1, is generally accepted as a method to determine the amount of mineral matter from the ash yield and sulphur content (Parr, cited by Arnold, 2013; Woodruff *et al*., 2017).

$$\text{Mineral matter} = 1.08\,(\text{ash }\%) + 0.55\,(\text{sulphur }\%) \qquad (2\text{-}1)$$

The amount of ash yield in coal can be classified in five categories, listed in Table 2-3 (ISO, 2005). A proximate analysis can be done to determine the percentage moisture content, volatile matter, ash yield and fixed carbon (by difference) of the coal and an ultimate analysis can be done to

determine the amount of carbon, hydrogen, sulphur, nitrogen and oxygen (by difference) (Arnold, 2013).

Table 2-3: Ash yield class categories retrieved from ISO (2005)

Ash class category	**Ash yield***
Very low	<5
Low	≥5 and <10
Medium	≥10 and <20
Moderately high	≥20 and <30
High	≥30 and <50

* % by mass, db

Clay minerals account for up to 80% of all mineral matter in coal and consequently influences coal agglomeration (Falcon, 2013; Mangena & du Cann, 2007). Clays can increase the strength of the agglomerates at the appropriate moisture content due to the plasticity of the minerals when they are wet, which causes the coal particles to adhere to each other (Mangena *et al.*, 2004). Kaolinite is a type of clay that swells due to the absorption of water and leads to a decrease in the water resistance of agglomerates with an ash yield larger than 15%, adb (Mangena *et al.*, 2004). Bentonite is a clay that has been used as a binder to agglomerate coal in past studies (Sastry, 1995). Mineral matter can be abrasive to equipment and coal with a low ash yield is therefore generally preferred for agglomeration (Couch, 2002).

b. Coal type

Coal type is described by the maceral composition of the coal, mainly vitrinite, inertinite and liptinite (Falcon, 2013). The maceral composition is determined by interrelated factors such as vegetation, climate, Eh (*i.e.* redox potential) and pH conditions and ground characteristics (Cook, 1975; O'Keefe *et al.*, 2013). Vitrinite creates a highly porous char that can cause a fast burn-out to occur at ignition, whereas inertinite creates a highly dense char with a long burn-out period (Falcon, 2016). Petrography can be used to determine the vitrinite reflectance or to do a maceral analysis on the coal (Laj & Barnikel, 2016). The vitrinite content of coal is independent of coal rank and the vitrinite class categories are listed in Table 2-4.

The maceral composition of coal plays an important role in the properties of coal agglomerates. High reflecting macerals, *viz.* vitrinite, liptinite and reactive inertinite, increases the strength and durability of agglomerates due to the vitrinite matrix that forms when the air in the voids between the coal particles is expelled and the particles become oriented and deformed during agglomeration (England, 2000; Kidena *et al.*, 2002; Mangena & du Cann, 2007; Waters, 1969).

Table 2-4: Vitrinite content class categories retrieved from ISO (2005)

Vitrinite class category	Vitrinite content*
Low	<40
Medium	≥40 and <60
Moderately high	≥60 and <80
High	≥80

* % by volume, dmmfb

This matrix binds the other macerals together and improves the elasticity of the agglomerates. The rigid, highly reflective macerals transmit shear forces during agglomeration (Gregory, 1960). The inert inertinite content of coal therefore has a negative effect on the agglomerate strength (Woods, cited by Modiri, 2016).

c. Coal rank

Coal rank is determined by the stage of coalification that was achieved, from peat to anthracite, which usually reflects the depth of burial and geothermal gradient prevailing at the time of coalification (O'Keefe *et al.*, 2013). Coal rank increases with an increase in fixed carbon content and calorific value and a decrease in moisture content, and it is independent of coal type and grade (Cairncross, 2001; Laj & Barnikel, 2016). A dry, mineral matter-free basis should therefore be considered to determine the coal rank (Arnold, 2013). A summary of the different coal ranks and their corresponding properties are shown in Table 2-5.

The moisture content of coal affects the agglomeration process due to surface tension and capillary pressure (Mangena, 2001; Pietsch, 2004; Waters, 1969). The binding mechanism is discussed in detail in Section 2.3.2.2. There is also a specific optimal moisture where clay minerals are plasticised (Mangena *et al.*, 2004). The optimal moisture content in coal is dependent on the properties of the coal that is being agglomerated. Briquettes are usually produced with coal that has a moisture content below 10%, however some studies have had success with higher moisture contents (Altun *et al.*, 2003; Clark *et al.*, 1997; England, 1993; Han *et al.*, 2013; Komarek, 1991; Mangena *et al.*, 2004; Venter & Naude, 2015). Coal rank is therefore important because moisture content decreases with an increase in coal rank. The strength of agglomerates increases for bituminous coal and semi-anthracites with a decrease in hardness, and decreases for anthracites with an increase in hardness (Mochida & Honda, 1963). This is because the strength of agglomerates increases with plasticity, which decreases with coal rank (Jones, 1963).

Table 2-5: Summary of coal ranks and their approximate properties adapted from Arnold (2013), Bowen and Irwin (2008), Laj and Barnikel (2016), Speight (2008), and Woodruff *et al.* (2017)

Rank	Proximate analysis (wt%)				Ultimate analysis[b,d,e] (wt%)					Reflectance of vitrinite[c] (%)	Calorific value[a,c] (MJ/kg)
	Moisture content[a,b]	Volatile matter content[c]	Fixed carbon content[a,b]	Ash yield[b]	Sulphur	Hydrogen	Carbon	Nitrogen	Oxygen		
Lignite	30–60	35–50	25–35	10–50	0.3–2.5	6.0–7.5	35–45	0.6–1.0	38–48	0.2–0.3	9–21
Subbituminous	10–45	27–50	35–45	≤10	<2.0	5.5–6.5	55–70	0.8–1.5	15–34	0.3–0.4	19–26
Bituminous	3–15	10–45	45–85	3–12	0.7–6.0	4.5–6.0	65–80	0.5–2.5	4.5–10	0.5–1.8	20–37
Anthracite	<15	<10	85–98	10–20	0.6–2.5	1.5–3.5	75–85	0.5–1.0	5.5–9.0	4.0	32–36

Source: [a] Laj & Barnikel (2016), [b] Bowen & Irwin (2008), [c] Arnold (2013), [d] Woodruff *et al*. (2017) and [e] Speight (2008)

Moisture content: arb, volatile matter: adb, fixed carbon content: dmmfb, ash yield: adb, ultimate analysis: arb, calorific value: mmmf

2.3.2.2 Particle size distribution

Particle size distribution (PSD) of coal is limited by the agglomeration process and can influence the strength of the agglomerates (Kaliyan & Morey, 2009; Mangena, 2001; Woodruff *et al.*, 2017). Agglomerating coal with a wide PSD can enhance the mechanical interlocking of the coal particles when the smaller particles fill the voids that are created by the larger particles (Dehont, 2006; Kaliyan & Morey, 2009; Young, 2015). The strength of agglomerates produced by coal with small particles also increases due to the ease with which fine coal particles plastically deform under pressure for high vitrinite coal and the increased contact between particles that facilitates adhesion/ bond formation (Ellison & Stanmore, 1981a; Gregory, 1960; Pietsch, 2004). The bonds that are only active below certain particle sizes are van der Waals forces (< 1 µm), adsorbed vapour layer (< 80 µm), and liquid bridges (< 500 µm) (Rumpf cited by Hapgood and Rhodes, 2008). Particles should be smaller than 1 mm because larger particles act as predetermined breaking points in an agglomerate (Franke & Rey, 2006). However, grinding the particles to a very small size increases the operational costs due to a high energy requirement for a low throughput, and it also makes handling difficult due to the propensity of the coal to block equipment and transportation mechanisms (Franke & Rey, 2006; Holuszko & Laskowski, 2004).

A suggested PSD for the agglomeration of coal particles as a percentage of the largest particle (3 mm) has been described by Dehont (2006) as 50% < 16.7% maximum size, 25% < 33.3% maximum size, and 20% < 66.7% maximum size. Trommer, cited by Ellison and Stanmore (1981a), used the Gates-Gaudin-Schumann distribution model, Equation 2-2, to determine the mean PSD of coal for agglomeration purposes.

$$Q(d) = \left(\frac{d}{d_{\max}}\right)^{n} \qquad (2\text{-}2)$$

In Equation 2-2, *Q(d)* is the cumulative distribution of the particles at size *d*, d_{max} is the diameter of the largest particles, and the distribution parameter, *n*, is a measure of the dispersion of particle sizes, *i.e.* if $n = 0$, the particles are all size d_{max}, and if $n = 1$, the PSD is linear. An intermediate value of *n* (≈ 0.6) showed the highest strength results due to the fines filling the voids between the larger particles, thereby giving maximum surface contact between the particles (Trommer cited by Ellison and Stanmore, 1981a).

2.3.2.3 Binding mechanisms

The forces associated with agglomeration are difficult to predict, but they can generally be divided into two groups: physical and applied (Lu, 1989; Sastry, 1995). There are five main groups of interparticle physical binding mechanisms, Table 2-6, described by Rumpf (cited by

Pietsch, 2004), *viz.* solid bridges, adhesion and cohesion forces, surface tension and capillary pressure, attraction forces between solids, and interlocking bonds. The applied forces from the agglomeration process decrease the interparticle voids and bring the coal particles into proximity with each other so that the physical forces can then become operational (Pietsch, 2004; Sastry, 1995; Waters, 1969). Binding mechanisms are complex and have been reviewed in detail in previous studies, so only a brief overview is given to aid in the analysis of the binder behaviour (Iveson & Litster, 1998; Iveson & Page, 2001; Iveson *et al.*, 2002; Iveson *et al.*, 2001; Pietsch, 1997, 2004; Zhang *et al.*, 2018).

Table 2-6: Agglomeration binding mechanisms and their respective bond types adapted from Rumpf (cited by Pietsch, 2004)

Binding mechanism	**Type**
Solid bridges	Crystalline Hardening liquid binder Solid binder
Adhesion and cohesion forces	Highly viscous binders Adsorption layers (<3 nm thickness)
Surface tension and capillary pressure	Liquid bridges Capillary pressure
Attraction forces between solids	Molecular forces Electric forces Magnetic forces
Interlocking bonds	

a. Solid bridges

Solid bridges form between particles when liquid is removed from the briquette and can develop as crystalline, hardening binder or solid binder bridges (Hapgood & Rhodes, 2008; Pietsch, 2004). Crystalline bridges form when a liquid binder containing a soluble material (*e.g.*, salt) is evaporated. This causes recrystallisation at the contact areas between the coal particles where a bridge structure then forms to increase the briquette strength. The strength of the recrystallised bridge structure depends on the amount of material and increases at higher crystallisation rates (Pietsch, 2004).

Hardening liquid binder or chemical reaction solid bridges usually form when a solvent (*e.g.*, water) containing a binder or chemical (*e.g.* glue) is added to the coal particles in liquid form and then evaporated to leave the hardened binder or chemical as a bridge between the particles (Hapgood & Rhodes, 2008; Pietsch, 2004). The binder properties, *i.e.* reactivity and tendency to

harden, and operational conditions, *i.e.* pressure and temperature, affect the strength of the bridges (Pietsch, 2004).

Solid binder bridges are also formed when a liquid binder containing suspended colloidal (*i.e.*, finely ground) particles is evaporated. When the liquid evaporates the suspended colloidal particles causes a pressure increase in the liquid bridges between coal particles which eventually compacts the colloidal particles to form a bridge by means of primarily attraction forces (Hapgood & Rhodes, 2008; Pietsch, 2004).

b. Adhesion and cohesion forces

Adhesion force refers to the molecular attraction exerted between the surfaces of the coal particles which causes them to stick to each other and cohesion force refers to the molecular attraction by which the coal and/ or binder particles in a briquette are united through the mass (Pietsch, 2004). Highly viscous binders, *e.g.* pitch, are used to agglomerate particles through the adhesion forces at the particle-binder border and cohesion forces in the binder itself, which increases the strength of the briquette until the weaker component, usually the liquid, fails (Green & Southard, 2019; Pietsch, 2004).

Particles in the presence of a condensable vapour is covered in a thin adsorbed layer of the vapour (Hapgood & Rhodes, 2008; Pietsch, 2004). If the adsorption layer is thinner than 3 nm, the molecular forces can be completely transmitted at the overlapping area between the particles (Pietsch, 2004). This often causes the particles to deform, thereby increasing the contact area and strength of the bond between adhering particles. The partial pressure of the vapour in the atmosphere affects the thickness and strength of the adsorbed layers, *i.e.* increased partial pressure leads to increased strength, such that there exists a critical partial pressure where the adsorbed layer bonding gives way to liquid bridge bonding (Coelho & Harnby, 1978; Hapgood & Rhodes, 2008).

c. Surface tension and capillary pressure

A small amount of liquid on the surface of the coal particles decreases the interparticle distance and has a smoothing effect, consequently increasing the interparticle forces (Hapgood & Rhodes, 2008). If a sufficient proportion of liquid is present however, interparticle liquid bridges will form (Green & Southard, 2019; Hapgood & Rhodes, 2008; Pietsch, 2004). Figure 2-6 is an illustration of the different liquid saturations in a briquette and the related liquid states (Hapgood & Rhodes, 2008; Pietsch, 2004).

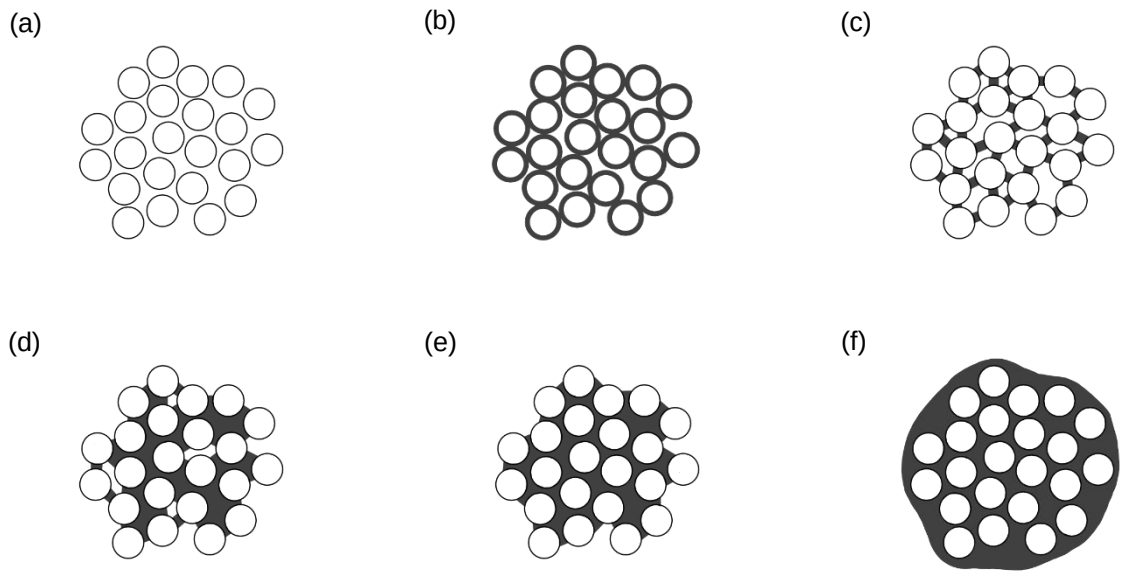

Figure 2-6: Illustrations of the liquid states in briquettes based on the liquid saturation for (a) dry, (b) adsorption layers, (c) liquid bridges – pendular sate, (d) transitional – funicular state, (e) fully saturated – capillary state, and (f) droplet, adapted from Pietsch (2004)

The coal particles will never be completely dry, Figure 2-6(a), under atmospheric conditions due to the adsorbed layer, Figure 2-6(b), that forms quickly on the surface of the particles. When the liquid saturation is increased to the pendular state, Figure 2-6(c), liquid bridges start to form between the coal particles (Green & Southard, 2019; Hapgood & Rhodes, 2008; Pietsch, 2004). These bridges connect the particles at a point contact on the surface and form curved bridge necks due to the interstitial space caused by porosity or voidage (Hapgood & Rhodes, 2008). The coal particles are pulled closer to each other due to the strong boundary forces created by the surface tension of the liquid, and the concave menisci that form at the pores on the surface of the briquettes that create a capillary pressure in the briquette (Green & Southard, 2019; Hapgood & Rhodes, 2008). An increase in liquid saturation in the pendular state increases the resistance of the bonds to rupturing, *i.e.* the particles can be pulled apart further without breaking the bridges, without significantly affecting the interparticle bond strength (Pietsch, 2004). However, if the liquid saturation is increased enough to move into the funicular state, Figure 2-6(d), the strength of the briquette decreases due to the free movement of the liquid and reduction in attractive force between the particles (Hapgood & Rhodes, 2008). The capillary state is reached when all the interstitial space is filled with liquid, *i.e.* complete saturation, and a further decline in briquette strength is observed due to fewer curved liquid surfaces and consequently less surface tension to pull the coal particles together (Hapgood & Rhodes, 2008). If the liquid exceeds complete saturation, the droplet state, Figure 2-6(f), is reached where the coal particles are suspended in the liquid and cannot be agglomerated via briquetting (Green & Southard, 2019; Hapgood & Rhodes, 2008; Pietsch, 2004).

d. Attraction forces between solids

Fine solid particles can adhere to each other without the presence of material bridges if they are very close to each other (Green & Southard, 2019; Pietsch, 2004). The three most important forces involved in solid-solid particle binding are molecular, electrostatic and magnetic forces (Pietsch, 2004). Van der Waals forces are molecularly based attractive forces that exist between all solids due to the electric polarization induced by the presence of other particles and has a maximum range of 3 nm (Hapgood & Rhodes, 2008; Pietsch, 2004). Coulomb force is an attractive/ repulsive electrostatic force that occurs due to the electrostatic charging of particles when they collide with each other or rub against external surfaces and has a maximum range of 1×10^{-6} nm (Encyclopedia Britannica, 2016; Hapgood & Rhodes, 2008; Pietsch, 2004). Magnetic forces are similar to electrostatic forces, but limited to ferromagnetic particles (Pietsch, 2004).

The non-valence associations of certain molecular groups are specifically important with respect to coal (Pietsch, 2004). Hydrogen bridges, which naturally binds organic macromolecules in coal, form when a hydrogen atom is bonded to a strongly electronegative atom, *e.g.* oxygen of a COOH group (Pietsch, 2004). The addition of water intensifies this association and can also lead to the formation of non-valence association bridges from the bipolar molecules, thereby increasing the strength of the briquette (Pietsch, 2004).

e. Interlocking bonds

Interlocking bonds usually occur when particles with an elongated shape, *e.g.* fibres, threads or lamellae, wrap around each other during agglomeration, consequently strengthening the briquette (Pietsch, 2004). If a combination of rigid and plastic particles are briquetted at high pressure, the plastic material may fill the interstitial space by wrapping around the rigid material to produce a strong structural bond (Pietsch, 2004).

f. Interaction of binding mechanisms

The interparticle forces that bind the particles in a briquette all occur simultaneously and the relative magnitude of each force is determined by the particle properties, interaction of the forces, and surrounding atmosphere (Hapgood & Rhodes, 2008; Pietsch, 2004). With the exception of capillary (*i.e.*, matrix) bonded briquettes, each particle will experience different bonding forces at different surface points due to the heterogeneity of coal, as well as the large number of particles in a briquette (Pietsch, 2004). An example of bonding forces interacting is an increase in adsorbed moisture layers increasing van der Waals forces, but decreasing the potential for particles to interlock due to its surface smoothing effect (Hapgood & Rhodes, 2008). Too much moisture can however form a barrier that prevents the van der Waals bond from forming (Gregory *et al.*, 1959).

An example of the effect of the surrounding atmosphere on the binding forces is an increase in humidity which decreases electrostatic forces, but a further increase may lead to the formation of liquid bridges (Coelho & Harnby, 1978; Hapgood & Rhodes, 2008; Karra & Fuerstenau, 1977).

2.3.2.4 Binders

Binders can increase the costs associated with agglomeration processes and many studies on binderless agglomeration have consequently been done (Couch, 2002; Ellison & Stanmore, 1981a; England, 2000; Gregory, 1960; Jones, 1963; Komarek, 1991; Mangena, 2001; Mangena & du Cann, 2007; Miller *et al.*, 1979; Motaung *et al.*, 2007; Olugbade & Ojo, 2021; Piersol, 1933). These studies were mostly on lignite coal. Binderless agglomeration relies mostly on capillary tension, van der Waals forces and particle interlocking, but the addition of a binder creates bonding due to bridging bonds (*i.e.* liquid and solid bridges) as well (Olugbade & Ojo, 2021; Zhang *et al.*, 2018). The influence of liquid binders on briquette strength mainly depends on the balance between interparticle friction, surface tension and capillary pressure, and adhesion and cohesion forces (Iveson & Litster, 1998).

a. Binder types by method

Binders can be grouped into five categories based on their binding method: inactive film, chemical film, inactive matrix, chemical matrix and chemical reaction (Holley, 1983; Komarek, 1967). Inactive film binders can be liquids that pull the particles together through surface tension or a solid that is mixed with the coal before a solvent is added (Holley, 1983; Lu, 1989; Young, 2015). The binder forms a solid bridge when the solvent dries. Film binders usually require thermal drying or high temperature sintering as a post-treatment (Engelleitner, 2001). Examples of this type of binder includes water, alcohol, oils, some starches, molasses, glucose, bentonite, lignosulphonate and alginates (Engelleitner, 2001; Young, 2015). Specialty inactive film binders are Brewex, Peridur, Fuller's earth, Alcotac, Avicel and Omnicel (Engelleitner, 2001).

Chemical film binders coat the coal particles and then cause a brief chemical reaction to occur which forms hardening binder solid bridges to bind the particles (Holley, 1983; Lu, 1989; Young, 2015). The agglomerates that are formed with these binders are usually water resistant and some examples are sodium silicate combined with either CO_2, dilute acid, lime or hydrated lime and molasses (Engelleitner, 2001; Young, 2015).

Inactive matrix binders embed the coal particles in a matrix of binding material (Holley, 1983; Lu, 1989; Young, 2015). These binders may need to be heated to coat the coal particles after which the binder sets and keeps the particles together. Examples include petroleum asphalt, carnauba wax, paraffin, coal tar pitch, bitumen, resins and Gilsonite (Engelleitner, 2001; Young, 2015).

Chemical matrix binders agglomerate coal particles due to a chemical reaction that takes place between two or more hardening liquid binder components which creates a matrix of solid bridges between the particles. Quick lime and water, molasses and slaked lime, and Portland cement and water are examples of this type of binder (Engelleitner, 2001; Young, 2015). Krystal Bond, LFI/SIVIA and Terravest are examples of specialty chemical matrix binders (Engelleitner, 2001).

Chemical reaction binders are used to form agglomerates by forming a strong bond between the coal particles and binder itself (Holley, 1983; Lu, 1989; Young, 2015). An example of this type of binder is water and a reagent, *e.g.* dilute sulphuric or phosphoric acid, may need to be added to increase the strength of the agglomerate.

Lubricants are an important additive in compaction agglomeration methods, such as briquetting and extruder pelletising (Engelleitner, 2001; Komarek, 1967; Pietsch, 2004). It can be mixed with the coal fines (internal) or applied to the compartments or dies in the agglomeration equipment (external). A lubricant improves briquette strength by reducing the coefficient of friction between particles, which leads to lower porosity and additional adhesion sites (Pietsch, 2004). A solid inactive film binder acts as a lubricant and a glue in the coal-binder mixture (Young, 2015). Examples of lubricants include water, glycerine, silicone, graphite and paraffin wax (Engelleitner, 2001; Kaliyan & Morey, 2009; Komarek, 1967).

b. Binder types by composition

Binders can also be sorted into three categories based on their material composition: organic, inorganic and compound (Mangena, 2001; Messman, 1977; Young, 2015; Zhang *et al.*, 2018). Organic binders include biomass, tar pitch, petroleum bitumen, lignosulphonate and polymers (Mills, 1908; Waters, 1969; Zhang *et al.*, 2018). Tar pitch, petroleum bitumen and lignosulphonate can be used to create strong agglomerates, but they are being phased out due to their hazardous properties (England, 2000; Leokaoke *et al.*, 2018; Mills, 1908; Strydom *et al.*, 2018; Zhang *et al.*, 2018). Biomass binders are inexpensive, easily accessible and they form strong agglomerates, however the agglomerates that are formed are not water resistant and they have a low ignition temperature (Zhang *et al.*, 2018). Polymer binders, *e.g.* starch and polyvinyl alcohol (PVA), create mechanically strong agglomerates, but they are expensive and do not increase the water resistance of agglomerates (Botha, 2019; Swanepoel, 2017; Venter & Naude, 2015; Zhang *et al.*, 2018).

Inorganic binders include clay, bentonite, kaolin, cement, water glass, lime and calcium carbide mud (Mangena, 2001; Zhang *et al.*, 2018). The advantages associated with this type of binder are the thermal stability, strong agglomeration affect and the desulphurisation properties of some

of them (Mills, 1908; Zhang *et al.*, 2018). The disadvantages are the poor water resistance of the agglomerates that are produced and the high ash yield (Mills, 1908; Zhang *et al.*, 2018).

Compound binders are used to combine the advantages of two or more binders, while eliminating or mitigating the disadvantages (Mangena, 2001; Zhang *et al.*, 2018). Both organic and inorganic binders can be combined to form organic-organic, organic-inorganic or inorganic-inorganic compound binders. Examples of compound binders include: kaolin, bentonite and sodium humate (increased mechanical strength and thermal stability, high ash yield), cements, hydrated lime and PVA (increased mechanical strength and water resistance, high ash yield and low calorific value), and asphalt, cationic emulsifier and water (increased mechanical strength and thermal stability, high cost) (Zhang *et al.*, 2018).

c. Industrial waste binders

An industrially acceptable binder can produce a strong, waterproof agglomerate, is environmentally friendly and economically feasible and does not decrease the quality of the coal or negatively impact the end-use process (England, 2000; Mills, 1908). Another criterion to consider is the quantity of binder that is readily available (Young, 1999). A method of reducing the costs associated with binders is by using wastes or processing by-products as a binder instead of commercially offered binders (Engelleitner, 2001).

The wastes in South Africa can be classified into two groups: general waste and hazardous waste (Department of Environmental Affairs, 2018). General waste does not pose an immediate threat to the environment or the health of the population and includes domestic waste, building and demolition waste, paper, and plastic. In 2017, South Africans generated approximately 54 Mtpa of general waste with only 38.6% of it having been recycled or recovered (Department of Environmental Affairs, 2018). Hazardous waste includes any waste that contains organic or inorganic compounds that may be harmful to the environment or the health of the population. Examples of this waste are waste oils, tarry and bituminous waste, fly ash and dust, mineral waste and sewage sludge. The total amount of hazardous waste generated in South Africa, in 2017, was approximately 67 Mtpa and only 6.3% of it was recycled or treated (Department of Environmental Affairs, 2018).

Some wastes have been investigated as possible binders for use during coal agglomeration, but it is still useful to do more tests to evaluate these wastes in new ways or to discover other useful waste binders. Approximately 2.4 Mt of plastic, specifically low-density polyethylene (LDPE), is available for recycling in South Africa and it is an example of a waste that has recently been tested as a binder for the use in coal agglomeration (GreenCape, 2019; Massaro *et al.*, 2014; Nwabue *et al.*, 2017).

2.3.2.5 Pressure and temperature

The ideal practice of coal agglomeration involves the production of an agglomerate with sufficient mechanical strength by using ambient temperature and a low compaction pressure during production (England, 2000). In coal briquetting either pressure or temperature and pressure is required to create mechanically strong briquettes from coal fines (England, 2000; Habib *et al.*, 2014; Mangena, 2001). The pressure and temperature required to agglomerate coal increases with coal rank (Waters, 1969). Compaction pressure and temperature also affect the solid bridge bonds, and adhesion and cohesion forces that form when a binder is used (Pietsch, 2004).

Briquetting is a high-pressure agglomeration process where plastic deformation, and breakage followed by rearrangement of brittle particles take place (Pietsch, 2004). Compaction pressure can increase the strength of agglomerates, due to the tighter packing of the coal particles (*i.e.* porosity <20%), and enhanced bonding until a limiting condition such as internal arching is encountered or the real density of the coal is reached (England, 2000; Green & Southard, 2019; Gregory, 1960; Pietsch, 2004). Coal agglomeration is usually conducted at a pressure of 50–150 MPa and the mechanical strength and density of the agglomerates mainly increases up to a pressure of 70 MPa, after which the increase is minor (Couch, 2002; Gregory, 1960; Miller *et al.*, 1979). During agglomeration, pressure can cause fibres and particles to interlock and fold about each other, creating interlocking bonds which are resistive to elastic recovery when the pressure is removed (Green & Southard, 2019; Kaliyan & Morey, 2010).

The temperature that is used during coal agglomeration can affect the chemical and physical properties of the coal, such as the improvement of plastic deformation under pressure at a temperature of 150°C (Gunnink & Zhuoxiong, 1994; Kaliyan & Morey, 2009; Mangena, 2001). High temperature briquetting (400–500°C) can drastically increase the plasticity of the coal and be used to remove volatiles, however, spontaneous combustion is also a possibility at these temperatures (England, 2000; Mangena, 2001). If the temperature is higher than two-thirds of the coal melting temperature the atoms/ molecules diffuse at the interparticle contact areas to form a type of solid bond called sinter bonds (Pietsch, 2004). Heat from interparticle friction may also melt the roughness peaks at the contact points, *i.e.* partial melting, which creates liquid bridges that quickly solidify into solid bridges (Pietsch, 2004). Adding heat during the agglomeration process is expensive and hazardous, but it is still preferred to using binders (Jones, 1963).

Post-treatment, *i.e.* curing, entails the treatment (*e.g.*, aging, drying or heating) of green, *i.e.* wet, agglomerates to modify their moisture content, strength or structure (Pietsch, 2004). Curing increases the strength of agglomerates that contain mainly liquid binder by removing the liquid and creating stronger bonds, *i.e.* solid bridges from sintering, partial melting, hardening binder

bridges, or crystalline bridges (Kaliyan & Morey, 2009; Pietsch, 2004). Curing is mainly used in low- and medium pressure agglomeration processes, such as drum agglomeration and pelletising, due to the higher liquid content of the of the feeds (Pietsch, 2004). Temperature also plays a part during the curing phase of the agglomeration process and it is impacted by the use of a binder (Habib *et al.*, 2014). The costs involved in curing agglomerates is high, but become more economical for facilities with capacities higher than 1000 Mtpa (Pietsch, 2004).

2.4 Physical properties of briquettes

There are six physical properties that should be considered while quantifying the quality of coal briquettes: compressive strength, impact resistance, abrasion resistance, water resistance, weathering, and density (Dohm *et al.*, 2012; Richards, 1990). These properties simulate some of the stresses that the briquettes will experience during transportation and end-use processes, as seen in Figure 2-7, such as (a) compressive force, (b) impact force and (c) attrition force.

The ability of a briquette to withstand the compressive forces, impact forces and attrition forces that it may experience can be described by its compressive strength, impact resistance and abrasion resistance, respectively (Dohm *et al.*, 2012). However, there are many different tests that can be used to determine these properties and a standard method is necessary for comparison purposes (Dohm *et al.*, 2012). The thermal degradation and swelling index of the briquettes may also be investigated due to the effect of these properties on end-use processes and equipment (England, 2000; Falcon & Ham, 1988; Mishra *et al.*, 2018).

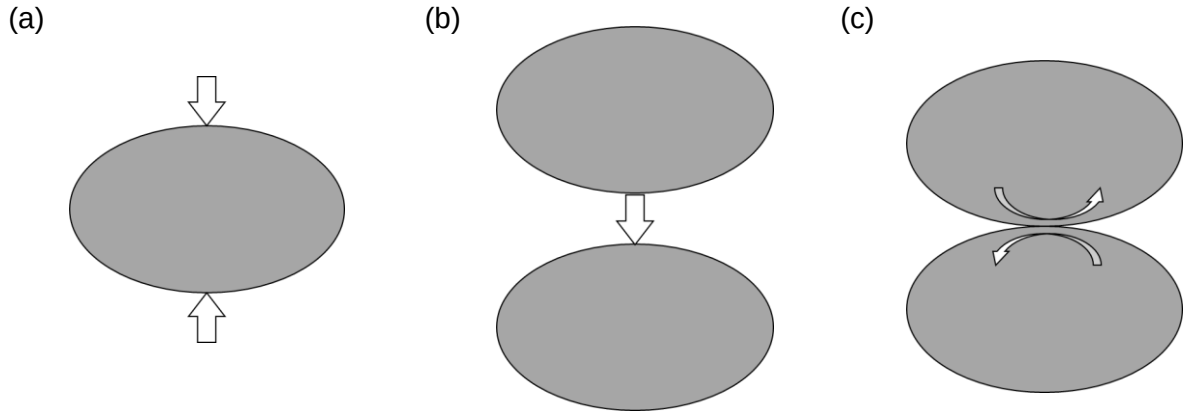

Figure 2-7: Forces briquettes encounter during storage, handling and transportation: (a) compressive force, (b) impact force and (c) attrition force, adapted from Dohm *et al.* (2012)

2.4.1 Compressive strength

Briquettes should be able to withstand the compressive force they may experience while they are stacked on each other during storage, handling and transportation without collapsing, which is why compressive strength (CS) is important even though a standard testing method does not

exist (Mangena, 2001; Rahman *et al.*, 1989). The shape of the briquettes has an impact on the CS; cylindrical-shaped briquettes are approximately 5 times stronger than pillow-shaped briquettes due to the higher density in the upper part of the briquette (Rahman *et al.*, 1989). The position that the cylindrical briquettes are in when the compression test is done also affects the strength of the briquettes*, i.e.* the surface CS is almost 10 times larger than the line or point CS due to dispersion of force over the larger contact area of the flat surface (Rahman *et al.*, 1989). Some deformation of the briquettes may occur before a crack forms, which can influence the results of the compression test (Kaliyan & Morey, 2009; Rahman *et al.*, 1989).

The minimum CS of a viable briquette has been acknowledged as 0.38 MPa, according to Richards (1990), while the CS of in situ ROM coal from South African coalfields has been specified as 5.4–7.4 MPa, by Mark and Barton (1996), and 2.1–17.2 MPa, by Speight (2005). Leokaoke *et al.* (2018) found that the CS of cylindrical shaped Highveld ROM coal was 14 MPa, which is at the higher end of the CS specified by Speight (2005).

The Richards (1990) method of determining the CS of a briquette entails a universal tensile testing machine applying an increasing load at a constant rate with two parallel plates to a single briquette, until it cracks. Equation 2-3 shows the calculation that is used to determine the CS of the briquette.

$$CS = \frac{F}{A} \tag{2-3}$$

In Equation 2-3, F (N) is the fracture load and A (m^2) is the area of the fracture. The average value of six identical tests is used as the CS (MPa). By expressing the CS as a stress, not a force, it is easier to compare to other studies with briquettes consisting of different shapes and sizes (England, 2000; Rahman *et al.*, 1989).

Taulbee *et al.* (2013) used a Lloyd LRX Plus compressive meter to test the CS of briquettes made with coal and biomass. The machine was equipped with a compression disk (d = 19 mm) on an automated test stand and a constant speed of 0.42 mm/s was used to apply force. The average of 20–30 identical tests was accepted as the CS in kilograms of compression (kg_F). The CS was classified as either poor (< 222 kg_F), marginally acceptable (≥ 222 kg_F, < 445 kg_F), good (≥ 445 kg_F, < 667 kg_F), or excellent (≥ 667 kg_F)(Dohm *et al.*, 2012).

Borowski and Hycnar (2013) tested the point CS of briquettes (flat horizontally) with a Zwick 100 materials testing machine that was connected to an automated test stand and used a moving plate speed of 0.2 mm/s. The CS was recorded in MPa.

Mangena (2001) also used an Instron 1195 Universal Strength testing machine to determine the point CS of binderless pillow-shaped briquettes by crushing a briquette between two plates (d_{lower} = 138 mm, d_{upper} = 152 mm) at a constant speed of 0.3 mm/s until a crack forms and the fracture load, *F*, is determined. The CS was then calculated with Equation 2-3 and the average of 10 tests was reported in kPa.

Mitchual *et al.* (2013) used an Instron Universal Strength testing machine to determine the CS of a briquette. The compression plates applied a load at a constant speed of 0.005 mm/s, until the briquette cracked. The fracture load, *F*, was then multiplied by three and divided by the sum of the length of the briquette measured at three points to calculate the CS (N/mm).

The Japanese Standard compression test (JIS Z 8841-1993) involves a briquette (2-20 mm) being placed between two plates where the top plate moves at a speed of 0.15-0.3 mm/s to apply pressure on the briquette until it cracks (England, 2000).

The CS of a briquette can therefore be determined by pressing it between two plates at a constant speed (< 0.5 mm/s) and converting the fracture load (N) and area (m^2) to CS (Pa).

2.4.2 Impact resistance

The impact resistance of a briquette is its ability to withstand a large force over a short period of time, such as falling to the ground or hitting a wall, which could happen during handling, transportation or loading (Dohm *et al.*, 2012).

The standard drop shatter test (ASTM D440-86) is used to determine the IRI of coal, but it is tailored for a large sample, *viz.* 50 kg (Dohm *et al.*, 2012). Richards (1990) adapted the standard drop shatter test to determine the impact resistance index (IRI_A) of a briquette. The test consists of dropping a single briquette from a height of 2 m onto a concrete floor and recording the number of pieces it breaks into. If the briquette does not shatter at first impact it is dropped again until it breaks, and the number of drops is also recorded. The results of three to six tests are averaged and substituted into Equation 2-4.

$$\mathrm{IRI_A} = \frac{N_{\mathrm{drops}}}{N_{\mathrm{pieces}}} \times 100 \qquad (2\text{-}4)$$

In Equation 2-4, N_{drops} is the average number of drops before the briquette shattered and N_{pieces} is the average number of pieces the briquette broke into (Adeleke *et al.*, 2019; Richards, 1990). The minimum IRI_A for a briquette is 50 (Richards, 1990). Chaiklangmuang *et al.* (2008), Li and Lui (2000), and Tembe *et al.* (2014) used a similar method. A limitation of this method is the fact that the fine particles are not considered when counting N_{pieces} (Li & Liu, 2000).

Holley and Antonetti (1977) developed a drop shatter test for briquettes that are approximately 1 cm^3 in size. During the test 10 briquettes were dropped simultaneously from a predetermined height after which the briquettes that did not shatter were dropped again. This was repeated a maximum of 10 times or until all the briquettes shattered. Equation 2-5 was then be used to calculate the IRI_B of the briquettes.

$$\mathrm{IRI_B} = \frac{N_{\mathrm{drops}}}{10} \tag{2-5}$$

In Equation 2-5, N_{drops} is the total number of drops for the 10 briquettes. The height of the drop was not specified, which means that this test is not suitable for comparison.

The Japanese drop shatter test (JIS Z 8841-1993) involves dropping a 400 cm^3 sample of briquettes, which is weighed, from a height of 2 m onto a steel plate in a drum five times (England, 2000). The sample is then sieved using a sieve approximately one-fifth the size of the briquette and the oversize is weighed (England, 2000). The shatter index (SI) of the briquettes can be determined using Equation 2-6.

$$\mathrm{SI} = \frac{m_{\mathrm{f}}}{m_0} \times 100 \tag{2-6}$$

In Equation 2-6, m_0 (g) is the weight of the sample and m_f (g) is the mass of the oversize (England, 2000). The method is like that of Richards (1990), but more accurate due to all the fines being taken into account when the briquette shatters.

Lindley and Vossoughi (1989) determined the SI for briquettes by dropping a briquette from a height of 1 m onto a concrete surface. The briquette was dropped a total of 10 times and the SI could be calculated with Equation 2-6. Conkle and Ragavan (1992) used a similar method.

The Richards (1990) drop shatter test can also be used to analyse the friability index (FR) of the briquettes with a method like that of the SI test. The FR, which is a measure of durability, can be calculated using Equation 2-7. In the equation m_0 is the weight of the briquette (g) and m_f *is* the weight of the largest piece after shattering (g). The minimum requirement for a viable briquette is an FR value of 80% (Kaliyan & Morey, 2009).

$$\mathrm{FR} = \frac{m_{\mathrm{f}}}{m_0} \times 100 \tag{2-7}$$

There are clearly various methods for testing the IRI of a briquette, but they all entail dropping a briquette(s) from a height and quantifying the breakage that occurs. The choice of methods therefore depends on sample size and available equipment.

2.4.3 Abrasion resistance

The transportation and handling of briquettes can cause them to rub against container walls and each other (Dohm *et al.*, 2012). The abrasion resistance (AR), or durability, of briquettes should therefore be quantified. The equation used to calculate the AR, Equation 2-8, is similar to that of the SI and FR, but the method is different. The shape of a briquette affects its AR, *i.e.* briquettes with a rounded shape will have a higher AR than briquettes with sharp edges (Richards, 1990). This is due to the sharp edges being abraded, while the central part remains intact.

Richards (1990) adapted the Micum Test for coke to a small-scale tumbler test that utilises a drum (l = 270 mm, d_i = 200 mm) that is fitted with a single lifter (w = 38 mm) on the entire length of the drum. A sample of approximately 20 ovoid-shaped briquettes (~1 200 g) was rotated in the sealed drum at 50 rpm for 100 revolutions, after which the sample was sieved on a 3 mm sieve and the AR was calculated as the oversize percentage as shown in Equation 2-8.

$$\mathrm{AR} = \frac{m_\mathrm{f}}{m_0} \times 100 \tag{2-8}$$

In Equation 2-8, m_0 (g) is the weight of the initial briquette sample and m_f (g) is the weight of the oversize sample after tumbling. The oversize value is regarded as the AR with a minimum value of 95% (Richards, 1990).

Botha (2019) used a modified version of the Richards tumbler test to determine the AR of briquettes. A stainless-steel cylindrical drum (d_i = 70 mm, l = 51 mm) with a lifter spanning the whole length of the drum was filled with a sample of four briquettes with a combined weight of ~20 g. The drum was rotated on roller-shafts connected to a Bongfioli variable speed drive at a speed of 80 rpm for 197 revolutions and then sieved on a 3 mm sieve to calculate the oversize as a percentage with Equation 2-8.

Kaliyan and Morey (2009) used the ASAE Standard (S 269.4) method to calculate the AR of the briquettes. A sample of ~500 g briquettes was rotated in a rectangular, stainless steel drum (l = 300 mm, w = 125 mm, h = 300 mm) with a baffle (l = 230 mm) extending 50 mm into the drum. The drum was rotated at 50 rpm for 10 min, after which the sample was sieved on a sieve with an aperture size of about 0.8 times the briquette diameter. The AR was then calculated with Equation 2-8.

Taulbee *et al.* (2013) determined the AR with a Plexiglas cylinder (l = 305 mm, d_i = 305 mm) equipped with three equally spaced lifters (w = 51 mm). A sample of 20-25 briquettes (~200 g) was tumbled at 40 rpm for 5 min. The sample was then sieved on a 4.76 mm sieve and the AR was calculated with the oversize as a fraction of the initial sample, but it can be converted to a

percentage value by multiplying the values by 100. The AR can be classified as poor (< 80%), marginally acceptable (≥ 80%, < 90%), good (≥ 90%, < 95%), and excellent (≥ 95%) (Dohm *et al.*, 2012; Taulbee *et al.*, 2010; Taulbee *et al.*, 2013).

Mangena (2001) adapted the Roga Test for coke to test the AR of briquettes. A drum (l = 70 mm, d_i = 200 mm, d = 202 mm) made of sheet iron with two baffles (w = 30 mm) was filled with a ~350 g sample of briquettes and tumbled at 50 rpm for 5 min. The sample was sieved on a sieve with 2 mm sized apertures and the AR was calculated with Equation 2-8.

The Japanese standard for the tumbler test (JIS Z 8841-1993) utilises a drum (l = 175 mm, d_i = 350 mm) with two baffles opposite each other on the inside (England, 2000). An agglomeration sample of 400 cm^3, that is weighed, is rotated 200 times and then sieved on a sieve that is one fifth the size of the briquettes. The oversize percentage, calculated with Equation 2-8, is the AR.

As observed for the IRI tests, the methods for AR testing are numerous and depends on sample size and available equipment.

2.4.4 Water resistance

Briquettes should be water resistant to avoid disintegration or loss of material when they come into contact with water (Dohm *et al.*, 2012). A weathering test is not always possible or reliable, but the water resistance test can give an indication of the briquettes' behaviour when exposed to wet conditions (England, 2000; Kaliyan & Morey, 2009).

Richards (1990) developed an immersion-in-water test to test the water resistance of a briquette, *viz*. a single briquette is immersed in water for a period of 30 min and light pressure is applied at 10 min intervals to check for disintegration. The water resistance index (WRI) can then be calculated using Equation 2-9.

$$\mathrm{WRI} = 100 - \%m_{\mathrm{w}} \tag{2-9}$$

In Equation 2-9, $\%m_w$ is the mass of water that was absorbed as a percentage of the overall mass of the briquette. The minimum WRI is 95% (Richards, 1990). The briquette can be wiped dry and tested afterwards to determine the wet compressive strength (CS_{wet}).

Lindley and Vossoughi (1989) measured the WRI of an briquette that was immersed for 0.5 min at 27°C as the percentage water that was absorbed, as shown in Equation 2-9. Borowski and Hycnar (2013) immersed the briquettes in water and defined the water resistance

as the percentage mass lost during the test, with briquettes that remained intact after 30-60 min being classified as water resistant.

Taulbee *et al.* (2013) determined the water resistance of briquettes by weighing 10 of them and then immersing them in water for 60 min, after which they were visually assessed and classified as intact, mostly intact, mostly degraded or degraded. The briquettes that were intact were left to dry for 30 min and then tested to establish the CS_{wet}. Mangena (2001) immersed 10 briquettes in water for 120 min and immediately tested the CS_{wet} as an indication of water resistance. Beker (1997) and Chaiklangmuang *et al.* (2008) immersed a briquette in cold tap water and measured the time until the onset of dispersion as the water resistance.

The method for water resistance should therefore be quantifiable and provide some indication of a briquette's ability to withstand contact with moisture.

2.4.5 Thermal degradation

Thermal degradation occurs when a coal briquette, or even sometimes ROM coal, disintegrates into small pieces due to the extreme heat that it suddenly experiences in some end-use processes (England, 2000). Coal degradation can be described by fragmentation, *i.e.* a single particle breaking up into two or more similarly sized particles, or attrition, *i.e.* a single particle retaining its shape and only losing very fine particles (Chirone *et al.*, 1982; Stubington & Linjewile, 1989). Coal fragmentation is caused by devolatilization (primary fragmentation), thermal stresses and/or combustion of the connective bridges between coal particles (secondary fragmentation), while coal attrition is due to the coal particles rubbing against bed inert solids and the internal surface of the combustor (Chirone *et al.*, 1982).

The effect of coal properties on fragmentation have been analysed in previous studies (Dacombe *et al.*, 1999; Gajewski & Kosowska, 2005; Senneca *et al.*, 2011; van Dyk, 2001; Zhang *et al.*, 2002). Primary fragmentation is the main cause of fragmentation in coal particles and increases with an increase in coal rank, *i.e.* carbon content (Dacombe *et al.*, 1999; Gajewski & Kosowska, 2005; Zhang *et al.*, 2002). Volatiles can create pressure in the particle during devolatilization and weaken the char structure during release and therefore primary fragmentation increases with an increase in volatile matter (Dacombe *et al.*, 1999; Gajewski & Kosowska, 2005; Senneca *et al.*, 2011; Zhang *et al.*, 2002). Primary fragmentation also increases with an increase in original particle size due to the higher number of volatiles and lower specific surfaces that cause larger inner pressure during devolatilization (Coetzee, 2011; Dacombe *et al.*, 1999; Zhang *et al.*, 2002). Briquettes made with a binder experience substantially more thermal degradation compared to binderless briquettes (Clark cited by England, 2000). This may be due to the binder creating a more rigid structure, thereby causing

higher thermal stresses inside the briquette when the volatile matter is removed. The extent of fragmentation decreases with an increase in particle CS (Dacombe *et al.*, 1999).

Van Dyk (2001) developed a laboratory testing method to determine the primary fragmentation of coal. A composite sample was sieved, and the Ergun index was calculated with Equation 2-10, where x and $y > 0$. The amount of sample between screen$_x$ and screen$_{x+1}$ is fraction$_x$.

$$\text{Ergun Index} = \left[\left(1 \Big/ \sum_{\text{Fraction } x}^{\text{Fraction } y} \%\ \text{of fraction}_x\right) \Big/ \frac{\text{screen size}_x + \text{screen size}_{x+1}}{2}\right] \times 100 \qquad (2\text{-}10)$$

The sample (PSD: 6.7–19 mm) was placed on a steel basin and covered with a lid. A muffle oven was pre-heated to 100°C and flushed with nitrogen to ensure that no secondary fragmentation takes place. The sample was then heated at a high heating rate of 12°C/min to 700°C, where the sample was kept for 60 min. The sample was cooled to room temperature and sieved again. The Ergun index after the test was used to calculate the percentage thermal fragmentation with Equation 2-11.

$$\%\ \text{Thermal fragmentation} = \frac{\text{Ergun index before test} - \text{Ergun index after test}}{\text{Ergun index before test}} \times 100 \qquad (2\text{-}11)$$

Leokaoke *et al.* (2019) used a similar method to test the thermal fragmentation of briquettes with an Elite Thermal Systems Ltd tube furnace. The briquettes were weighed and inserted into a pre-heated oven, at 100°C, in an inert environment created by nitrogen gas flowing into the furnace at 5 NL/min. A lower heating rate of 5°C/min was used to increase the temperature to 700°C where it was kept for 60 min. The remaining sample was weighed to determine the thermal fragmentation. The briquettes did not fragment, and a qualitative analysis of the briquettes were made. This could be due to the lower heating rate that was used creating an insufficient thermal shock effect.

Dakič *et al.* (1989) proposed a correlation between the pore resistance number (PRN) and free swelling index (FSI) of coal with various sizes (2–15 mm), shown in Equation 2-12, as a more precise way of categorising low rank coals that do not exhibit measurable swelling during the FSI standard test, *i.e.* have a score below one.

$$\text{FSI} = 10^{-2}\text{PRN}^{1.9} \qquad (2\text{-}12)$$

The PRN is calculated from the volatile matter content divided by the inherent moisture in the coal and is therefore dependent on coal type. A higher PNR indicates more resistance for volatiles to escape from the coal which leads to fragmentation.

2.5 Reactivity of coal

The thermal reactivity of coal is a complex process that is affected by numerous variables and therefore difficult to predict. However, it is still important to strive to understand and analyse the thermal behaviour in coal for use in industrial processes, *viz*. combustion, carbonization, liquefaction, and gasification (Speight, 2012).

Combustion is essentially the complete oxidation of coal in air/ oxygen to produce thermal energy, while gasification can be considered as an incomplete combustion of coal due to insufficient oxygen, converting the energy in the coal into chemical energy contained in the resulting crude gas instead of thermal energy (Bell *et al.*, 2011; Fernando, 2008; Speight, 2012). The steps in both processes therefore entails:

- Step 1: Drying.
- Step 2: Pyrolysis, *i.e*. de-volatilisation.
- Step 3: Volatile combustion.
- Step 4: Char reactions.

The reactions that occur during the combustion and gasification steps occur simultaneously and consecutively and may sometimes approach a condition of equilibrium (Bell *et al.*, 2011).

Pyrolysis is the thermal decomposition of coal in an inert environment at temperatures above 300°C and produces char (*i.e*., coke), tar, (*i.e.,* high-molecular-weight liquids), liquor (*i.e*., low-molecular-weight liquids), and gas (*i.e*., CO, CO_2, H_2O, and low-molecular-weight hydrocarbons such as C_1–C_5 up to C_{10}) (Bell *et al.*, 2011; Dong *et al.*, 2019; Speight, 2012). The pyrolysis temperature has a large effect on the product formation and can be classified as low (400–750°C), medium (750–900°C), high (900–1100°), or plasma (> 1650°C), Table 2-7 (Ladner, 1988; Speight, 2012; Xu & Tomita, 1987). As the temperature increases, the gas yield increases and the char yield decreases (Ladner, 1988; Speight, 2012; Uwaoma *et al.*, 2019). The gas composition also changes based on the temperature range (Hu *et al.*, 2004; Ladner, 1988; Meyer, 2020; Speight, 2012; Xu & Tomita, 1987).

In the temperature region below 350°C mainly moisture is evaporated, but some hydrocarbons (*e.g*., benzene, toluene, HCl) are also removed from the coal matrix (Ladner, 1988). In the low-temperature region (400–750°C) the gas yield increases with hydrocarbons, especially CH_4, accounting for most of the gas, the tar/ liquor yield decreases, and the char yield slightly increases due to the formation of some carbonaceous products (Ladner, 1988). In the high-temperature region (900–1100°C) the char (~75%) and gas (~17%) yield accounts for more than 90% of the product yield with the gas consisting of mostly H_2 and hydrocarbons (Hu *et al.*, 2004;

Ladner, 1988; Pretorius *et al.*, 2017; Xu & Tomita, 1987). The H_2 evolves from the dehydrogenation reaction of the aromatic cluster at higher temperatures and some CO evolves from the decomposition of phenolic hydroxyl groups (Hu *et al.*, 2004; Xu & Tomita, 1987). In the plasma-temperature region (> 1650°C) a negligible amount of tar is formed and the gas is rich in acetylene (Ladner, 1988).

Table 2-7: Pyrolysis reactions and products at low, medium, high and plasma temperature ranges adapted from Speight (2012)

Region	Temperature (°C)	Reactions	Products
–	< 350	Mainly evaporation	Water and volatiles
Low	400–750	Primary degradation	Gas, tar and liquor
Medium	750–900	Secondary reactions	Gas, tar, liquor and additional hydrogen
High	900–1100		
Plasma	> 1650		Acetylene; carbon black

Other coal properties that affect pyrolysis behaviour are coal rank, density, heating rate, and gas environment (Smoot & Smith, 1985; Speight, 2012; Wu, 2005).

2.6 Industrial applications of coal

This section provides a brief overview of potential end-use industries for the briquettes based on the effect of the coal characteristics on the processes. Co-firing specifications are discussed where relevant literature is available, otherwise raw coal properties are used. The coal briquettes will primarily be used in local coal markets due to the low quality of the raw fine coal discards compared to export qualities; therefore only end-use processes that are based in South Africa will be considered in this section.

The industries that consumed the most coal in South Africa, in 2015, were electricity generation, 53%, basic iron and steel manufacturing, 20%, and synthetic fuel and chemical industries, 10%, with the rest being used in various other smaller industries, 17% (CMSA, 2018). Other industries that use coal on smaller scale are cement manufacturers, pulp and paper manufacturers and sugar mills (FFF, 2011). However only electricity generation, steel manufacturing, and liquid fuels and chemicals production will be considered due to the possible hazardous nature of the binders that are added to the coal briquettes.

Figure 2-8 depicts the different types of coal based on their rank and the end-use industries of each type (Speight, 2008). The lower ranked coals (lignite and subbituminous) and low-quality bituminous coals are primarily used for electricity generation and to a lesser extent cement production. Coal used in steel manufacturing is coking (*i.e.* better) quality coal and some binders

may increase the calorific value of the coal briquettes to make them useable in this industry. Therefore, to determine the suitability of certain binders for use in these industries, a summary of the processes and the effects of coal quality on them will be given in the following sections.

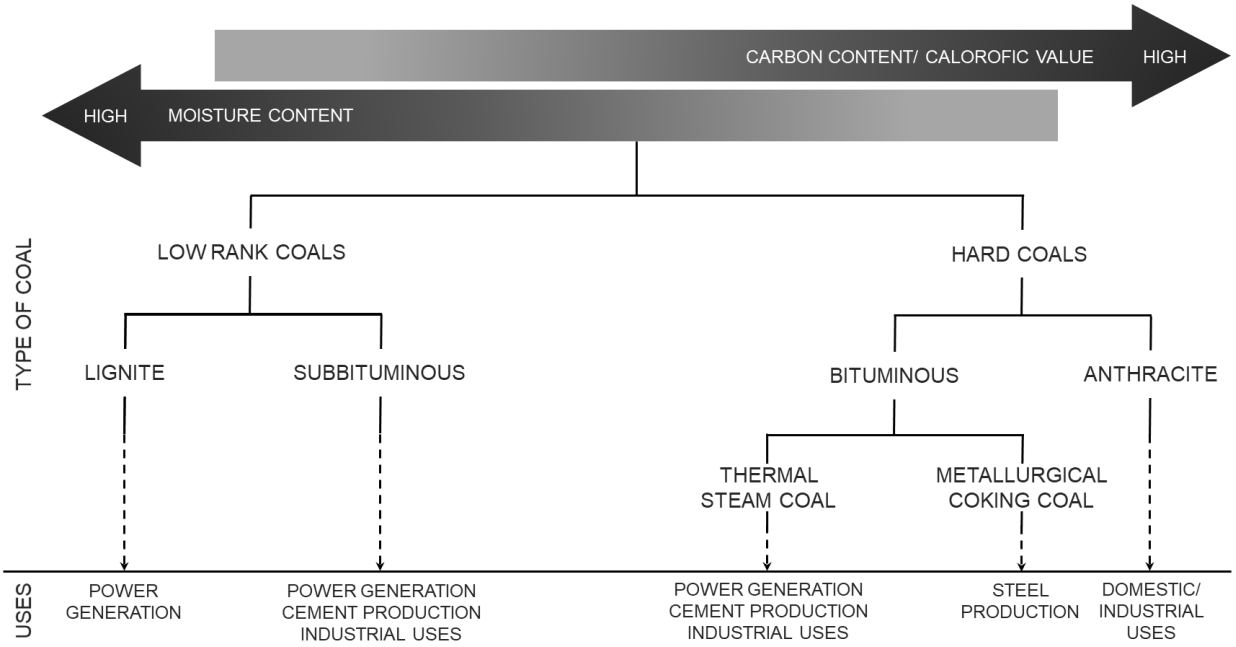

Figure 2-8: The different types of coal and their respective uses retrieved from Speight (2008)

2.6.1 Electricity generation

A simplified coal-fired electricity generation process is depicted in Figure 2-9 (Department of Energy, 2018; FFF, 2011; Speight, 2008). Coal is fed to boiler where the particles react with air and combust due to the high temperature, releasing more heat that is used to convert water into steam. The steam propels the turbine which powers the generator, where electricity is generated. The water is in a closed circuit and another open circuit of cooling water is used to condense the steam so it can be reheated. The ash that is formed during the combustion process falls to the bottom of the boiler where it is removed to an ash dam. The gaseous emissions, *e.g.* CO_2, SO_2 and NO_X, and particulate matter emissions are called flue gas and removed through a chimney, *i.e.* a flue. Some of the components in the flue gas can be reduced with emission control technologies.

There are three types of technology that is used in coal-fired power stations: pulverised coal combustion (PCC), fluidised bed combustion (FBC), and integrated gasification combined cycle (IGCC) (Fernando, 2004). As of 2011, all of Eskom's (the primary electricity provider in South Africa), coal-fired plants are PCC plants (Department of Energy, 2018; FFF, 2011). FBC may play a larger role in the future of coal-fired plants in South Africa and will also be considered (Hotta, 2009; Mamaila, 2020; Schreuder, 2017). The ACTOM (Pty.) Ltd. John Thompson

industrial boilers have been used to successfully co-fire coal and bagasse due to the versatility of stokers with regards to fuel feed (Fernando, 2007; Whyle, 2016). Chain grate stokers may be able to handle a feed with 40% ash yield, but they have a lower efficiency and throughput compared to other combustion technologies (Ban, 1981; Fernando, 2007).

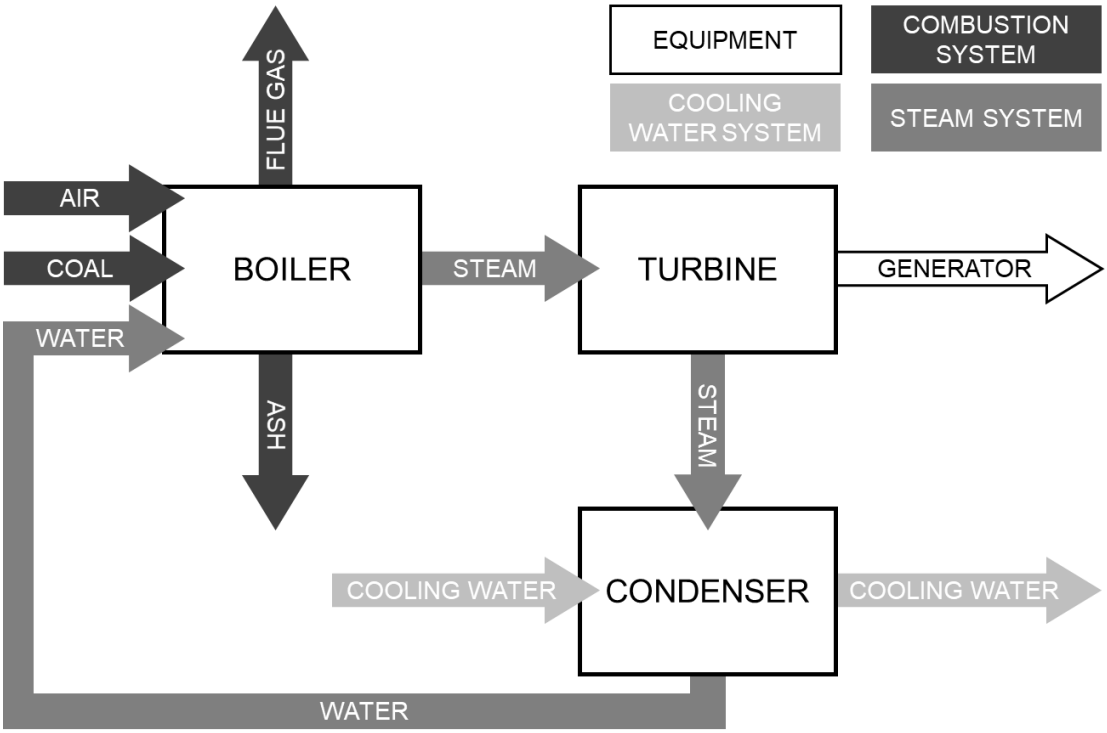

Figure 2-9: Simplified diagram of a coal-fired electricity generation process adapted from Speight (2008)

2.6.1.1 Pulverised coal combustion

In a PCC plant, the feed coal is pulverised to a particle size of 5-400 µm before being blown into the boiler by air through the furnace burners that are usually positioned in the walls of the boiler (FFF, 2011). The combustion process, described in Section 2.5, takes place at a temperature of 1300-1700°C, depending on the coal rank (FFF, 2011; Wu, 2005)

Co-firing is the substitution of some of the coal feed by a biomass or gas feed and there are four methods for directly co-firing waste fuels in a PCC boiler (Fernando, 2001; FFF, 2011). The first method is feeding and burning the waste together; this has the lowest cost implications, but the highest risk of malfunction. The second method is by only burning the coal and waste together; the cost of installing a new transport line should be considered and it may also cause congestion and a lower burner performance. The third method entails burning the waste in dedicated burners; the risk is minimised by this method, but it is an expensive option. The fourth option is to use the waste as a re-burn fuel, but this method is still in development (Fernando, 2001).

Table 2-8: Summary of some coal properties and their desired values and effects on pulverised coal combustion adapted from de Korte and Jeffrey (2016), Skorupska (1993), and Wu (2005)

Property	Unit	Value			Comments
		Minimum	Desired	Maximum	
Moisture content[a,b]	wt%	-	4–8	12*	-
Volatile matter content[a,b]	wt%	20–23*	20–35	-	Side-fired furnace
		-	15–20	20	Down-fired furnace
Ash yield[a,b]	wt%	-	low	20–30*	-
Sulphur[a,b]	wt%	-	low	0.5–2.0	Depends on local regulations
Vitrinite[b]	wt%	-	-	55–80	-
Inertinite[b]	wt%	-	-	10–25	-
Calorific value[a,b]	MJ/kg	23*–25	high	-	-
Particle size (to pulveriser)[a]	mm	3.0	30–40	50	Maximum 30% <3 mm
Particle size (to boiler)[c]	mm	-	0.005–0.400	-	Maximum 70–75% <0.075 mm and 2% >0.3 mm for bituminous coal

Source: [a] De Korte & Jeffrey (2016), [b] Skorupska (1993) and [c] Wu (2005)

* Outer limits

Moisture content: ar, volatile matter content: db, ash yield: db, calorific value: ar

The quality of the coal that is fed to the boiler has a significant effect on the ignition, capacity, heat rate, availability and maintenance requirements of the plant (Carpenter, 2006). The properties of the coal fines and binders that are used for agglomeration that are important include, but are not limited to the moisture content, volatile matter content, ash yield and calorific value, shown in Table 2-8. The effect of coal and waste properties on PCC plants have been studied in detail by Fernando (2007), Skorupska (1993) and Wu (2003), therefore only a brief overview will be given in this section.

The moisture content of the boiler feed should be low due to the negative effect it has on the handling and thermal efficiency of the process (Carpenter, 2010). A high moisture content (> 8%) can also increase the flue gas volume and necessitate excess air flow which will negatively influence the fans, air preheater and emission control equipment. (Carpenter, 2010; Fernando, 2007).

The volatile matter content can negatively impact the storage of the coal due to the danger of spontaneous combustion or the loss of calorific value, the required size for pulverisation, burner settings, combustion behaviour and carbon content of the fly ash (Carpenter, 2010).

2.6.1.2 Fluidised bed combustion

The FBC systems have been investigated by Wu (2003) and only a brief overview of the process will be given in this section. In a FBC plant the coal is fed to the boiler where it is burnt in a bed of heated particles suspended in flowing air (Fernando, 2007; Wu, 2003). The air flowing into the boiler keeps the particles suspended which promotes mixing and a uniform temperature throughout the combustion zone. The ash that forms eventually constitutes the bulk of the suspended particles and the surplus is periodically removed to maintain the correct bed depth.

There are two different forms of FBC based on the fluidising gas velocity, namely bubbling fluidised bed combustion (BFBC) and circulating fluidised bed combustion (CFBC). CFBC is currently the most promising alternative to PCC (Aziz & Dittus, 2011; Barišić *et al.*, 2009; Belaid, 2017; Fernando, 2007). The advantages of CFBC are the lower operating temperature of 800–900°C, an increased rate of heat transfer, greater fuel flexibility, reduced NO_X formation and easier capturing of SO_2 with sorbents (Belaid, 2017; Wu, 2003). The disadvantages include the relatively small scale in current commercial use, large amounts of solid residues, higher carbon-in-ash levels and increased N_2O formation (Moodley, 2007; Skinner & Brown, 2011; Wu, 2003).

Table 2-9: Summary of some coal properties and their desired values and effects on fluidised bed combustion adapted from Aziz and Dittus (2011), Belaid (2017), Fernando (2004), Henderson (2003), Hotta (2009), Jin *et al.* (2003), and Wu (2006)

Property	**Unit**	**Value**			**Comments**
		Minimum	Desired	Maximum	
Moisture content[a–e]	wt%	-	~12	23–55, 65*	-
Volatile matter content[b,e]	wt%	-	10–55	-	-
Ash yield[a–e]	wt%	-	10–17	25–65	-
Sulphur[a,b,d]	wt%	-	0.1–1.0	1.5	-
Calorific value[b–e]	MJ/kg	5–6	20–25	-	-
Particle size (feed)[b,f,g]	mm	0	3–6	25	Anthracite: 0–6 mm Semi-anthracite: 0–8 mm Bituminous: 0–10 mm Lignite: 0–13 mm Less than 10% <0.1 mm, 50-60% <0.1–1.0 mm, and 30-40% >1.0 mm

Source: [a]Hotta (2009) , [b]Henderson (2003), [c]Fernando (2004), [d]Aziz and Dittus (2011), [e]Belaid (2017), [f]Wu (2006), and [g]Jin *et al.* (2003)

* Outer limits

Moisture content: ar, volatile matter content: dafb, ash yield: db, calorific value: ar

The advantage of most interest in briquette use is the greater fuel flexibility that is observed in CFBC plants. The types of material that has been used in the past either alone or via co-firing include coals of different ranks (from lignite to anthracite), solid waste fuels (*e.g.*, peat, municipal refuse, industrial waste, coal waste, sewage sludge), and biomass (Aziz & Dittus, 2011; Fernando, 2004; Koornneef *et al.*, 2007; Wu, 2003; Zhu, 2013). The amount of co-firing material is usually added to the coal feed in the range of 5–30 wt% (Barišić *et al.*, 2009; Hotta, 2009).

The properties of the fuel that is fed to the boiler has an impact on its operations and therefore some co-firing fuels are preferable (Koornneef *et al.*, 2007; Zhu, 2013). A summary of the possible ranges for the fuel characteristics is given in Table 2-9. The four main fuel qualities that may affect the operations of the boiler are the preparation requirements, ash yield, CV, and chlorine content (Koornneef *et al.*, 2007). A summary of the various co-firing materials that have been used in the past and their challenges vs. CV has been evaluated by Koornneef *et al.* (2007). Biomass has been successful as a co-firing material, however its higher moisture content will require a pre-treatment with mills that have an increased drying capacity (Henderson, 2014; Zhu, 2013). Petroleum coke is a good choice for co-firing because it has a high CV and does not require any design changes to the boiler. Municipal solid waste (MSW) and refuse derived fuels (RDF) are poor choices due to low CV and multiple design and operation challenges.

2.6.2 Liquid fuels and chemicals production

Coal gasification entails the conversion of a solid fuel into a gas, which is easier to use, through the reaction of the fuel with a gasifying agent such as air, carbon dioxide, oxygen and steam (Bell *et al.*, 2011; Fernando, 2008). Gasification can be considered as an incomplete combustion of coal due to insufficient oxygen, converting the energy in the coal into chemical energy contained in the resulting crude gas, instead of thermal energy (Bell *et al.*, 2011; Fernando, 2008). The steps that are involved in coal gasification are consequently similar to those of combustion: (1) drying, (2) de-volatilisation, (3) volatile combustion, and (4) char reactions (Bell *et al.*, 2011).

There are two process routes for the conversion of coal-to-liquids (CTL), *i.e.* liquefaction: direct and indirect (Couch, 2008; Osbourne & Gupta, 2013). Direct coal liquefaction (DCL) involves the addition of hydrogen to the coal and the dissolution of coal in solvents at a high temperature and pressure. This process is very efficient; however, significant purification processes are required to obtain a good quality product. Indirect coal liquefaction (ICL) entails the complete destruction of the coal structure by gasification, followed by purification to produce a synthesis gas (syngas) consisting of mainly carbon monoxide, hydrogen and some light hydrocarbons (Couch, 2008; Osbourne & Gupta, 2013). A simplified diagram of the process is shown in Figure 2-10

(Mahinpey & Gomez, 2016; Sasol, 2018). The sulphur is converted to mainly H_2S, instead of SO_2, and the nitrogen is almost completely converted to NH_3, instead of NO_X, which makes it easier to remove and gasification is consequently considered a clean coal technology (Vamvuka, 1999). The condition of the ash that is removed from the gasifier can be classified as dry or wet/ slagging (Couch, 2008). The impurities should also be removed before the coal is gasified to prevent the downstream gas phase reaction catalysts from being poisoned in Fischer-Tropsch (FT) synthesis reactions (Couch, 2008; Osbourne & Gupta, 2013).

There are three types of gasifiers based on their fluidisation regime: moving bed, fluidised bed and entrained flow (Bell *et al.*, 2011; Fernando, 2008; Mahinpey & Gomez, 2016; Vamvuka, 1999). In a moving (*i.e.* fixed) bed gasifier, the coal is fed from the top of the gasifier, and the gasifying agent is fed from the bottom while the gases from the reactions flow upward and are removed at the top, and the ash is removed from the bottom. In a fluidised bed reactor, the coal and gasifying agent is fed from the bottom and gasified in a bed of heated particles suspended in flowing air. In an entrained flow gasifier, the pulverised coal and gasifying agent is fed from the top and flow concurrently through the gasifier at high speed. The properties of the coal that are used differ for each type of gasifier, however Sasol (the main CTL company in South-Africa) uses the Lurgi® FBDB™ (fixed bed dry bottom) gasifier and therefore only the properties for moving bed gasifiers will be evaluated in this section (Bell *et al.*, 2011; Sasol, 2018; van Dyk *et al.*, 2001).

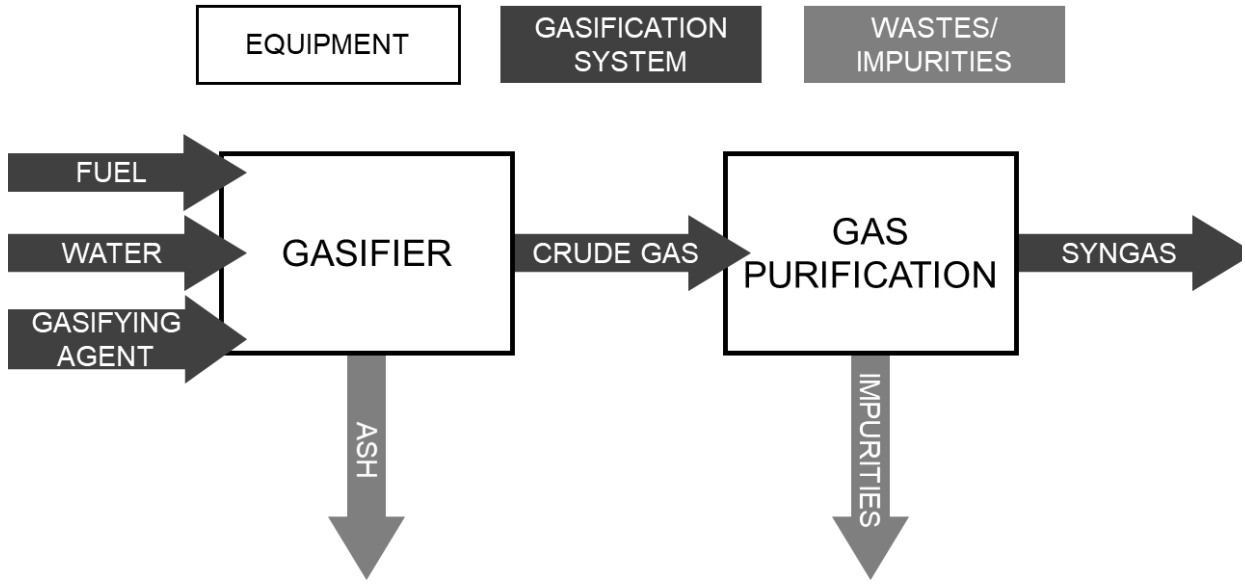

Figure 2-10: Simplified diagram of an ICL gasification process adapted from Mahinpey and Gomez (2016)

Table 2-10: Summary of some coal properties and their desired values and effects on coal gasification adapted from Couch (2008), Vamvuka (1999), van Dyk *et al.* (2001), van Dyk *et al.* (2006), and Weiss and Turna (2009)

Property	**Unit**	**Value**			**Comments**
		Minimum	Desired	Maximum	
Moisture content[a,b]	wt%	-	~5	30*	Σ (moisture + ash) ≈ 50%
Ash yield[a,c]	wt%	4*	~28	35	
Volatile matter content[a]	wt%	-	~20	-	-
Sulphur[a]	wt%	-	low	0.6	Depends on local regulations
Thermal fragmentation[c]	%	-	low	~55	-
Caking propensity[d]	%	-	low	~20	
Ash fusion temperature[a,c]	°C	~1 200	-	-	-
Calorific value[a]	MJ/kg	-	~30	-	-
Particle size[b,d,e]	mm	-	5–70	100*	Maximum 5% <5 mm

Source: [a] Vamvuka (1999), [b] Van Dyk *et al.* (2006), [c] Weiss & Turna (2009), [d] Van Dyk *et al*. (2001) and [e] Couch (2008)

* Outer limits

Moisture content: ar, volatile matter content: mmfb, ash yield: adb, calorific value: mafb

The effects of coal characteristics on gasification have been intensively evaluated and only a brief overview will be discussed in this study (Fernando, 2008; Mahinpey & Gomez, 2016; Mishra *et al.*, 2018; van Dyk *et al.*, 2001). The characteristics of the coal affect gasification in many ways, but some of the most important factors, which can also be tested, are volatile matter content, moisture and oxygen content, caking properties, ash characteristics, sulphur content and reactivity (van Dyk *et al.*, 2001). The desired values and limits of the coal properties are summarised in Table 2-10.

The volatile matter content of the coal gives an indication of the number of liquid hydrocarbons that can be produced during gasification and it is also directly proportional to the reactivity of the coal (Mahinpey & Gomez, 2016; Mishra *et al.*, 2018).

Thermal fragmentation can affect the gas purification equipment due to the fines that are carried out of the gasifier with the gas stream and should consequently be minimised (Couch, 2008). It is affected by the moisture content and oxidation of the coal; the moisture content contributes to ~75% of the thermal fragmentation (van Dyk *et al.*, 2001).

Coal caking is caused when the coal particles melt or sinter together to form larger particles due to their plasticity at higher temperatures (van Dyk *et al.*, 2001). This can cause gas channelling and pressure drop fluctuations which can lead to unstable operation and in severe cases oxygen break-through which may cause downstream explosions (Couch, 2008; van Dyk *et al.*, 2001). Pressure has a significant influence on the caking propensity of coal; the caking propensity is directly proportional to the pressure in the gasifier (van Dyk *et al.*, 2001). The caking propensity may be decreased by blending coal samples (Couch, 2008; van Dyk *et al.*, 2001).

The ash fusion temperature (AFT) analysis of coal provides an indication of the likelihood of ash agglomeration/ clinkering during gasification (van Dyk *et al.*, 2001). Ash fusion can cause problems similar to coal caking and the gasifier should therefore be operated at a temperature above the initial deformation temperature (IDT), but below the melting temperature in a dry-bottom (non/slagging) fixed bed gasifier (Couch, 2008; van Dyk *et al.*, 2001). The ash composition affects the ash fusion behaviour; ash with a higher content of Ca, Na and Fe, has a lower AFT due to the fluxing properties of the minerals (Couch, 2008; van Dyk *et al.*, 2001). The AFT may also be decreased by blending coal samples (Couch, 2008; van Dyk *et al.*, 2001).

2.6.3 Metallurgical use

The steel manufacturing process consists of four stages: mining, iron making, primary steel production and fabrication (FFF, 2011). There are three main types of iron making methods: blast furnace, direct reduction and smelting reduction (Carpenter, 2004; SEAISI, 2016; WCA, 2019a).

In South Africa, the primary method that is used is the blast furnace (55%), followed by direct reduction (23%), with the electric furnace (14%) and other methods (8%) accounting for the rest of the iron manufacturing (FFF, 2011). The focus of this study will consequently be on blast furnaces and direct reduction.

2.6.3.1 Blast furnace method

An integrated steel plant consisting of a coking plant, iron ore agglomeration plant, blast furnace (BF), basic oxygen furnace plant, and continuous casting, rolling and finishing operations is the main setup for iron production with a BF (Carpenter, 2004; WCA, 2019a). A simplified diagram of the process is illustrated in Figure 2-11 (Carpenter, 2004; SEAISI, 2016; WCA, 2019a). The metallurgical coal is crushed and fed to the coking ovens where it is heated up (~1 200°) in an inert atmosphere to drive off volatiles and some impurities. The sponge-like mass of carbon-rich material (*i.e.* the coke) is then quenched with water and screened. Large coke (25–80 mm) and small nut coke are fed separately to the BF and the smallest coke (*i.e.* coke breeze) is used at the sinter plants. The gas that was produced is piped to a gas processing plant where by-products (*e.g.,* coke oven gas and tar) are extracted from the gas, after which some coke oven gas may be returned and mixed with the blast furnace gas to heat the coking ovens or as a fuel around the steelworks.

Iron ore is fed to the BF as lump ore, pellets or sinter where it is charged into the top of the BF along with coke and fluxes such as limestone or sometimes dolomite. The coke is gasified when it reacts with the air and heat in the BF which produces more heat, carbon monoxide and carbon dioxide. The iron ore reacts with the carbon monoxide (reductant) to produce a high-quality molten iron that is called hot metal/ molten pig iron, which can then be removed through tapping and refined to produce steel. The chemistry of the slag can be controlled by the fluxes and it can be cooled and sold or dumped in a landfill. The gas that is produced is handled similarly to the gas from the coking ovens and the extracted blast furnace gas can be used to preheat the air entering the BF.

The air that is used for the gasification of the coke contains a supplementary fuel such as natural gas or pulverised coal (SEAISI, 2016). The coal that is used to produce the coke, *i.e.* metallurgical coal, is usually a high rank, hard coal and it is therefore preferable to use lower quality coals for pulverised coal injection (PCI) rather than coke production (Carpenter, 2004; WCA, 2019a). PCI technology has many benefits, it reduces the overall costs due to lower consumption of expensive metallurgical coals, it extends the coke oven lifetime due to less coke production, it increases BF productivity and flexibility due to the thermal conditions in the BF and the coal injection rate being easier to adjust, and it reduces overall emissions due to less coal being manufactured (Carpenter, 2004; WCA, 2019c). However, there are some disadvantages, especially at high coal

injection rates (>150 kg/thm) and if no operational changes are implemented (Carpenter, 2006). This is due to not enough coke being available to maintain a permeable bed in the BF, which can lead to production loss and a shorter BF lifetime (Carpenter, 2006).

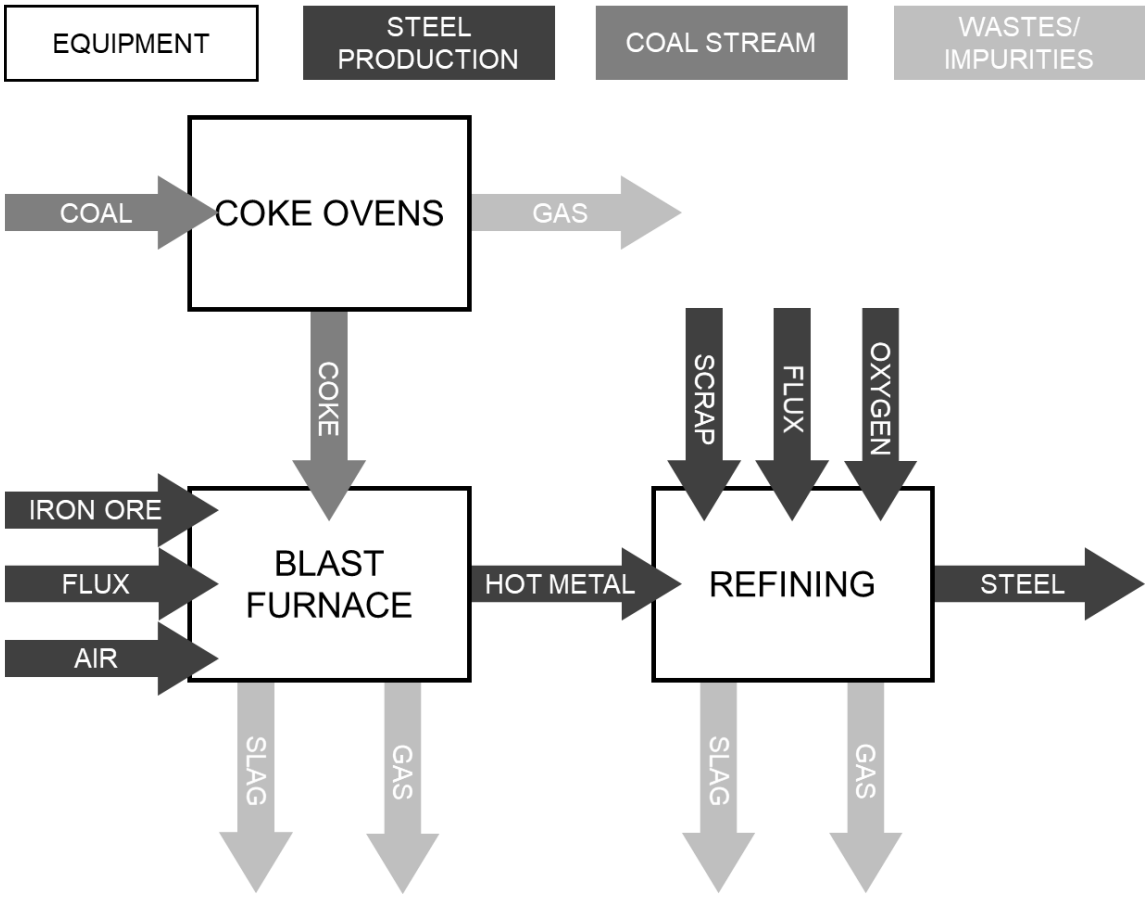

Figure 2-11: Simplified diagram of the blast furnace iron making process adapted from Carpenter (2006) and SEAISI (2016)

The considerations of using PCI in a BF to manufacture iron has been intensively reviewed by Carpenter (2006). The properties of the coal that is used affects the performance of the BF at injection rates higher than 100 kg/thm and the volatile matter content, carbon content, moisture, ash yield, calorific value, AFT and sulphur should therefore be evaluated (Carpenter, 2006).

The volatile matter content can affect the char formation, blast momentum and coke fines generation due to the pyrolysis of the coal and the resulting volatiles (Carpenter, 2006). The carbon content of the coal increases the coke replacement ratio, which is the mass (kg) of coke replaced per kilogram of coal, decreases the blast oxygen enrichment requirements, and decreases the blast momentum if the content is more than 85% dafb (Carpenter, 2006). A high moisture content can decrease the efficiency of the pulverisers, block the equipment and require more energy in the BF to evaporate the moisture (Carpenter, 2006). The ash yield of the coal should be low because of the propensity of the mineral matter to cause lance blockages and

increase the wear on the equipment, the reduced flux requirements and the lower slag production (Carpenter, 2006). The ash composition can also affect the efficiency of the BF and the quality of the hot metal. The calorific value of the coal should be high to increase the coke replacement ratio and the stability of the BF due to increased reactivity (Carpenter, 2006). The AFT of the coal should be high enough that ash deposition on the injection equipment does not occur (Carpenter, 2006). The sulphur in the coal can increase the volume of slag formation and the sulphur content of the hot metal and should therefore be low (Carpenter, 2006).

2.6.3.2 Direct reduction method

Another method of incorporating coal into the iron making process is with coal based direct reduction (Carpenter, 2006; SEAISI, 2016). The most used reactor type to produce direct reduced iron (DRI) is the rotary kiln (Carpenter, 2006; SEAISI, 2016). A simplified diagram of the process is shown in Figure 2-12 (Carpenter, 2006; SEAISI, 2016).

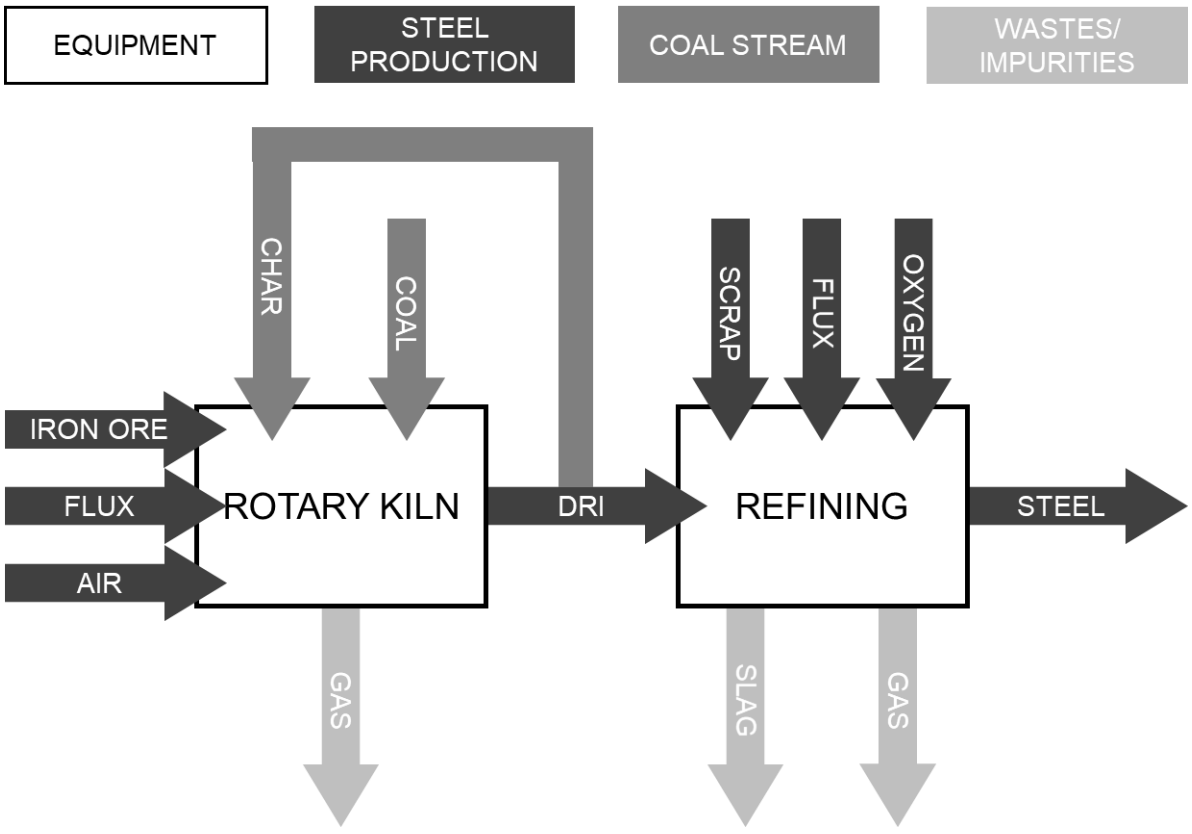

Figure 2-12: Simplified diagram of the direct reduction iron making process adapted from Carpenter (2006) and SEAISI (2016)

Table 2-11: Summary of some coal properties and their desired values and effects on blast furnace and direct reduction iron making adapted from Carpenter (2004) and Chatterjee (2010)

Property	Unit	Blast furnace method			Direct reduction method		
		Minimum	Desired	Maximum	Minimum	Desired	Maximum
Moisture content[a]	wt%	-	6–8	10	-	~6	10
Ash yield[a]	wt%	-	low	8	-	low	25
Volatile matter content[a]	wt%	-	20–38	-	-	28–35	-
Sulphur[a]	wt%	-	low	0.8	-	low	0.8
Ash fusion temperature[a]	°C		-	-	1 150	-	-
Calorific value[a,b]	MJ/kg	-	30–34	-	-	20–30	-
Particle size[a]	mm	-	-	-	-	1–10	-

Source: [a] Carpenter (2004), [b] Chatterjee (2010)

* Outer limits

Moisture content: ar, volatile matter content: db, ash yield: adb, calorific value: mafb

Iron ore (lump, pellets or iron sands), coal and the fluxes (limestone/ dolomite) are fed to the rotating kiln which is tilted 3-4° from the horizontal. The solids move through the kiln due to gravity and rotation. Gasification and reduction both take place in the kiln: the coal is devolatilised in an inert atmosphere and then gasified to produce carbon monoxide and carbon dioxide, after which the iron undergoes a reduction reaction with the carbon monoxide. The carbon monoxide and hydrogen gas from the reactions partially combusts with air to produce heat in the kiln. The burner at the discharge end of the kiln may fire pulverised coal, fuel oil or natural gas as a fuel, like PCI. The DRI product can be removed cold or hot and then passed through magnetic separators to separate the DRI, ash and char. The gas that is produced can be fed to a gas processing plant to produce off-gas, which can be used to preheat the feed to the kiln or to dry the coal.

Carpenter (2004) reviewed the coal quality requirements for direct reduction processes and the desired values are summarised in Table 2-11.

CHAPTER 3: METHODOLOGY

3.1 Overview

In this chapter the materials, methods and equipment that were used during the study are described. Section 3.2 contains a description of the materials that were used. The coal preparation and sampling methods are described in Section 3.3 and the characteristics of the coal were determined using the methods in Section 3.4. The laboratory-scale and pilot-scale briquetting methods used are given in Section 3.5 and Section 3.6, respectively. The mechanical strength tests that were conducted on the briquettes are described in Section 3.7 and the reactivity tests are described in Section 3.8. The coal characteristics are provided in Section 3.9.

3.2 Materials

A description of the coal and binders used in this study is provided in this section, as well as the chemicals, liquids and gasses that were used for tests.

3.2.1 Coal

Highveld inertinite-rich coal fines (-272 µm) from a filter cake was used in this study. A more detailed characterisation of the coal is given in Section 3.9.

3.2.2 Binders

Five industrial wastes were evaluated to determine their efficacy in the agglomeration of coal fines. The binders will be referred to as Binder A–E for ease of reference. These binders are:

- A: waterworks bio-sludge from a petrochemical industry
- B: acrylic acid containing a hydrocarbon by-product from a petrochemical industry
- C: pitch from a petrochemical industry
- D: wax emulsion from a petrochemical industry
- E: recycled low-density polyethylene (LDPE) from a North-West plastic recycling company

In addition to waste reduction, all these binders were selected due to properties they possess which may be advantageous with regards to agglomeration or reactivity. The notable advantages and disadvantages based on the material safety datasheets (MSDS) of the binders are summarised in Table 3-1. The specific SDSs will not be referenced due to confidentiality agreements, but a summary of the physical and chemical properties of the binders is provided in Appendix A.

Table 3-1: Overview of the binder properties which may be beneficial in briquetting coal fines

Binder	Properties	
	Agglomeration	Reactivity
A	✓ Relatively harmless to the environment Type: Inactive film	X High moisture content
B	✓ Contains components that are used to make sealants and adhesives ✓ Polymerisation occurs when exposed to white light, ultraviolet light or heat X Contains hazardous components Type: Inactive matrix	X May produce hazardous emissions
C	✓ Contains components that are used to make sealants and adhesives ✓ Pitch has been successfully used as a binder in previous studies X Contains hazardous components Type: Inactive matrix	X High sulphur content
D	✓ Hydrophobic component Type: Inactive film	X High moisture content
E	X Should have a particle size ≤ coal fines Type: Inactive matrix	✓ High heating value

Source: MSDS

✓: advantages, X: disadvantages

The water used for the binderless briquettes, Binder A, and Binder D are all inactive film binders, where a liquid uses surface tension to pull the coal particles together (Engelleitner, 2001; Holley, 1983; Young, 2015). Binder B, C and E are all inactive matrix binders, where the coal particles are imbedded in an almost continuous matrix of the binder (Engelleitner, 2001; Holley, 1983; Young, 2015).

3.2.3 Liquids

Liquid nitrogen was used to pulverise Binder E and toluene was used as a solvent in the Fischer assay experiments to wash the gas and trap the tar from the briquette pyrolysis reaction of the optimal pilot-scale briquettes. Tap water from the Potchefstroom area was used during the coal agglomeration process and during the water resistance tests, demineralised water was used

during the particle size distribution (PSD) and the bomb calorimeter tests, and ice was used to keep the toluene cold in the Fischer assay experiments, as per the relevant standard procedures.

3.2.4 Gases

The gases that were used to test the briquettes were supplied by Afrox. Oxygen (99.9% purity) was used during the bomb calorimeter test, nitrogen (99.9% purity) was used to devolatilise the briquettes, carbon dioxide (99.9% purity) was used during gasification experiments, and dry air (<2 ppm water) was used during combustion experiments.

3.3 Coal preparation and sampling

A coal sample of ~500 kg was received and prepared to ensure that a homogeneous sample was used during the study. A grab sample of approximately 20 g was taken to test the surface moisture content (ar) of the coal. The coal was spread over a clean, flat area and left to air dry for four days, after which another grab sample was taken to test the surface moisture (adb) of the coal. The coal sample was mixed while coning and quartering, as shown in Figure 3-1 (Crosby & Patel, 1995). The coal was piled with a shovel into a cone-shaped heap, Figure 3-1(a), and then flattened on the top, Figure 3-1(b). The heap was divided into four equally sized quarters, Figure 3-1(c), and the coal on the outside was piled into the middle of the heap to form a cone-shape again. This was repeated and two of the equally sized quarters, Figure 3-1(c), were removed to reduce the size of the sample, Figure 3-1(d).

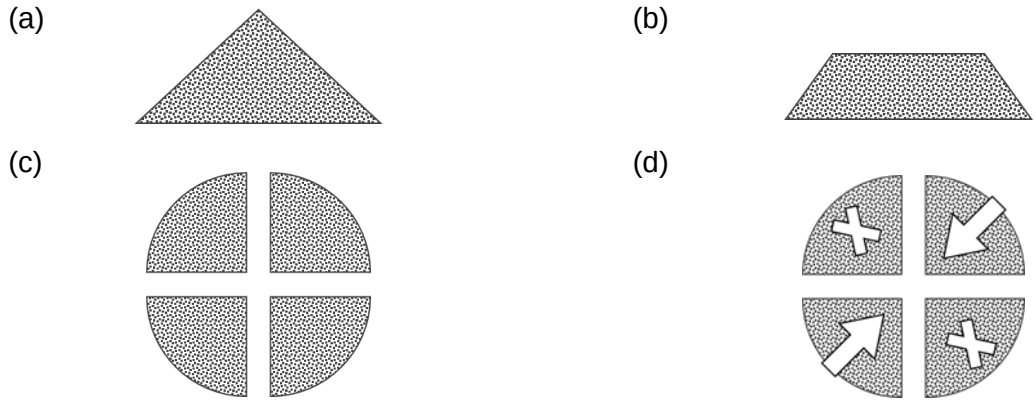

Figure 3-1: Coal preparation – coning and quartering, adapted from Crosby and Patel (1995)

The smaller coal sample was separated into two using a manual riffle divider and any large clumps of coal/ impurities were removed by sieving the coal on a sieve with an aperture size of 1 mm. This also ensured that the coal that was used during the study can be classified as fine coal. The oversize and unused coal sample was stored in separate 20 L containers and nitrogen gas was injected into the containers to prevent oxidation of the coal.

3.4 Coal and briquette characterisation

The PSD, composition and calorific value of the coal was determined, while only the proximate analysis and calorific value of the optimal pilot-scale produced briquettes was determined to evaluate the suitability of the briquettes as feedstock to various industrial applications and are incorporated into the reactivity results in Chapter 5.

3.4.1 Particle size distribution

A Malvern Panalytical Ltd. Mastersizer® 3000 was used to determine the PSD of the coal fines. The procedure adheres to the ISO 13320 (2009a) standard for laser diffraction methods to analyse particle sizes and the results are shown in Section 3.9 on a cumulative distribution curve according to the ISO 9276-1 (1998) standard for the representation of PSD results.

3.4.2 Coal and briquette composition

The proximate and ultimate analyses of the coal that was used for the experiments were outsourced to Bureau Veritas Testing and Inspection (BVT) in South Africa. The standards that BVT used to determine the characteristics of the coal are listed in Table 3-2. The proximate analyses of the optimal briquettes, as determined during the pilot-scale tests, were conducted in-house in a Labotec Inc. EcoTherm Economy oven, a Carbolite® Gero VMF–100 muffle furnace and a Carbolite® Gero AAF–1100 muffle furnace, according to the standards listed in Table 3-2.

Table 3-2: Standards for proximate analysis, ultimate analysis, XRD and XRF

Description	Procedure/ Test method
Sample preparation	BV-TPM-001 based on ISO 13909-4 (2001)
Moisture content (%)	BV-TPM-010 based on ISO 11722 (2008)
Ash content (%)	BV-TPM-011 based on ISO 1171 (2010a)
Volatile matter content (%)	BV-TPM-012 based on ISO 562 (2010b)
Fixed carbon content (%)	Calculated by difference
Total sulphur (%)	BV-TPM-013 based on ISO 19579 (2006)
Elemental analysis (%)	CHN Instrumental method based on ISO 12902 (2001)
Mineral composition (%)	Rietveld method
Ash composition (%)	ASTM D4326-4 XRF – By fusion bead (2004)

3.4.3 Gross calorific value

A bomb calorimeter was used to determine the gross calorific value (CV), also known as the higher heating value, of the coal fines and optimal briquettes. The standard procedure described by ISO 1928 (2009b) was used for the analysis.

3.5 Laboratory-scale briquetting

Phase 1 of the study entails the manufacturing of cylindrical briquettes on laboratory-scale to evaluate the effect of the binders on the agglomeration process. Two batches of briquettes were manufactured to test the effect of different parameters on the mechanical strength of the briquettes.

3.5.1 Binder preparation

The initial batch of laboratory-scale tests focused on the handleability of the binders and the effect of a large moisture addition on the compressive strength (CS) and water resistance index (WRI) of the briquettes. This was done to determine if air-drying is necessary before the coal and binders were mixed and agglomerated. Venter and Naude (2015) could make briquettes with a moisture addition of up to 18%, and a maximum moisture addition of ~17% was therefore used. The moisture and binder additions were based on weight percentage and the mass of binder that was added to the mass of coal fines was calculated using Equation 3-1.

$$m_{\text{binder}} = \frac{m_{\text{coal}}}{(1 - x_{\text{binder}})} - m_{\text{coal}} \tag{3-1}$$

In Equation 3-1, m_{binder} (g) is the mass of binder that was added to a coal sample with a mass of m_{coal} (g) to achieve a binder mass fraction of x_{binder}. This equation was also used to calculate the amount of water that should be added by substituting x_{binder} with the moisture fraction. The diameter (13 mm) and mass (~2 g) of the briquettes were kept constant, but the length differed based on the type and amount of binder that was added. The moisture addition of 17% was kept constant while the binder was added from 5%, increasing in intervals of 5%, until the mixture could not hold its form during agglomeration.

The second batch of laboratory-scale tests focused on maximising the binder addition to air-dried coal fines. Usually, the goal is to find a compromise between minimising the binder addition and maximising the quality of the briquettes due to the costs involved (Couch, 2002; Engelleitner, 2001). Binders A–D considered in this study are all classified as hazardous wastes and getting rid of these wastes can be a costly process (Lewitt, 2011). Maximising the binder addition in the briquettes therefore creates an opportunity to reduce or even eliminate the costs involved in disposing of these wastes, while also making the waste materials useful and decreasing environmental pollution (Couch, 1998). Binder E was not considered during this phase due to the extra costs involved in sourcing and processing the binder.

Binders A and D were used as is while Binders B and C were heated before briquetting the second batch of briquettes due to the high viscosity of the binders hindering homogeneous mixing

(Mills, 1908). This was not an issue during the first batch due to the higher moisture content facilitating mixing. The equipment used included a beaker (100 mL) to heat the binders, a beaker (100 mL) to mix the coal and binder, a spatula to handle the materials and an eyedropper to add water to the mixture. A laboratory mass balance (0.01 g readability) was used to measure the mass of the materials.

Binder E had an average particle size of approximately 5 mm (ar) and the particle size was consequently reduced to -1 mm to ensure that the plastic and coal particles had enough contact to properly bind and to avoid excessively large voids caused by the larger plastic particles (Dehont, 2006; Kaliyan & Morey, 2009; Massaro *et al.*, 2014). The crystalline structure of LDPE deforms instead of shattering and the plastic had to be cooled with liquid nitrogen while a Kambrook® electric blender was used to reduce the size of the particles to below 1 mm in size. A D_{90} of 826 µm was obtained.

3.5.2 Batch briquetting process

The briquettes were manufactured using an Ametek® Lloyd Instruments™ LRX Plus press in a stainless-steel Specac® die with a 13 mm diameter. A schematic of the process is illustrated in Figure 3-2. Each briquette was pressed individually by inserting the coal-binder mixture into the die, and placing it between two plates, *viz*. the fixed lower punch and the moving upper punch, shown in Figure 3-2(a). A guide pin was used to push the upper punch down until a pressure of 1.5 kN was reached, after which the position was held for 15 s before being released (Maree *et al.*, 2020). The briquette, shown in Figure 3-2(b), was removed and stored for further testing. Approximately 50 briquettes (~2 g each) were manufactured for each respective binder and concentration.

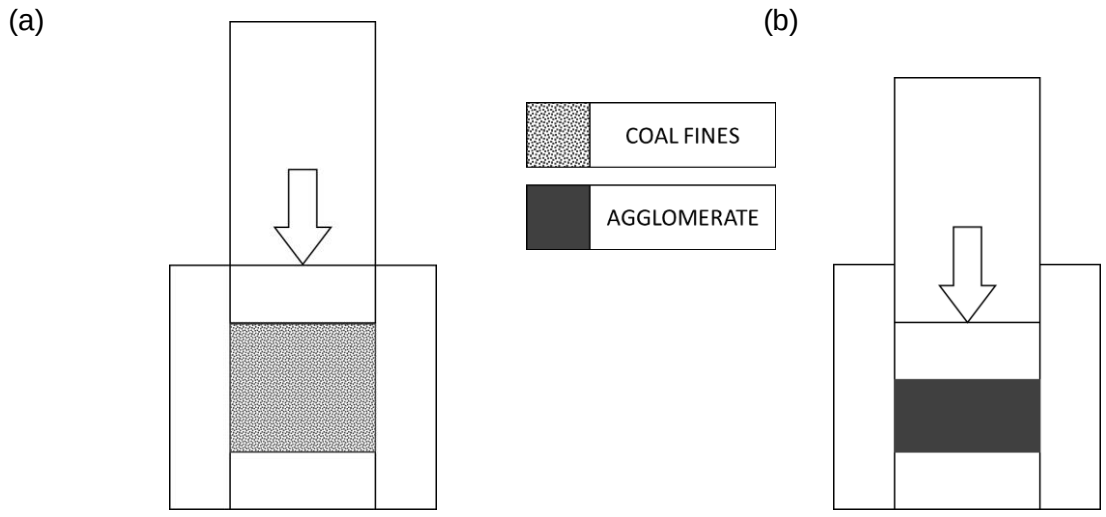

Figure 3-2: Briquetting process: (a) before and (b) after

3.5.3 Curing

The curing step facilitates the evaporation of moisture from the briquettes to increase capillary pressure and/or enables solid bridge bond formation which increases their strength (Green & Southard, 2019; Hapgood & Rhodes, 2008; Pietsch, 2004). Briquette curing conditions were dependent on the properties of the binders and therefore differed between some binders.

The first batch of briquettes bound with Binders A and D were cured at ambient temperature and the briquettes bound with Binders B and C were cured in a Labotec Inc. EcoTherm Economy oven at 60°C for 30 min, as the binders start to decompose above 60°C. The Binders B and C bound briquettes were heated due to the high viscosity of the binders to ensure that the binder sufficiently fills the voids between the coal particles. Some briquettes containing Binder B were also cured under an 18 W UV lamp due to its propensity of plasticising under UV light (based on SDS) (Pietsch, 2004). The briquettes manufactured with Binder E were cured in the oven at 150°C for 12 hrs due to its higher melting point (Gug *et al.*, 2015; Massaro *et al.*, 2014). The briquettes were then stored in a well-ventilated area at room temperature.

The second batch of briquettes were cured under ambient temperature in a well-ventilated area as Binders B and C were heated before briquetting, thereby reducing binder viscosity. Binder E was not tested during the second batch of tests due to handling issues.

3.6 Pilot-scale briquetting

Phase 2 of the study entails the manufacturing of pillow-shaped briquettes at pilot scale to determine the optimal briquette concentrations for each binder based on the mechanical strength (CS, AR, FR, IRI) and water resistance (WRI) of the briquettes. The handleability, cost implications and hazardous nature of the binders are also considered.

3.6.1 Binder preparation

The addition of moisture was found to act as a lubricant during the mixing of the binders and coal fines, however due to the binders needing to be maximised, a compromise between moisture and binder addition was found (Engelleitner, 2001; Komarek, 1967). The minimum moisture addition that was considered to create binderless briquettes was 2.5%. The moisture addition was therefore kept constant at 2.5%, while the binder addition was increased from 5%, at intervals of 5%, until the briquettes no longer retained their shape during the briquetting process. If the mixture could not be agglomerated at 10%, the binder concentration was lowered to 2.5% to determine if a lower concentration could create a stronger briquette.

Binders A, D and E were used at room temperature, while Binders B and C were heated before use as described in Section 3.5.1.

3.6.2 Continuous briquetting process

The pillow-shaped briquettes were manufactured on pilot-scale using a K.R. Komarek Inc. B050 roll press. A schematic of the process is shown in Figure 2-4. The coal-binder mixture (~2 kg) was agitated at 80 rpm with a Kenwood® electric mixer and then fed through a hopper-setup to a feed screw. The mixture was then fed at a speed of 80 ± 0.1 rpm to two roller dies rotating at 3.8 ± 0.1 rpm with a roll gap and force of 0.3 mm and 30 ± 0.5 kN, respectively, where the briquettes where formed (Botha, 2019). Each briquette (l = 35 mm, w = 22 mm, h = 12 mm) weighed approximately 5 g.

3.6.3 Curing

The briquettes produced with Binders A–E, as well as the binderless briquettes, were cured under a controlled temperature (25°C) and humidity (40% relative humidity) to reduce the adsorption of moisture from the atmosphere (Himbane *et al.*, 2018). Additionally, the briquettes produced using Binder E were cured in a Labotec EcoTherm oven at 150°C overnight (~18 hours) to melt and sufficiently spread the binder between the coal particles (Gug *et al.*, 2015; Massaro *et al.*, 2014).

3.7 Mechanical strength tests

Four tests were performed to determine the compressive strength (CS), abrasion resistance (AR), impact resistance (IRI), durability (FR) and water resistance (WRI) of the briquettes. The mechanical strength tests were performed on specific days: 0 (green strength), 7, 14 and 21. Phase 1 testing only entailed the compressive strength test and the water-immersion test, whereas Phase 2 included all four tests.

3.7.1 Compressive strength test

The Richards (1990) test was used to determine the CS of the briquettes using an Ametek® Lloyd Instruments™ LRX press. The cylindrical briquettes were tested for surface CS, *i.e.* axially vertical position as shown in Figure 3-3(a), while the pillow-shaped briquettes were tested for point CS, *i.e.* flat-horizontal position as shown in Figure 3-3(b), due to it being the natural resting orientation of the briquettes (Rahman *et al.*, 1989). The top plate (d = 500 mm) pressed on the briquette resting on an equal sized plate at a speed of 0.25 mm/s, until a cracked formed and the CS could be calculated using Equation 2-3:

$$\mathrm{CS} = \frac{F}{A} \tag{2-3}$$

In Equation 2-3, *F* (N) is the fracture load and *A* is the area of the fracture, *i.e.* the area that touches the plate. The circular flat area of the cylindrical briquette was 1.33 x 10^{-4} m^2 and the rectangular flat area at the topmost part of the pillow-shaped briquette was 6.80 x 10^{-4} m^2. The test was repeated five times and the average CS was reported. The minimum acceptable CS is 0.38 MPa for briquettes and 2.1 MPa for South African ROM coal (Mark & Barton, 1996; Richards, 1990; Speight, 2005).

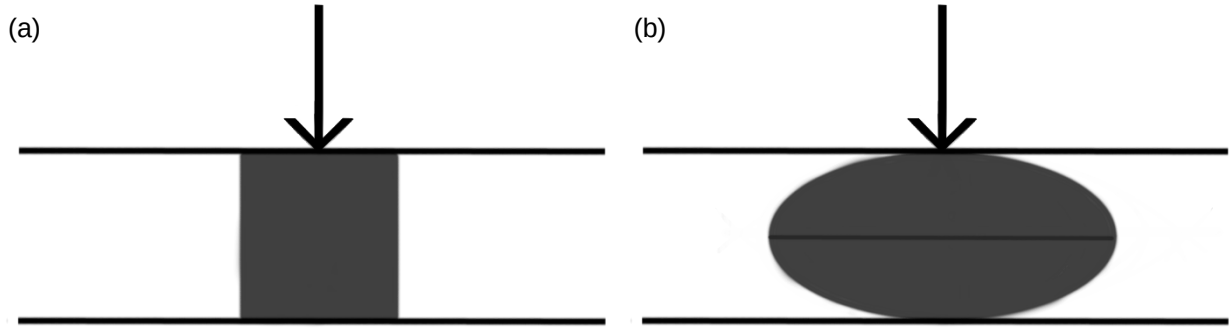

Figure 3-3: Schematic of the (a) axially vertical and (b) flat-horizontal positions for testing compressive strength

3.7.2 Drop shatter test

The Richards (1990) drop shatter test was used to determine the impact resistance index (IRI) and the friability (FR) of the briquettes. FR provides information on the durability of the briquettes. The test consisted of dropping a single briquette from a height of 2 m onto a concrete floor until it breaks. The number of times it was dropped, N_{drops}, the number of pieces it broke into, N_{pieces}, the initial mass, m_0 (g), and the mass of the largest broken piece, m_f (g), was recorded. A laboratory mass balance (0.01 g readability) was used. The values were substituted into Equation 2-4 and Equation 2-7 to calculate the IRI and FR, respectively.

$$\mathrm{IRI} = \frac{N_{\mathrm{drops}}}{N_{\mathrm{pieces}}} \times 100 \tag{2-4}$$

$$\mathrm{FR} = \frac{m_{\mathrm{f}}}{m_0} \times 100 \tag{2-7}$$

The minimum acceptable IRI and FR are 50 and 80%, respectively (Kaliyan & Morey, 2009; Richards, 1990).

3.7.3 Tumbler test

A modified Richards (1990) test, constructed by Botha (2019), was used to establish the AR of a smaller sample size of briquettes, which is an indication of the durability of the briquettes. A

stainless-steel cylindrical drum (d_i = 70 mm, l = 51 mm) with a lifter spanning the whole length of the drum was used in the experiment. The drum contained a sample of four briquettes with a combined weight of approximately 20 g, which was rotated on roller-shafts connected to a Bonfiglioli® variable speed drive controlled at a speed of 80 rpm for 197 revolutions. The sample was sieved on 6 mm and 1 mm sieves to determine the amount of sample that can be classified as peas (+6 mm), duff (-6 mm, +1 mm) and fines (-1 mm) (Steyn & Minnitt, 2010). The oversize of the 6 mm sieve was used to calculate the AR as a percentage using Equation 2-8.

$$\mathrm{AR} = \frac{m_\mathrm{f}}{m_0} \times 100 \qquad (2\text{-}8)$$

In Equation 2-8, m_0 (g) is the weight of the initial briquette sample and m_f (g) is the weight of the oversize sample after tumbling, determined with a laboratory mass balance (0.001 g readability). To ensure accuracy the test was repeated twice, and the average of the results was used. The minimum acceptable AR value is 95% (Richards, 1990).

3.7.4 Water-immersion test

The water resistance of the briquettes was tested with the Richards (1990) immersion-in-water test where a briquette is immersed in water for 30 min, with light pressure being applied every 10 min. If the briquettes were not water resistant the time until dispersion was classified as 5, 10 or 30 min with the state of the waterlogged briquette being evaluated as intact, mostly intact, mostly degraded, or degraded (Taulbee *et al.*, 2013). The intact briquettes were then weighed to determine the mass of water that was absorbed, and the water resistance index (WRI) was calculated using Equation 2-9.

$$\mathrm{WRI} = 100 - \%m_\mathrm{w} \qquad (2\text{-}9)$$

In Equation 2-9, $\%m_w$ is the mass of water that was absorbed as a percentage of the overall mass of the briquette. The test was repeated three times and the average value was used to ensure accuracy. The minimum acceptable WRI is 95% and the briquette was wiped dry and tested afterwards to determine the wet compressive strength (CS_{wet}) (Richards, 1990).

3.8 Reactivity tests

Phase 3 entails the matching of the different binders to end-use processes they can possibly be used in. It is therefore important to know how the different binders react during pyrolysis, gasification and combustion to predict their suitability to the four processes that are considered in this study. The briquettes that have the best mechanical strength tests results for each binder will be considered in these tests.

3.8.1 Free swelling index

The free swelling index (FSI), *i.e.* crucible swelling number, of the coal and optimal coal-binder blends were tested to determine if the coal or binders had any swelling properties for use in the metallurgical industry. The standard procedure is described in ISO 501 (2003). The FSI was also calculated with the pore resistance number (PRN) correlation suggested by Dakič *et al.* (1989), as shown in Equation 2-12. The PRN is calculated from the volatile matter content divided by the inherent moisture in the coal.

$$\mathrm{FSI} = 10^{-2}\mathrm{PRN}^{1.9} \tag{2-12}$$

3.8.2 Thermal degradation

The method that van Dyk (2001) and Leokaoke *et al*. (2019) used was modified to test the primary thermal degradation of the briquettes. A Carbolite® Gero VMF–100 muffle furnace was used due to its high heating rate capability. The briquettes were placed inside the ceramic crucibles used for the proximate analysis (volatile matter content) and covered with a lid to prevent air from entering. The muffle oven was pre-heated to 100 ± 25°C and the briquettes were weighed and inserted into the furnace. The furnace was then heated at a rate of 45°C/min to 700 ± 25°C and kept there for 60 min. The fragmentation that occurred could then be measured with the Ergun index, Equations 2-10 and 2-11, or through visual assessment if no fragmentation occurred.

3.8.3 Pyrolysis

The briquettes were charred in an Elite Thermal Systems Ltd. TMH16/75/610 horizontal tube furnace before undergoing either combustion or gasification reactivity tests. The briquettes were charred in an inert environment created by streaming 5 ± 0.1 sL/min nitrogen gas into the furnace while the furnace was heated to 1000 ± 25°C at a heating rate of 5°C/min. The briquettes were held isothermally for 120 min to ensure that all the volatiles were removed before the furnace was cooled down to room temperature (Vamvuka, 1999). The charred briquettes were stored under nitrogen atmosphere in air-tight containers at ambient temperature.

3.8.4 Thermogravimetric analysis

The combustion and gasification tests were both performed in an in-house designed Elite Thermal Systems Ltd. TSV15/50/180 vertical tube furnace setup with different gases and experimental parameters. A schematic of the process is shown in Figure 3-4. The furnace was heated via elements around the tube and a ceramic encasing insulated the furnace from the surrounding area. A maximum heating rate of 7°C/min and temperature of 1 400°C could be obtained in the furnace. The gas-flow was controlled using a mass flow controller (*viz*. Brooks® model 0254 for

air and Sierra® SmartTrak® 50 series for CO_2) and entered the furnace at the top. The gas then flowed through the furnace where the briquette was held in a quartz bucket, placed on top of a laboratory mass balance (0.001 g readability). The mass, temperature and time were logged at 2 second intervals with a computer program, VisiDAQ®. The mass loss versus time data was filtered with the least square's method to smooth out the TG-curves for data analysis.

The isothermal combustion tests were performed on the charred coal briquettes with a dry air flowrate of 0.15 ± 0.01 sL/min at three temperatures, *viz.* 850, 875 and 900 ± 5°C (Botha, 2019). The isothermal gasification tests were conducted using carbon dioxide with a flow rate of 2 sL/min at two different temperatures, *viz.* 1000 and 1025 ± 5°C.

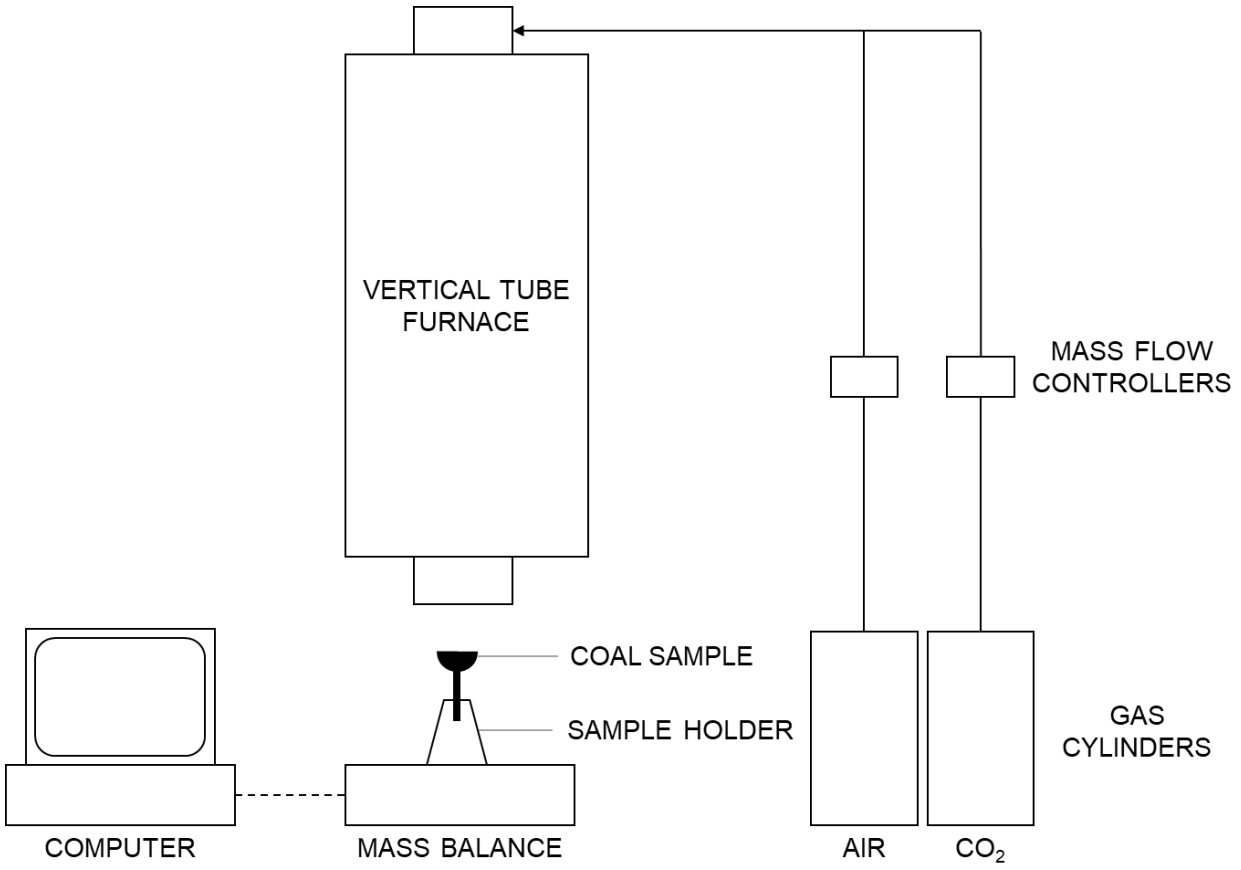

Figure 3-4: Schematic of the in-house testing rig setup for thermogravimetric analysis

3.8.5 Fischer assay

An adapted Fischer assay rig, based on the ISO 647 (2007) standard, was used to evaluate the pyrolysis products of the briquettes (Roets *et al.*, 2014). Nitrogen was sent through the setup to generate an inert environment. The Fischer assay was conducted using a temperature of 900°C, with an oven ramp rate of 10°C/min and a retort ramp rate of 5°C/min. The volatiles that were released during the heating process bubbled through a toluene tar trap and gas washing phase that was kept cool with an ice bath. This was used to separate the gas fractions from the tars for

capture in Tedlar® gas sampling bags. A Dean-Stark distillation system was used to remove the water fractions from the tar and toluene mixture and a Büchi® Rotavapor® R-100 and Büchi® Vacuum pump V-100 were used to perform rotary evaporation on the remaining mixture at 60°C and 77 mbar. The ISO 647 (2007) method was used to determine the gas yields, while the weights of the different fractions were used to gain the pyrolysis product distributions.

An SRI Instruments gas chromatograph (GC) model 8610C, fitted with a 1mL sample loop, was used to analyse the composition of gaseous products and a Restek® Molecular sieve 13X column, with argon gas as a carrier, was used to separate the gas components. Each analysis started with the sample flowing through the separation column and being detected by the thermal conductivity detector (TCD). The sample gas components were eluted and then detected in the order of H_2, N_2, CH_4 and CO within the first six minutes. The sample loop was then switched so that the flow of argon was reversed at 6.3 min which ensures that the CO_2 is eluted to the TCD. At the time that the sample was injected into the GC column the temperature was 50°C where it was held for 3 min. The oven temperature was then increased to 25°C/min until a temperature of 200°C was reached in 9 min. To ensure that the CO_2 peak was completely eluted and detected by the TDC it was left for another minute at 200°C. A detection error of less than 1% was ensured with the calibration graphs of the gaseous components.

3.9 Coal characterisation results

This section contains the PSD, XRD, XRF and CV results of the coal used in the study. The results are discussed based on their effect on the briquetting of the coal fines.

Table 3-3: Comparison of the proximate analysis, ultimate analysis and gross calorific value of the coal fines and ROM coal from the same area adapted from Leokaoke *et al.* (2019)

Property	Coal fines	ROM coal[a]
Proximate analysis (wt%, db)		
Ash yield	30.4	19.8
Volatile matter	24.4	24.1
Fixed carbon yield*	45.2	56.0
Ultimate analysis (wt%, afb)		
Carbon	77.6	78.6
Hydrogen	4.3	4.0
Nitrogen	1.9	2.1
Oxygen*	15.0	14.7
Sulphur	1.2	0.6
Gross calorific value (MJ/kg, adb)		
CV	20.1	26.0

[a] Leokaoke *et al.* (2019)

* calculated by difference

The proximate analysis, ultimate analysis and CV results of the coal fines are shown in Table 3-3. The values for ROM coal from the same area are also given for comparison (Leokaoke *et al.*, 2019). The inherent moisture content of the coal fines was found to be 4.7 wt% (adb). The ash yield for the coal fines is categorised as high (≥ 30), but still below the ash yield of coal from discard dumps (40–50%) (Arnold, 2013; Department of Minerals and Energy, 2001; ISO, 2005). The volatile matter content of the coal fines is comparable to that of the ROM coal and is in line with that of a medium volatile bituminous coal (Arnold, 2013; ISO, 2005). The fixed carbon yield is also acceptable for a bituminous coal (Laj & Barnikel, 2016). The volatile matter is within the range (20–28%) where the compressive strength of the briquettes are expected to increase with an increase in volatile matter content (England, 1993). The CV of the coal fines is low compared to that of ROM coal, but above that of coal from discard dumps (10–20 MJ/kg, adb) (Department of Minerals and Energy, 2001). Overall, the coal fines are comparable to coal from

the upper part of the No. 4 Seam in the Highveld Coalfield (Hancox & Götz, 2014; Jeffrey, 2005; Jordaan, 1986).

Table 3-4: Mineralogical composition from the XRD analysis results for the coal fines

Mineral	Coal
XRD analysis (wt%, graphite basis)	
Graphite	68.2
Kaolinite	16.3
Quartz	8.4
Calcite	1.5
Gypsum	1.4
Microcline	1.4
Muscovite	1.0
Dolomite	1.0
Magnetite	0.7
Pyrite	0.2

The crystalline mineral matter composition of the coal fines from XRD analysis is presented in Table 3-4. The approximate amount of mineral matter (33.5 wt%) can be calculated using the Parr formula, Equation 2-1, by using the ash yield and sulphur content given in Table 3-3. This value concurs with the results from the XRD analysis where the crystalline mineral matter was determined to be 31.8 wt%. Mineral matter can be abrasive and a low value is therefore preferable (Couch, 2002). The most abundant crystalline minerals are kaolinite (16.3%) and quartz (8.4%), which is typical for Highveld coal (Leokaoke *et al.*, 2018; Matjie *et al.*, 2012; Strydom *et al.*, 2018). Kaolinite is a clay mineral that can cause a low WRI in briquettes with an ash yield above 15 wt% (db) due to the clay plasticising and swelling when encountering water (Mangena *et al.*, 2004). Since kaolinite, shown in Table 3-4, accounts for more than half of the minerals present in the coal fines and the ash yield is larger than 15 wt%, the WRI of the briquettes may be poor.

The ash composition of the coal fines from XRF analysis is shown in Table 3-5 and compared to ROM coal from the same area (Leokaoke *et al.*, 2019). The ash consists primarily of metallic oxides, *e.g.* SiO_2 and Al_2O_3, which may derive from the kaolinite and quartz minerals shown in Table 3-4 (Spears, 2000). The alkali index, AI, was calculated with the equation proposed by Sakawa *et al.* (1982) and represents the catalytic effect of the ash components. The increased

AI of the coal fines suggests an increased reactivity compared to the ROM coal (Coetzee *et al.*, 2013; Sakawa *et al.*, 1982; Zhang *et al.*, 2006)

Table 3-5: Ash composition from the XRF analysis results for the coal fines

Ash composition	**Coal fines**	**ROM coal**[a]
XRF analysis (wt%, LOIfb*)		
SiO_2	50.3	50.1
Al_2O_3	26.4	24.4
CaO	7.5	10.7
Fe_2O_3	5.4	1.8
SO_3	3.8	5.6
MgO	2.1	3.3
TiO_2	1.4	1.3
K_2O	1.2	0.6
P_2O_5	0.8	0.6
SrO	0.4	0.4
Na_2O	0.4	0.8
BaO	0.3	0.2
MnO	0.1	0.1
ZrO_2	0.1	0.1
Alkali Index**	6.5	4.6

[a] (Leokaoke *et al.*, 2019)

*Loss on ignition free basis

** $\mathrm{AI} = \frac{\mathrm{CaO}+\mathrm{Fe_2O_3}+\mathrm{MgO}+\mathrm{K_2O}+\mathrm{Na_2O}}{\mathrm{SiO_2}+\mathrm{Al_2O_3}} \times \mathrm{Ash}(\%)$

The cumulative density distribution graph of the coal particle sizes is shown in Figure 3-5. The graph shows that the particle sizes are distributed between a minimum size of 0.46 µm and a maximum size of 272 µm and the coal can therefore be classified as fine (-1000 µm) (Hardman & Lind, 2003). The Dv90 is however 178 µm, which means that most of the particles are ultra-fine (-150 µm) (Hardman & Lind, 2003). The increased contact between the surfaces of the smaller particles may increase the bond formation and adhesion between them to create stronger briquettes (Ellison & Stanmore, 1981a, 1981b; Gunnink & Zhuoxiong, 1994; Motaung *et al.*, 2007; Pietsch, 2004). The small particle size also allows van der Waals forces (< 1 µm), adsorbed vapour layers (< 80 µm), and liquid bridges (< 500 µm) to all be active in binding the particles (Rumpf cited by Hapgood and Rhodes, 2008).

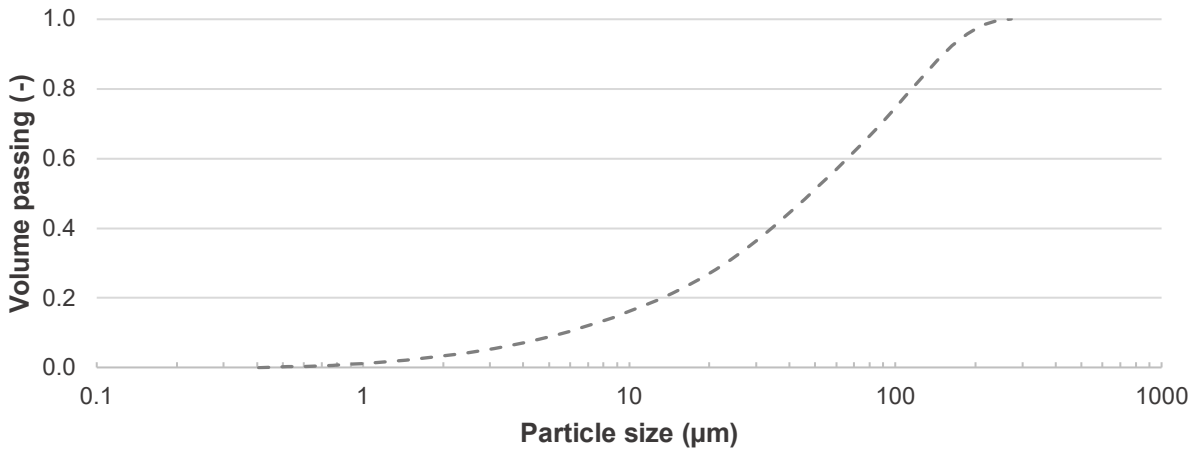

Figure 3-5: Cumulative density particle size distribution of the coal fines (-1 mm)

CHAPTER 4: MECHANICAL STRENGTH RESULTS

4.1 Overview

The mechanical strength of the briquettes bound with Binders A–E was evaluated. Section 4.2 contains the results for the laboratory-scale briquettes and provides insight into behaviour of the binders. Section 4.2 contains the results for the pilot-scale briquettes which expands on the mechanical strength of the briquettes and leads to the optimisation of the binder concentrations for further reactivity testing.

4.2 Phase 1: Laboratory-scale briquetting

The compressive strength, CS (MPa), and water resistance index, WRI (%), results of the lab-scale produced, cylindrical briquettes are discussed in this section. The binding mechanisms involved for each binder are hypothesised based on the performance of the binder and the CS of the briquettes. Some notes on the handling and behaviour of the binders are also listed for the next phase of testing.

4.2.1 Compressive strength results

The CS of the briquettes with 95% confidence level over a 21-day period is given in Figure 4-2 to Figure 4-6. The effect of the various binders on the CS of the briquettes is compared to the CS of the binderless briquettes, as well as the minimum CS for bituminous ROM coal (2.1 MPa) (Speight, 2005). It can be noted that all the briquettes surpassed the minimum limit of 0.38 MPa set by Richards (1990) on day 0 as well as the minimum ROM coal CS of 2.1 MPa from Speight (2005) on day 7. The evaporation/ adsorption of moisture in the Phase 1 briquettes is shown in Figure B-1 (Appendix B) to aid in discussing the theorised binding mechanisms of each binder.

The binderless briquettes were manufactured with an additional 17% moisture, however the briquettes had a lower moisture content because some of the moisture was removed at the sides of the die during pressing. This is caused by pressure decreasing the interstitial space, *i.e.* pores, created by air between the coal particles which are occupied by incompressible fluids which then need to escape (Iveson & Page, 2001; Pietsch, 2004). The CS of the binderless briquettes, Figure 4-1, peaked on day 0 at 3.4 MPa (green strength), after which it decreased with time. Figure B-1 shows that the briquettes lost a relatively large amount of weight (9.0%) between day 0 and 7, before gaining back some weight between day 14 (0.9%) and 21 (0.3%). The initial weight loss can be attributed to moisture evaporating from the briquettes which may have decreased the adhesion and cohesion forces created by the water layer and the small amount of re-adsorbed moisture was not enough to increase the strength (Hapgood & Rhodes, 2008;

Karra & Fuerstenau, 1977; Pietsch, 2004). The maximum CS obtained for the binderless briquettes (3.4 MPa) will be used for comparison with the binder bound briquettes.

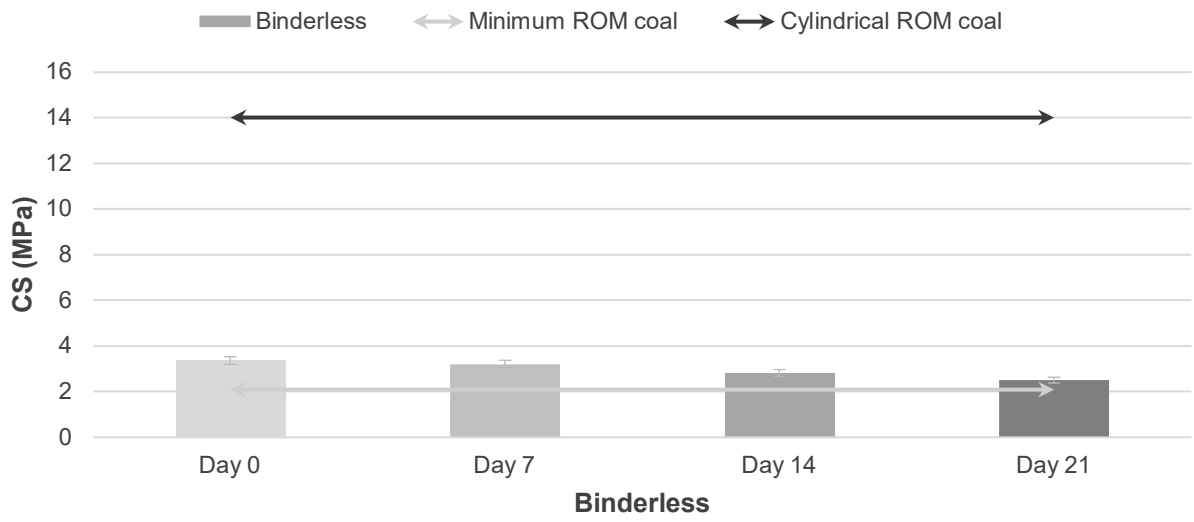

Figure 4-1: Compressive strength results over a period of 21 days for the lab-scale binderless briquettes

a. Binder A bound briquettes

The CS of briquettes produced with Binder A (5–15%) and a 17% moisture addition is shown in Figure 4-2. Binder A is a film binder and consists of small particles (< 10%) suspended in water which is why the binder did not have a large effect on the CS of the briquettes when compared to binderless briquettes. Figure B-1 shows that the weight changes of briquettes bound with different concentrations were almost identical. This may be due to the water escaping from the coal particles during pressing, leaving the solid colloidal particles in the briquette. The increase in CS (1–3 MPa) when the concentration is increased could therefore be due to solid bridges that are formed between the coal particles by the colloidal particles in the binder (Hapgood & Rhodes, 2008; Pietsch, 2004). Solid binder bridges are held together by mainly attraction forces and the adsorption of moisture, indicated by the weight gain after day 7 (1.3%), may have weakened these bonds and decreased the CS (Coelho & Harnby, 1978; Hapgood & Rhodes, 2008). The highest CS (5.6 MPa) was achieved with a binder concentration of 15% on day 7.

In the second batch of tests the concentration of Binder A could be increased to 20, 30 and 40%, without additional moisture. The same behaviour was observed as in Phase 1 because even though no extra water was added, Binder A mostly consists of water which leads to less liquid escaping during pressing compared to Phase 1, but similar liquid retention. The highest CS of the 20, 30 and 40% Binder A bound briquettes were 2.3, 3.8 and 4.1 MPa respectively, all on day 7.

These values are below those obtained in the first phase (binder dosages of 5–15%), although only by a small measure (1–2 MPa). There is therefore no observable benefit in increasing the binder concentration above 15%, except to use the briquettes as a carrier for the waste binder.

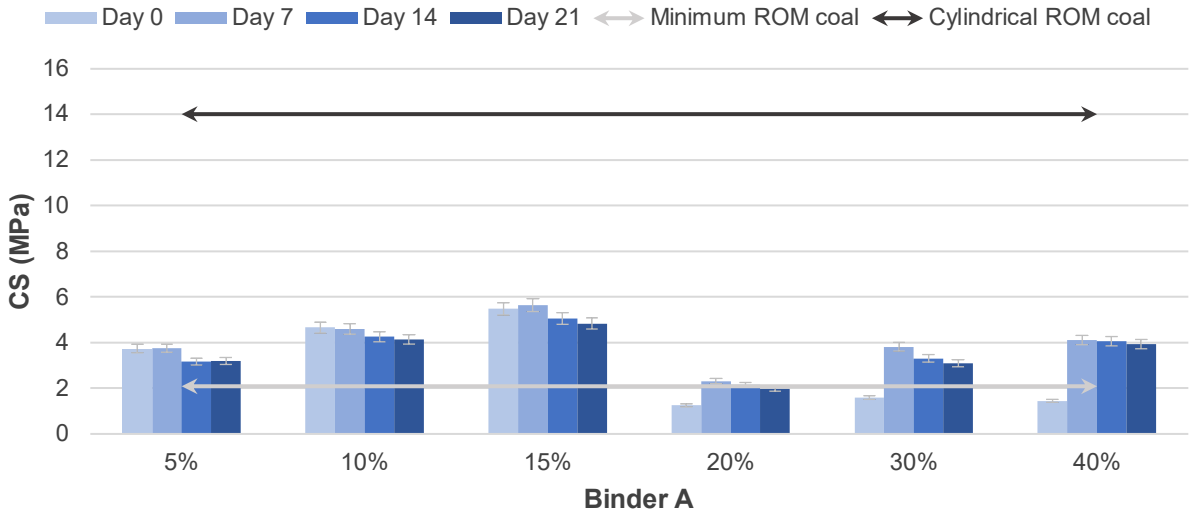

Figure 4-2: Compressive strength results over a period of 21 days for the lab-scale briquettes manufactured with Binder A

b. Binder B bound briquettes

Figure 4-3 shows the 21-day CS results of briquettes that were manufactured with maximum moisture addition (~17%) and Binder B (5–15%) then cured in an oven (60°C, 30 min). The CS results of the briquettes that underwent additional curing under a UV lamp as an attempt to activate the plasticising effect of the binder are also shown on the graph. Binder B is a somewhat viscous binder and therefore creates adhesion and cohesion forces as well as liquid bridges between the coal particles (Green & Southard, 2019; Pietsch, 2004). Binder B is both insoluble in water and denser (~1.025 g/cm^3) than water thus it can be assumed that more water escaped during pressing than binder. Briquettes bound with 5% Binder B had a relatively large weight loss (8.3%) before day 7 compared to the 10% (0.5%) and 15% (1.1%) bound briquettes, as shown in Figure B-1. This weight loss may be caused by moisture evaporating from the briquette and is higher due to the lower binder concentration allowing more water to be retained in the briquette. The slight increase in CS when the concentration is increased could therefore be caused by more adhesion and cohesion forces, and binder liquid bridges being present which supports the theory that more water than Binder B escapes during pressing. The CS of the 5, 10 and 15% bound briquettes peaked on day 7 at 5.1, 6.8 and 7.8 MPa, respectively. After day 7 the briquettes all regained some weight (0.4–1.0%) indicating adsorption of moisture on the surface of the particles which corresponds to the slight fluctuation in CS after day 7.

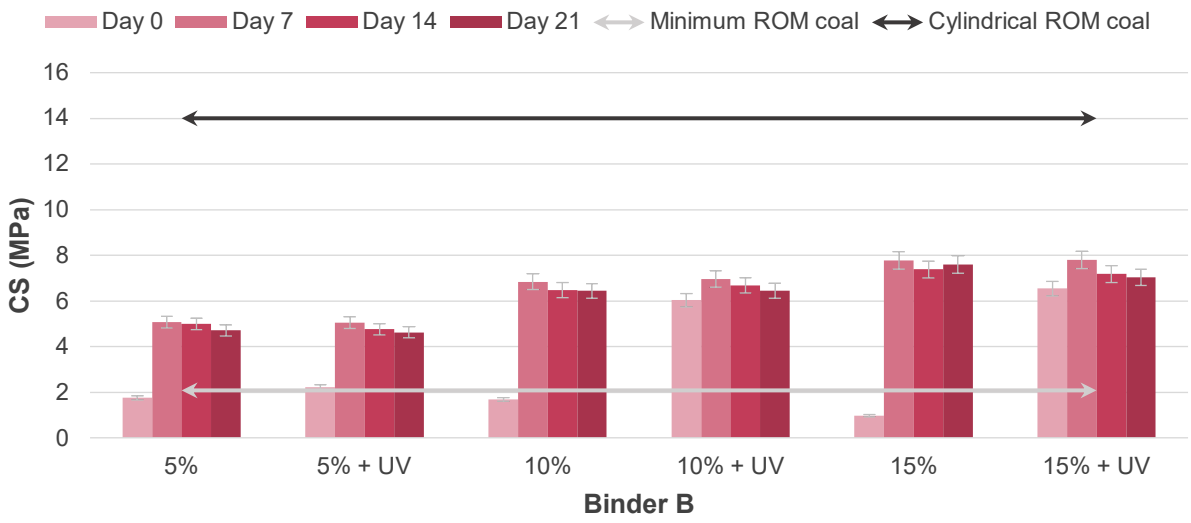

Figure 4-3: Compressive strength results over a period of 21 days of the lab-scale briquettes manufactured with Binder B

The peak CS of the UV cured Binder B bound briquettes at a concentration of 5, 10 and 15% was 5.0, 7.0 and 7.8 MPa, respectively. UV light seems to expedite the curing that the briquettes experience in the first week but did not significantly affect the peak CS of the briquettes; a finding that was also reported by Venter and Naude (2015). This might be due to the UV light removing some of the moisture in the green briquette instead of plasticising the binder. The addition of an initiator, *e.g.* hydrogen peroxide, can induce the polymerization of the binder (Rife & Walker, 1953). The UV cured briquettes had the same behaviour as the uncured briquette with regards to weight change, shown in Figure B-1, but at a smaller magnitude.

In the second batch no extra moisture was added, but the concentration of Binder B could not be increased beyond 15% due to the high viscosity of the binder preventing it from escaping during densification (Hapgood & Rhodes, 2008). The coal-binder mixture was also tacky and difficult to handle due to the absence of the additional moisture that acted as a lubricant (Engelleitner, 2001; Komarek, 1967). This is similar to the maximum viscous liquid saturation of 20–30% that is observed for the granulation of fine particle systems (Iveson & Page, 2001; Iveson *et al.*, 2002; Keningley *et al.*, 1997).

c. Binder C bound briquettes

The CS measured over a period of 21 days for the briquettes containing a moisture addition of 17% and Binder C (5–15%) is shown in Figure 4-4. The green strength of the briquettes (~1.6 MPa) was below even the binderless CS (3.4 MPa). A sharp increase in CS was observed in the first 7 days where the CS of the briquettes bound with 5, 10 and 15% Binder C peaked at 5.6, 9.5 and 14.5 MPa, respectively. The corresponding weight, Figure B-1, of the briquettes

bound with 5, 10 and 15% Binder C was reduced by 3.6, 5.1 and 7.8% over this period. Binder C is a highly viscous (500 mPa.s at 100°C) binder and therefore acts as a matrix between the coal particles to create strong viscous binder bridges that exhibit strong surface tension, capillary pressure, and adhesion and cohesion forces (Ennis *et al.*, 1990; Keningley *et al.*, 1997; Mazzone *et al.*, 1987; Simons, 2007). The declining CS after day 7 corresponds to a weight gain which could be due to moisture adsorption decreasing the capillary pressure in the briquette. The peak CS of the 15% binder containing briquettes (14.5 MPa) is comparable to that of cylindrical ROM coal (14 MPa) (Leokaoke *et al.*, 2018).

The issues observed during the second batch (> 15%) for Binder C were similar to those of Binder B. Theoretically a higher binder concentration should be able to provide stronger briquettes when considering the trend in Figure 4-4, but the mixing and pressing of briquettes with such a high viscous liquid content was found to be unfeasible.

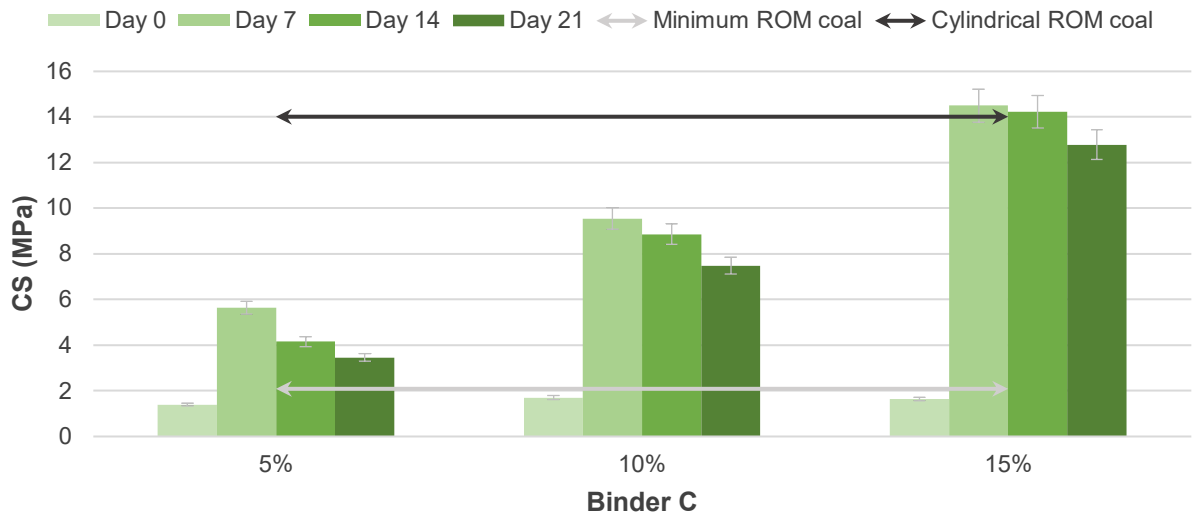

Figure 4-4: Compressive strength results over a period of 21 days of the lab-scale briquettes manufactured with Binder C

d. Binder D bound briquettes

Figure 4-5 shows the CS results for Binder D (5–15%) bound briquettes over a period of 21 days. The same escape of liquid during densification was observed as with the previous binders which decreased the moisture content of the pressed briquettes. The peak CS of the 5, 10 and 15% Binder D bound briquettes, *viz*. 3.7, 4.0 and 4.1 MPa, were comparable to that of the binderless briquettes (3.4 MPa). Binder D is a wax emulsion and mostly consists of water which is why the briquette strength depends on attractive forces, surface tension and capillary pressure (Pietsch, 2004). The weight loss, Figure B-1, of the Binder D bound briquettes is similar to the weight loss seen in the binderless briquettes which explains the peak in CS on day 7 and subsequent decrease.

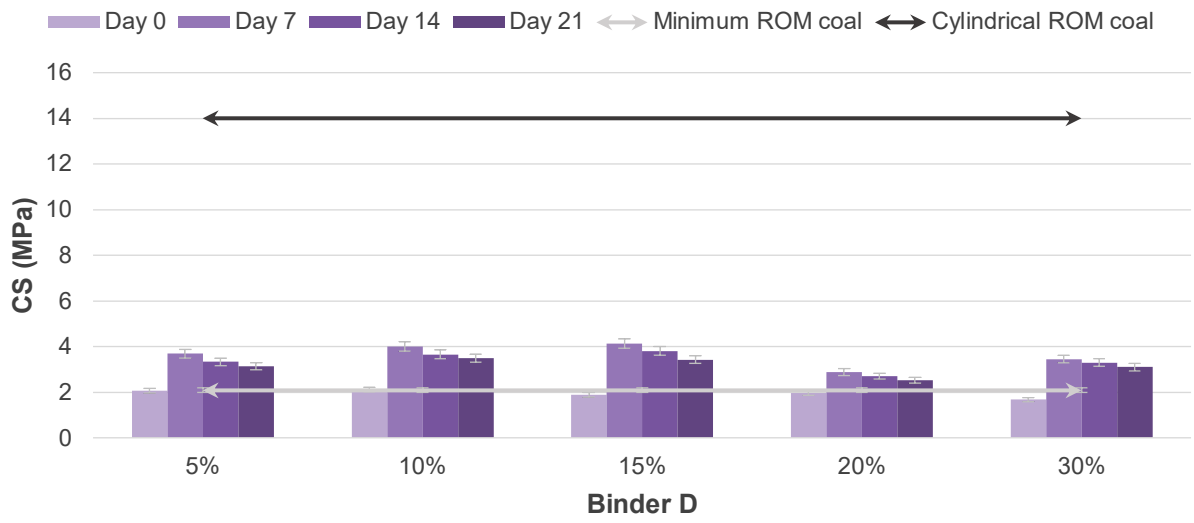

Figure 4-5: Compressive strength results over a period of 21 days of the lab-scale briquettes manufactured with Binder D

During the second batch of tests the concentration of Binder D could be increased to 20% and 30%, with a peak CS on day 7 of 2.9 MPa and 3.5 MPa, respectively. This is slightly lower than the CS of the first batch of briquettes.

e. Binder E bound briquettes

Binder E was handled differently to the previous liquid binders due to it being a solid. The CS of the briquettes was not evaluated over time as the coal particles are bound by solid bridges and the effect of adsorbed moisture was deemed negligible (Pietsch, 2004). The focus for Binder E was therefore on the CS of the briquettes at different concentrations. Figure 4-6 shows the CS of briquettes bound with 5, 10, 15 and 20% Binder E and a moisture addition of 17% (lubricant).

The hypothesis was that Binder E would function as an inactive matrix binder by melting and coating the coal particles, thereby creating a matrix that bonds the particles together (Engelleitner, 2001; Gug *et al.*, 2015; Massaro *et al.*, 2014; Pietsch, 2004). Binder E is, however, a plastic and the finely comminuted plastic particles (-1 mm) that were mixed with the coal swelled when the briquettes were cured (150°C), thereby creating cracks in the briquette surface and weakening the briquette structure which caused the CS to decrease above 10% binder addition. Technology, such as extruder pelletising, should therefore be considered in future studies to ensure that the binder is moulded while hot, thereby eliminating the cracks that form due to the particles swelling. The CS of the 5, 10 and 15% Binder E bound briquettes were still high at 10.0, 11.1 and 6.4 MPa, respectively, and further testing with the roller press will be implemented.

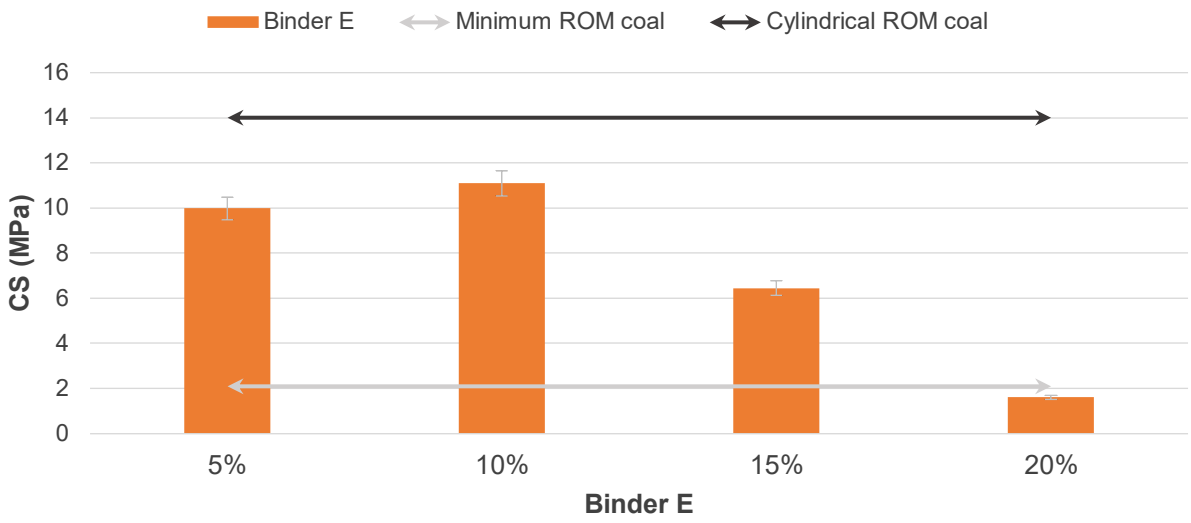

Figure 4-6: Compressive strength results of the lab-scale briquettes manufactured with Binder E

4.2.2 Water resistance results

The water resistance test determined that briquettes manufactured using Binders A–D were not water resistant. On the other hand, the briquettes manufactured with Binder E were water resistant and could be kept immersed for up to 3 hrs without disintegrating. The WRI of the Binder E bound briquettes at different time intervals are shown in Table 4-1. The minimum WRI is 95% and Binder E bound briquettes (5, 10 and 15%) all meet this requirement (Richards, 1990). Additionally, the 5% and 10% briquettes could be immersed for up to 120 min and still conform to the minimum WRI.

Table 4-1: Water resistance index, WRI (%), of lab-scale briquettes with Binder E at 30, 60, 120 and 180 min

Binder E	**Time immersed in water (min)**			
	30	**60**	**120**	**180**
5%	98.2	96.8	95.7	94.7
10%	97.6	96.6	95.2	93.9
15%	97.2	94	85.7	84.7
20%	92.9	80	53	44.8

Binder E bound briquettes with WRI ≥ 95%

The CS_{wet} of the 5 and 10% Binder E bound briquettes after 30 min of immersion, shown in Figure 4-7, were 8.3 and 9.7 MPa, respectively. The CS_{wet} of both the 5 and 10% binder E containing briquettes were below their original CS (10.0 and 11.1 MPa, respectively) but exceeded that of

literature (0.38 MPa). The 15% Binder E bound briquettes could only withstand 30 min immersed in water and had a CS_{wet} of 3.9 MPa, compared to an original CS of 6.4 MPa which may be due to the swelling of the plastic damaging the briquette structure. The CS_{wet} also decreased with an increase in immersion time, however the CS_{wet} of the briquettes at 120 min (5.5 and 6.8 MPa, respectively) were still above the minimum acceptable values (Richards, 1990; Speight, 2005).

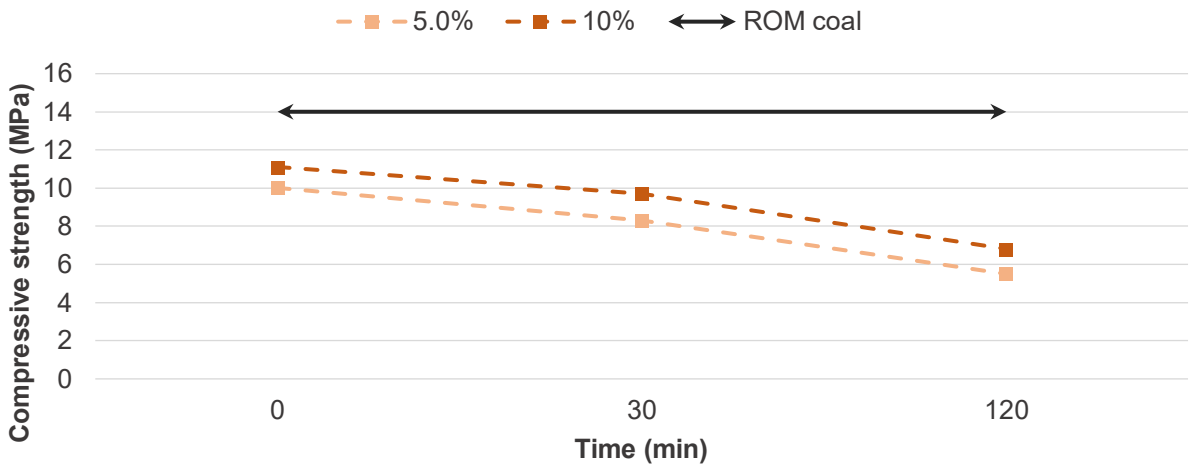

Figure 4-7: Wet compressive strength results of the lab-scale briquettes bound with 10 and 15% Binder E

4.2.3 Summary of lab-scale briquettes

The optimal concentrations for the cylindrical briquettes, as well as their respective CS and WRI, are summarised in Table 4-2. The binders (descending) can be ranked based on their CS as: C > E > B > A > D.

Table 4-2: Summary of the lab-scale briquettes manufactured with Binders A–E

Binder		Moisture (wt%)	CS (MPa)	WRI (%)	CS_{wet} (MPa)
Type	**Concentration (wt%)**				
A	15	17	5.6	–	–
B			7.8		
C			14.5		
D			4.1		
E	10		11.1	97.6	9.7

The lab-scale cylindrical tests have provided some valuable insight into the binders that were used in this study. Some of these insights are:

- Binders A and D had the lowest CS due to the primary binding mechanism being surface tension and capillary pressure from liquid bridges between the coal particles.
- Binder B and C are viscous liquids and increase the CS of the briquettes, at a magnitude relating to their viscosities, due to added adhesion and cohesion forces.
- Binder E created solid bridges in the briquette by melting and interlocking around coal particles.
- Binder E was the only binder that increased the water resistance of the briquettes enough to satisfy the minimum WRI parameter.
- Binders B, C and E all significantly increase the CS of the briquettes, but only Binder C matched the CS of ROM coal.
- Additional moisture has a lubricating effect on binder mixing and may be necessary when highly viscous binders are used.

4.3 Phase 2: Pilot-scale briquetting

The CS (MPa), IRI (-), FR (%), AR (%), and WRI (%) results of the Phase 2 pilot-scale pillow-shaped briquettes are presented and discussed in this section. The optimal binder concentrations are also determined based on the mechanical strength, water resistance, handleability, hazardous nature and cost implications of the binders prior to further reactivity testing.

4.3.1 Compressive strength results

The CS results of the pilot-scale briquettes manufactured with moisture (2.5–10%), Binder A (5–15%), Binder B (5–20%), Binder C (5–20%), Binder D (2.5–5%), and Binder E (5–10%) were evaluated and compared with the minimum CS of South African ROM coal (2.1 MPa) and cylinder-shaped ROM coal (14 MPa) (Leokaoke *et al.*, 2018; Speight, 2005). It can be noted that all the briquettes surpassed the minimum limit of 0.38 MPa set out by Richards (1990). The briquettes were stored in a temperature (25°C) and humidity-controlled (40% relative humidity) room to diminish the effects of moisture adsorption on the mechanical strength of the briquettes during the 21-day curing period.

The CS of the binderless briquettes with a moisture (*i.e*. water) addition of 2.5, 5 and 10% are shown in Figure 4-8. The CS of the binderless briquettes increased with curing time due to the evaporating liquid increasing the capillary pressure in the briquette, but it still did not reach the CS of ROM coal (2.1 MPa) (Botha, 2019; de Assis *et al.*, 2019; Iveson *et al.*, 2001;

Patil *et al.*, 2009). The peak CS for the 2.5, 5 and 10% briquettes was 1.8, 2.2 and 2.3 MPa, respectively. It can be observed that the moisture content did not have a significant impact on the CS of the briquettes and the lowest concentration (2.5%) was therefore chosen to complete the pilot-scale briquette manufacturing of the liquid and slurry containing binders (A, B, C and D), while the highest addition of water (10%) was chosen for the solid binder (E) to enable capillary forces (Massaro *et al.*, 2014).

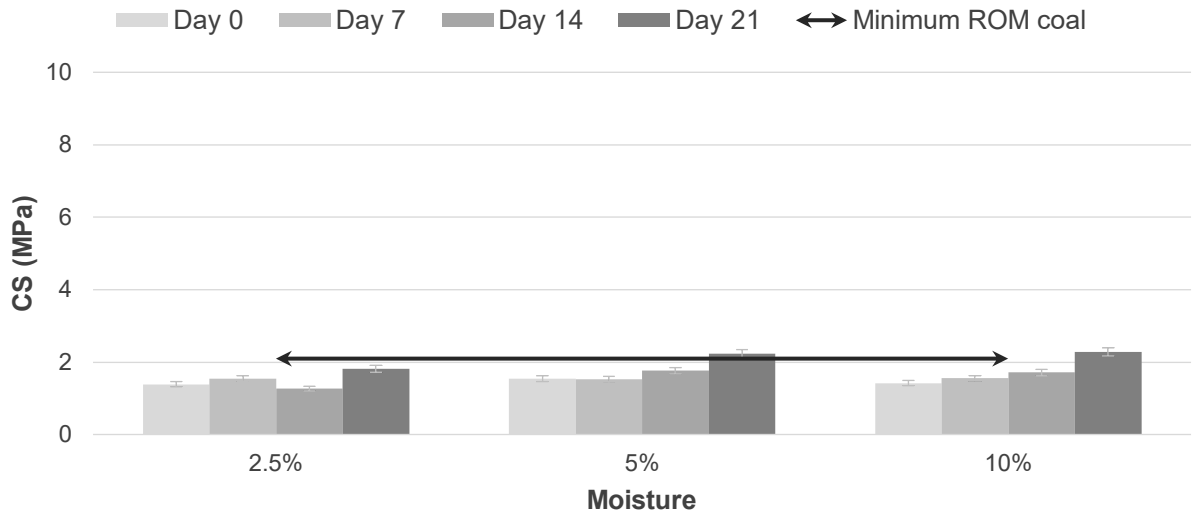

Figure 4-8: Compressive strength results over a period of 21 days of the pilot-scale binderless briquettes manufactured with a moisture addition of 2.5, 5.0 and 10.0%

The CS results for the briquettes bound with Binders A–E are shown in Figure 4-9. The CS of the binders showed similar trends as seen in Phase 1 but peaked at lower values which indicates that the binding mechanisms proposed in Section 4.2 are still valid. The briquettes also took longer to cure due to their larger size. Some variation in the CS trends was observed which may be due to poorer mixing caused by the higher volume of coal and binder batches that were prepared for the pilot-scale briquettes, resulting in the uneven distribution of materials within the briquettes (Rubio *et al.*, 1999). All the briquettes exceeded the minimum ROM coal CS of 2.1 MPa except the Binder D and 10% Binder E bound briquettes thus the binders can be ranked as: C>E>A>B>D.

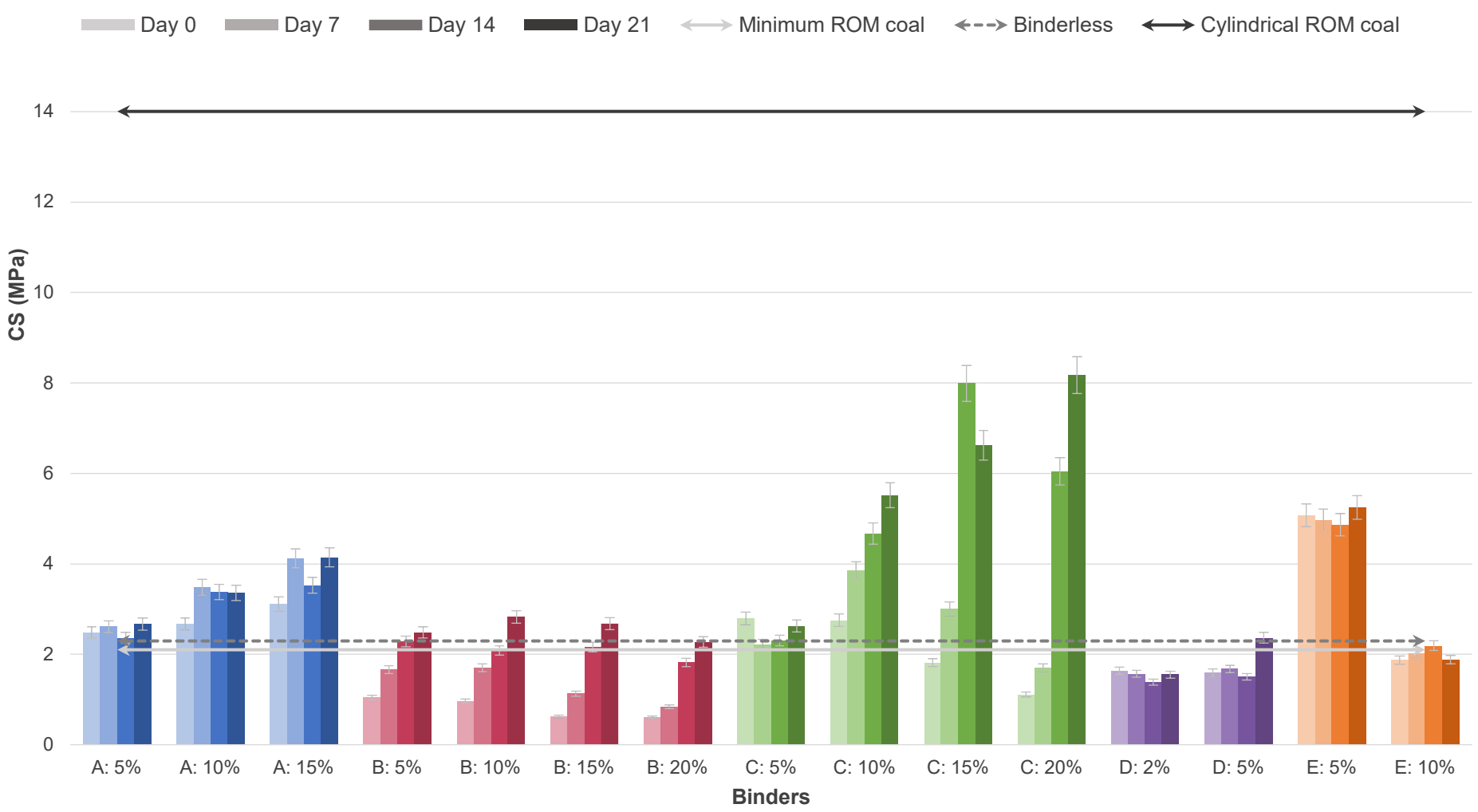

Figure 4-9: Compressive strength results over a period of 21 days of the pilot-scale briquettes manufactured with Binders A–E

4.3.2 Impact resistance results

The IRI is a measure of the briquette's ability to withstand impact forces, *e.g.* hitting a surface during transportation, handling or loading (Dohm *et al.*, 2012). The minimum acceptable IRI is 50 with the briquettes dropped a maximum of 10 times (Richards, 1990). The IRI tabulated results of the briquettes over a 21-day period is shown in Table C-1, Appendix C. The average for each binder type and concentration was calculated and can be seen in Figure 4-10. The effect of the impact when the briquette hits the floor, on the bonds created by each respective binder (as detailed in Section 4.2.1), are discussed in this section.

The briquettes bound with water (2.5–10%) and Binder D (2.5–5%), respectively, did not achieve the minimum IRI. Both binders are mainly dependent on attraction forces and liquid bridges with resulting surface tension and capillary pressure created by the water in the briquette. The impact from hitting the ground during the drop shatter test could therefore easily break these bonds, causing the briquettes to shatter, thereby decreasing the IRI. Binder A is also a film-type binder consisting of mostly water, however the colloidal particles in the binder that form colloidal solid bridges increased the IRI with concentration, resulting in an above minimum IRI of 68 ± 13 at a concentration of 15%.

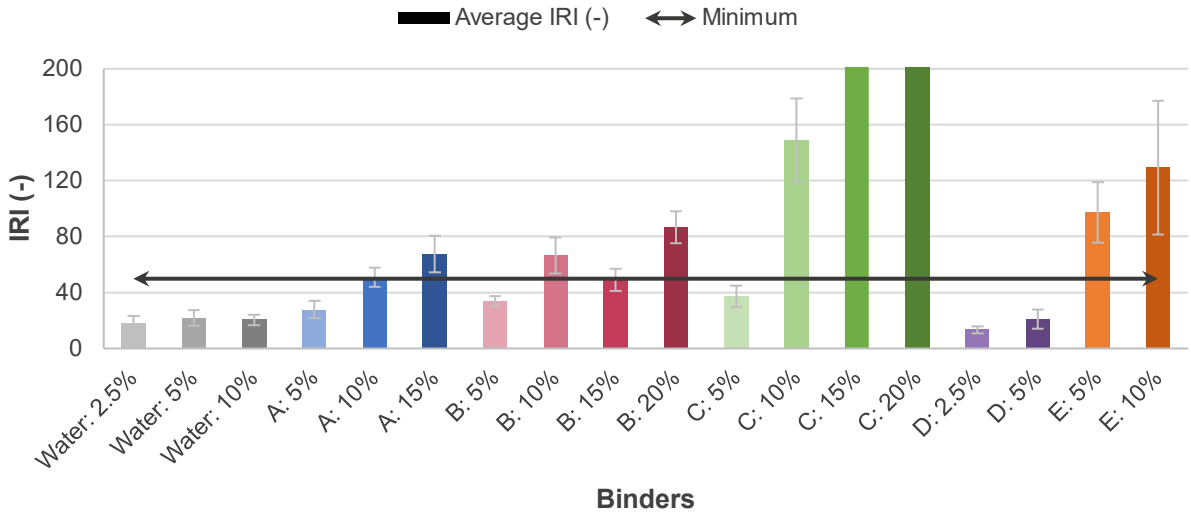

Figure 4-10: Average impact resistance index results of the pilot-scale binderless briquettes and briquettes bound with Binders A–E

The higher viscosities of Binders B and C resulted in an increase in impact resistance with an increase in concentration due to viscosity being the dominant mechanism of energy dissipation (Adams *et al.*, 1994; Ennis *et al.*, 1990; Iveson & Page, 2001; Keningley *et al.*, 1997; Mazzone *et al.*, 1987). Binder B had an acceptable IRI of 66 ± 13 and 87 ± 11 at concentrations of 10 and 20%, respectively. The IRI seems to increase with Binder B concentration, except at a concentration of 15%. This could be due to the large error caused by the limitations of the drop

shatter test discussed in Appendix C, *e.g.* not taking the small pieces/ fines into account when counting the number of pieces the briquette breaks into (Li & Liu, 2000). The IRI of Binder C increases with concentration, and at a concentration larger than 15%, the briquettes do not shatter when they hit the ground after 10 drops, *i.e.* the IRI is 1000 (Blesa *et al.*, 2003; Rubio *et al.*, 1999). This may be a result of Binder C creating a matrix of very high viscosity binder around the coal particles (Iveson & Page, 2001).

4.3.3 Durability results

Friability index, FR (%), and abrasion resistance, AR (%), are both measurements of a briquette's durability, *i.e.* resistance to the formation of fines (Dohm *et al.*, 2012). The FR results of the briquettes, Table C-2 in Appendix C, showed no clear trend based on time and the average for each binder and concentration was therefore calculated and shown in Figure 4-11.

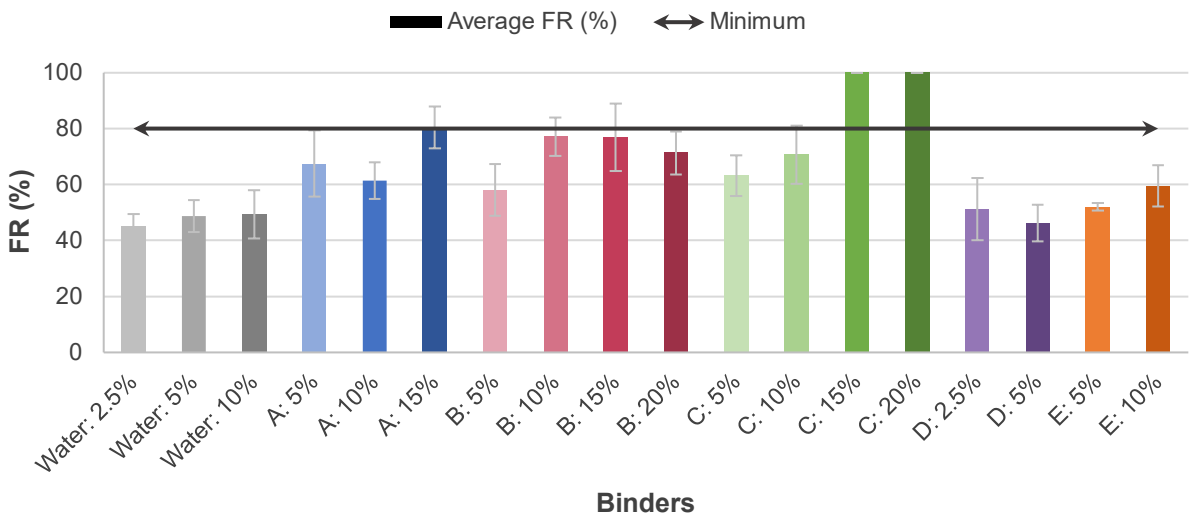

Figure 4-11: Average friability index results of the pilot-scale binderless briquettes and briquettes bound with Binders A–E

The FR of a briquette is calculated from the weight of the largest piece after breaking as a percentage of the initial briquette weight and has a minimum acceptable value of 80% (Kaliyan & Morey, 2009). The goal of this is to limit the amount of smaller, *e.g.* fine, pieces to 20%, though the pillow-shaped briquettes frequently broke in half at the seam where it is weakest (Botha, 2019). This skews the results because the largest piece is approximately half the briquette weight (~50%), but virtually no fines are generated giving an inaccurately low FR. Conversely, the briquette splitting could give an inaccurately high FR if the briquette splitting prevented the briquette from shattering. The FR of most of the briquettes were below the acceptable minimum of 80%, with some Binder A, B and C bound briquettes exceeding it (Kaliyan & Morey, 2009).

Massaro *et al.* (2014) also observed scattered results for the attrition index of plastic bound pillow-shaped briquettes due to inherent inconsistencies in the briquetting process.

The AR results of the briquettes also showed no clear trend and had a maximum difference of 1% so the average for each binder and concentration, Figure 4-12, will be used for analysis. The AR of the binderless briquettes with a lower moisture addition (2.5 and 5%) and the Binder D bound (2.5 and 5%) briquettes had the lowest AR. The AR of the briquettes in Figure 4-12 showed some variation based on concentration.

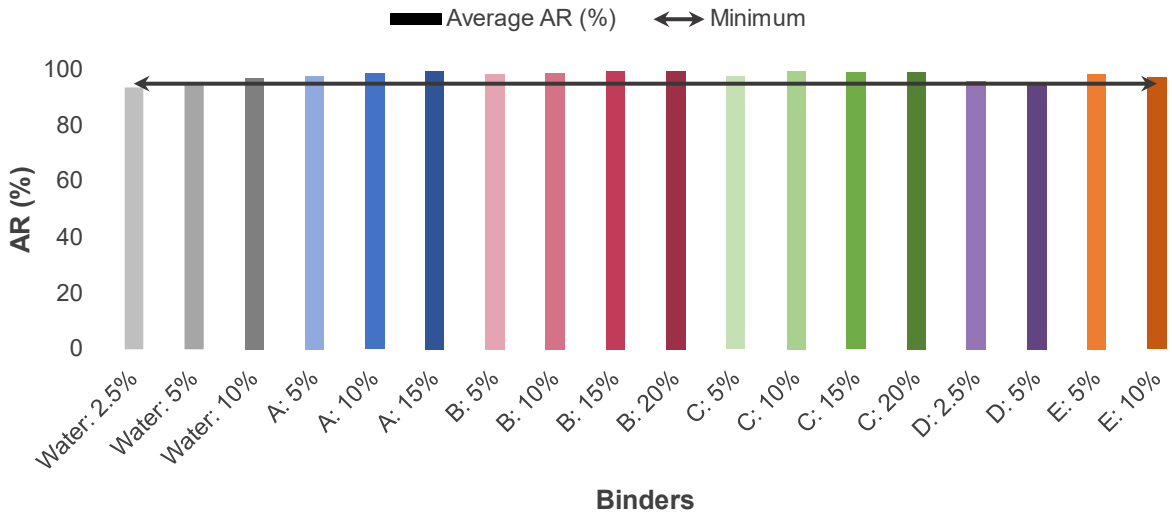

Figure 4-12: Average abrasion resistance results of the pilot-scale binderless briquettes and briquettes bound with Binders A–E

4.3.4 Water resistance results

Most of the briquettes were not very water resistant, however the effect of the binders on the water resistance of the briquettes can still be visually assessed to describe their performance as shown in Appendix D. The briquettes were classified as intact, mostly intact, mostly degraded, or degraded and the time (1, 5, 10, 20, 30 min) when the briquettes were degraded was recorded (Taulbee *et al.*, 2013). The results are tabulated in Table 4-3. The water and Binder D bound briquettes degraded before 5 min which is similar to the briquettes made from lignite and waste materials that were tested by Beker (1997). The poor water resistance of the briquettes is caused by the high kaolinite content in the coal swelling when it is wetted (Leokaoke *et al.*, 2018; Mangena *et al.*, 2004; Motaung *et al.*, 2007). The other binders increased the water resistance of the briquettes to different degrees due to their hydrophobic properties. Binder B is insoluble in water and the water resistance of the 10, 15 and 20% Binder B bound briquettes can therefore be attributed to enough binder coating the coal particles in the briquette and keeping the water out of the briquette matrix (de Assis *et al.*, 2019). The increased water resistance of the

pilot-scale briquettes compared to the lab-scale Binder B bound briquettes can consequently be explained by the higher water addition in the lab-scale briquettes inhibiting the complete coating of coal particles with Binder B. The markedly improved water resistance of the 20% Binder C bound briquettes compared to the briquettes with lower concentrations (≤ 15%) can be explained by the higher viscosity of the binder requiring more binder to sufficiently coat the coal particles (Mills, 1908). The Binder E bound briquettes were all water resistant due to the binder (plastic) creating a solid bridge matrix in the briquette that does not dissolve in water (Massaro *et al.*, 2014).

Table 4-3: Water resistance of the pilot-scale briquettes manufactured with water and Binders A–E based on their condition

Binder		Immersion time (min)	Condition (-)
Type	**Concentration (wt%)**		
Water	2.5	5	Degraded
	10	5	
	15	5	
A	5	10	Mostly degraded
	10	10	
	15	10	Mostly intact
B	5	10	Mostly intact
	10	30	Intact
	15	30	
	20	30	
C	5	5	Degraded
	10	5	
	15	5	
	20	30	Mostly intact
D	2.5	5	Degraded
	5	5	
E	5	30	Intact
	10	30	

If the briquettes were still fully intact after 30 min they were accepted to be water resistant and the WRI and wet compressive strength, CS_{wet}, were determined, Table 4-4 (Richards, 1990). The briquettes bound with 20% Binder B, 5% Binder E and 10% Binder E met the minimum WRI requirement of 95% (Richards, 1990). The CS_{wet} is lower than the original CS of the briquettes,

also observed by Leokaoke *et al.* (2018) and Massaro *et al.* (2014), but still above the minimum CS of 0.373 MPa set by Richards (1990).

Table 4-4: Water resistance index and wet compressive strength of the briquettes bound with Binders B (10, 15, 20%) and E (5, 10%) that were intact after 30 min

Binder		WRI (%)	CS_{wet} (MPa)
Type	**Concentration (wt%)**		
B	**10**	89	0.44
	15	92	0.49
	20	97	0.59
E	**5**	96	1.30
	10	97	1.45

Binder B bound briquettes with WRI ≥ 95%, Binder E bound briquettes with WRI ≥ 95%

4.3.5 Optimisation of binder concentrations for pilot-scale briquettes

The optimisation, or rather satisficing, of the binder concentrations was done with an a posteriori weighing method and equal weights, as shown in Equation 4-1 (Einhorn & Hogarth, 1975; Ennis & Ennis, 2012; Miettinen, 2008). The method is discussed in Appendix E and the optimal binder concentrations and their respective mechanical strength values are tabulated in Table E-1 and summarised in Table 4-5. The optimal briquettes were used for further reactivity testing and the results are presented in Chapter 5.

$$y = 0.143\left(x_{\mathrm{CS}} + x_{\mathrm{IRI}} + x_{\mathrm{durability}} + x_{\mathrm{WRI}} + x_{\mathrm{handling}} + x_{\mathrm{cost}} + x_{\mathrm{hazard}}\right) \qquad (4\text{-}1)$$

Table 4-5: Optimal concentrations for the pilot-scale briquettes manufactured with water and Binders A–E and their mechanical strength and water resistance

Binder		Moisture (wt%)	CS (MPa)	IRI (-)	FR (%)	AR (%)	WRI (%)	CS_{wet} (MPa)
Type	**Concentration (wt%)**							
Water	–	5	2.2	22	49	95.2	–	–
A	15	2.5	4.1	68	80	99.3		
B	20		2.3	87	71	99.5	97.4	0.59
C			8.2	1000	100	99.2	–	–
D	5		2.4	21	46	95.3		
E		10	5.3	97	52	98.3	98.3	1.30

CHAPTER 5: REACTIVITY RESULTS

5.1 Overview

The briquettes with the optimal concentration for each binder (5% water, 15% Binder A, 20% Binder B, 20% Binder C, 5% Binder D and 5% Binder E) were evaluated to determine the effect of the binders on the briquette reactivity. The results were mainly compared to the performance of the binderless briquettes as a deeper investigation is beyond the scope of this study. Section 5.2 contains the proximate analysis and calorific value results of the optimal briquettes, while the pyrolysis, combustion and gasification behaviour of the briquettes are discussed in Sections 5.3–5.5. The results of the reactivity tests are used to match the binders to possible end-use industries in Section 5.6. The reproducibility of the tests is discussed in Appendix I.

5.2 Proximate analysis and calorific value results

The proximate analysis of the binderless and optimal Binder A–E bound briquettes is shown in Table 5-1. The properties were used to evaluate the behaviour of the briquettes during the reactivity tests and to compare with the yields that were obtained.

Table 5-1: Proximate analysis and calorific value results of the optimal concentration briquettes compared to ROM coal adapted from Leokaoke *et al.* (2019)

Property	ROM[a]	Water	A	B	C	D	E
Proximate analysis (wt%, db)							
Ash yield	19.8	30.8	29.3	28.1	26.1	31.3	28.1
Volatile matter	24.1	25.0	27.2	32.6	34.2	25.2	29.4
Fixed carbon content*	56.0	44.2	43.4	39.3	39.7	43.5	42.5
Gross calorific value (MJ/kg, adb)							
CV	26.0	20.1	20.7	20.8	21.7	20.4	20.6

[a] Leokaoke et al. (2019)

* by difference

The inherent moisture of the briquettes were similar and can be ordered as: water bound (*i.e.* binderless) and Binder A bound briquettes (5.1%) > Binders D and E bound briquettes (4.8%) > Binder C bound briquettes (4.4%) > Binder B bound briquettes (3.5%). The ash yield for the binder bound briquettes generally decreased, which may be due to the binders comprising of mostly liquids which did not leave a substantial residue, *i.e*. ash, behind. The increase in volatile matter and decrease in fixed carbon can be attributed to the volatile nature of some of the binders and corresponds to the behaviour of similar binders from literature (Fernando, 2007; Folgueras *et al.*, 2003; Gao & Li, 2019; Gwenzi *et al.*, 2020; Leckner & Lind, 2020; Massaro *et al.*, 2014; Nwabue *et al.*, 2017; Otero *et al.*, 2008). The increase in CV due to binder addition was very small, with Binder C bound briquettes having the highest CV (~1.6 MJ/kg) and

Binder E bound briquettes exhibiting almost no increase in CV (~0.5 MJ/kg), which contradicts most previous studies with plastics (Gao & Li, 2019; Massaro *et al.*, 2014; Nwabue *et al.*, 2017).

5.3 Pyrolysis results

The thermal fragmentation and Fischer assay results are provided in this section to evaluate the effect of Binders A–E on the behaviour of the briquettes during pyrolysis.

5.3.1 Thermal fragmentation results

The thermal fragmentation test results provide insight into the primary fragmentation that occurs during pyrolysis, *i.e.* heating in an inert environment. The binderless and Binder A–E bound briquettes, Figure 5-1, were heated at a high heating rate (45°C/min) and the resulting briquettes are shown in Figure 5-2. The discoloration at the ends of the briquettes can be attributed to the small amount of air that was trapped in the crucibles reacting with the coal.

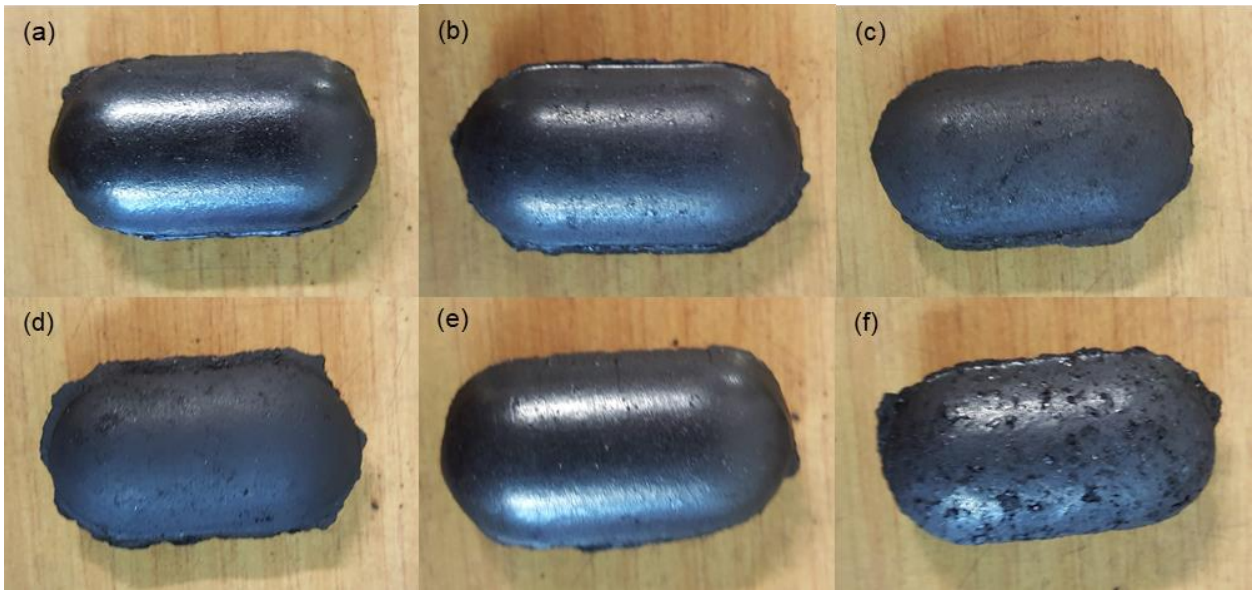

Figure 5-1: Thermal fragmentation pre-test images of the optimal concentration briquettes with (a) 5% moisture, (b) 15% Binder A, (c) 20% Binder B, (d) 20% Binder C, (e) 5% Binder D, and (f) 5% Binder E

No significant fragmentation, *i.e.* breakage, was observed and the fragmentation could therefore not be calculated with the Ergun index as described by Equations 2-10 and 2-11. This is in contradiction to the high volatile matter (> 24%, adb), as indicated in Table 5-1, and the binder content in the briquettes suggesting that some fragmentation will occur. This observation may be attributed to the higher porosity in the briquettes allowing the volatile matter to escape and reducing internal pressure build-up (England, 2000; Gajewski & Kosowska, 2005; Senneca *et al.*, 2011). Leokaoke *et al.* (2019) also did not observe fragmentation for briquettes bound with resin or lignosulphonate and attributed it to the findings of Bunt and Waanders (2008) stating that small Highveld coal particles (< 25 mm) do not have a high propensity for thermal

fragmentation. The micropore surface area of the resin and lignosulphonate bound briquettes in the previously stated study increased during pyrolysis due to the decomposition of the binders and the reduced interparticle bonding could also have provided less resistance to the escape of volatiles. The possible effect of the binders on attrition fragmentation, *i.e.* formation of fines, is discussed in Appendix F.

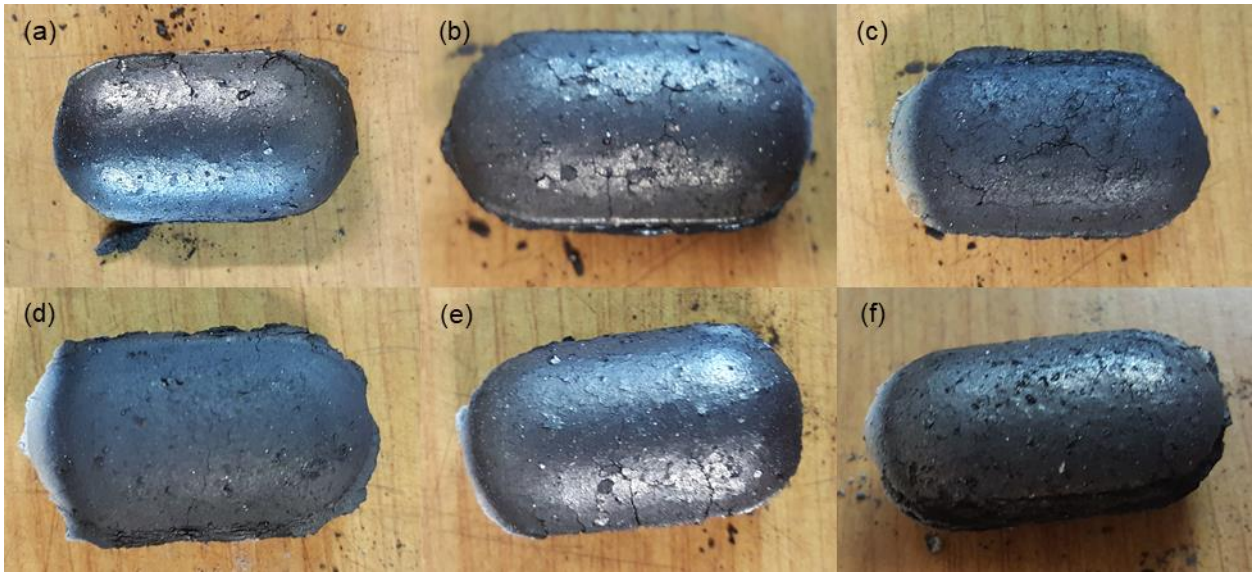

Figure 5-2: Thermal fragmentation post-test images of the optimal concentration briquettes with (a) 5% moisture, (b) 15% Binder A, (c) 20% Binder B, (d) 20% Binder C, (e) 5% Binder D, and (f) 5% Binder E

The result of the free swelling index (FSI) test is shown and discussed in Appendix G. Binders A and D had no effect on the FSI of the coal calculated with Equation 2-12, while Binders B, C and D only produced a slight increase due to their higher volatile matter contents (Dakič *et al.*, 1989). A low FSI usually correlates with more thermal fragmentation due to the decreased swelling ability increasing the internal pressure so the lack of briquette fragmentation supports the theory that the porosity of the briquettes allowed the volatiles to more easily escape (Stubington & Linjewile, 1989). Further tests will however be necessary to substantiate this.

5.3.2 Fischer assay results

The pyrolysis product yields (wt%), *i.e.* char, tar, water and gas, of the Fischer assay test that was conducted at 900°C are shown in Table 5-2. The water yield (5–10%) is comprised of surface and pore moisture, inherent moisture and pyrolytic water, and is aptly higher than the respective inherent moistures of the briquettes, listed in Table 5-1 (3.5–5.1%) (Meyer, 2020; Pretorius *et al.*, 2017). The difference in char yields of the briquettes can be explained by their respective fixed carbon contents, as seen in Table 5-1, and is in the range (70–75%) that can be expected for medium to high-temperature pyrolysis (Ladner, 1988; Meyer, 2020). The char yield was compared to that of the pyrolysis and proximate analyses of the briquettes in Appendix I and

shows a good correlation (error < 1%). The Binder B and C bound briquettes had the highest volatile matter content and consequently the highest evolved volatile yield, *i.e.* tar and gas (Ladner, 1988; Xu & Tomita, 1987). The relatively high tar yield (9.4%) of the 20% Binder C bound briquettes can be attributed to the high binder concentration and pitch being the main component of tar at 900°C (Hu *et al.*, 2004; Ladner, 1988).

Table 5-2: Fischer assay results of the optimal briquettes

Property	Water	A	B	C	D	E
			Pyrolysis yields (wt%)			
Water	6.4	8.8	5.9	7.6	5.4	9.8
Char	71.0	71.0	66.6	63.5	71.5	68.3
Tar	2.5	3.0	4.5	8.7	1.8	3.2
Gas	20.1	17.2	23.0	20.2	21.3	18.8

The gas product contains low-molecular weight volatiles and consists mainly of H_2, CH_4, CO and CO_2 (Bell *et al.*, 2011; Dong *et al.*, 2019; Speight, 2012). The normalised (N_2 and C_2-C_6 hydrocarbon-free basis) composition (%) of these components in the pyrolysis gas are shown in Figure 5-3.

The gas compositions were all comparatively similar to the binderless briquettes, especially the Binder B and D bound briquettes which contained primarily water. A high H_2 yield is typical for pyrolysis above 900°C due to the dehydrogenation reaction of the aromatic clusters occurring at high temperatures (Hu *et al.*, 2004; Xu & Tomita, 1987). The small differences in the compositions of the Binder B, C and E briquettes are due to the binders containing more chemicals, with the most important being hydrocarbons and oxygen-containing polymers (Andreikova *et al.*, 2017; Massaro *et al.*, 2014; Sørum *et al.*, 2001; Straka *et al.*, 1998).

The pyrolysis product yields, and gas compositions were all comparable to that of other studies done at high 900°C and no noteworthy impact was observed from the addition of Binders A–E (Meyer, 2020; Pretorius *et al.*, 2017; Roets *et al.*, 2015; Uwaoma *et al.*, 2019). The effects on the char and tar yields were not investigated and may provide more insight into the specific effects of the hydrocarbons and polymers in Binders B, C and E.

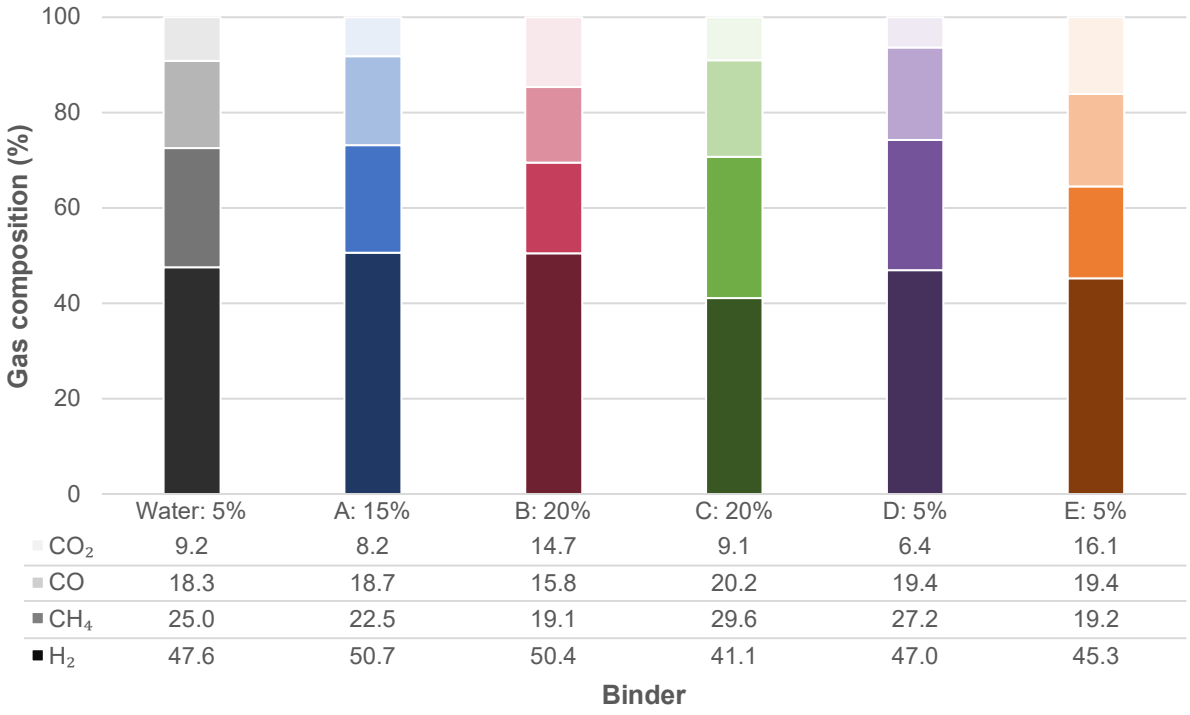

Figure 5-3: Pyrolysis gas composition (H_2, CH_4, CO, CO_2) of the optimal concentration briquettes

5.4 Combustion results

The mass loss (g) and time (s) data of the combustion experiments were refined with the least squares method and plotted in Excel® to obtain a 4th order polynomial trendline ($R^2 > 0.999$). This was done to reduce the number of data points and to create an equation to differentiate. The carbon conversion, X (-), was calculated with Equation 5-1, as previously done by Coetzee *et al.* (2013), du Toit (2013), and Leokaoke *et al.* (2019). In Equation 5-1, m_0 is the initial mass of the charred briquette, m_{ash} is the mass of residual ash and m_i is the mass at time t_i. The conversion graphs (X vs. t) of the combustion tests are provided in Appendix H and the repeatability of the results are shown in Appendix I.

$$X = \frac{m_0 - m_i}{m_0 - m_{\text{ash}}} \tag{5-1}$$

The conversion rate, dX/dt (min^{-1}), was then determined with Equation 5-2.

$$\frac{\mathrm{d}X}{\mathrm{d}t} = \frac{X_i - X_{i-1}}{t_i - t_{i-1}} \tag{5-2}$$

Figu shows the conversion rates versus conversion (up to 50%) with a 95% confidence level for all the briquettes, *i.e.* binderless and Binders A–E bound, obtained from the combustion tests at (a) 850°C, (b) 875°C, and (c) 900°C. No clear trend was observed based on binder addition and the effect of temperature seems to be negligible. A maximum initial conversion rate with

subsequent decrease was observed with an increasing carbon conversion and can be attributed to pore coalescence and collapse decreasing the available reaction surface area and active sites (Coetzee, 2011; Leokaoke *et al.*, 2019; Liu *et al.*, 2000; Rambuda, 2015).

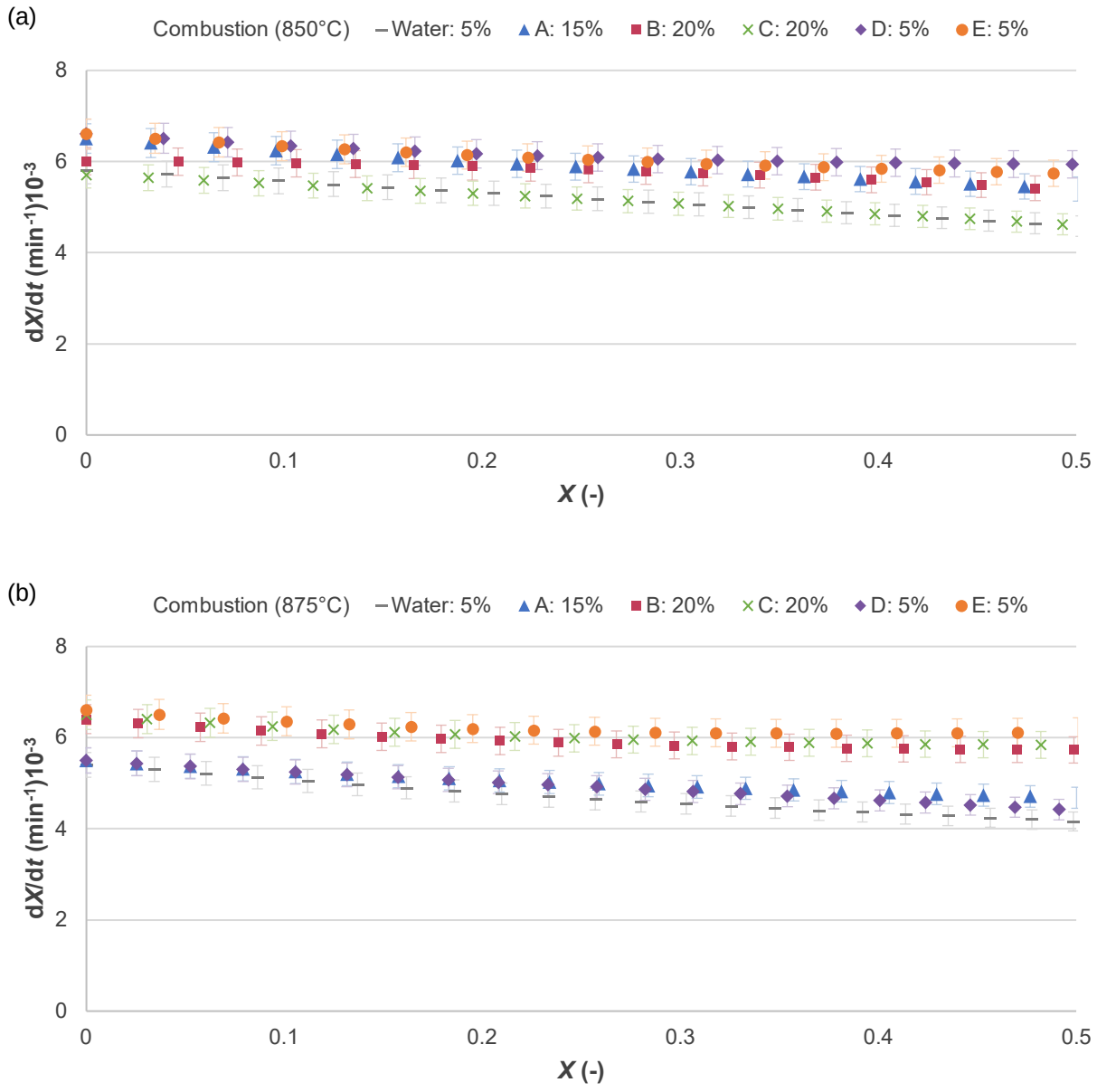

Figure 5-4: Graphs of the conversion rate versus conversion for the binderless and Binder A–E bound briquettes during combustion at (a) 850°C, (b) 875°C, and (c) 900°C

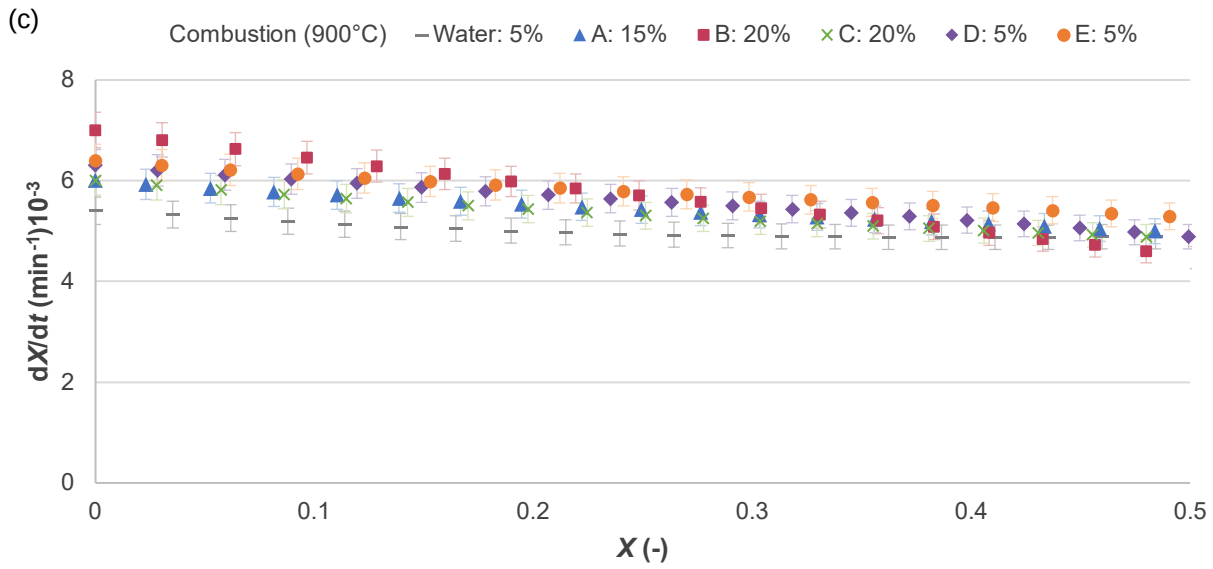

Figure 5-4 (continued)

Binders A–E all decomposed at ≤ 500°C, based on literature values of similar binders, and therefore did not significantly influence the combustion process aside from the char formation during pyrolysis (Andreikova *et al.*, 2017; Botha, 2019; Cozzani *et al.*, 1995; Leokaoke *et al.*, 2019; Massaro *et al.*, 2014; Sørum *et al.*, 2001; Wallouch *et al.*, 1972).

5.5 Gasification results

The gasification results were refined as discussed for the combustion results in Section 5.4 and the repeatability of the test is demonstrated in Appendix I. Figure 5-5 shows the conversion rate versus conversion (up to 20%) with a 95% confidence level for the binderless and Binders A–E bound briquettes during gasification at (a) 1000°C and (b) 1025°C.

An increase in initial conversion rate was observed with an increased in temperature from 1000 to 1025°C. Bunt *et al.* (2015) and Leokaoke *et al.* (2019) also noted an increased gasification rate for coal briquettes with an increase in temperature at 1000°C. The gasification rates of the briquettes were also higher than ROM coal in both studies. The initial conversion rates for gasification (2.0–4.6 min^{-1}) were lower than those for combustion (5.4–7.0 min^{-1}), which agrees with literature (Rambuda, 2015; Smoot & Smith, 1985). There is no apparent trend based on the binder addition, also observed for the combustion results, due to the binders decomposing at ≤ 500°C (Andreikova *et al.*, 2017; Botha, 2019; Cozzani *et al.*, 1995; Leokaoke *et al.*, 2019; Massaro *et al.*, 2014; Sørum *et al.*, 2001; Wallouch *et al.*, 1972).

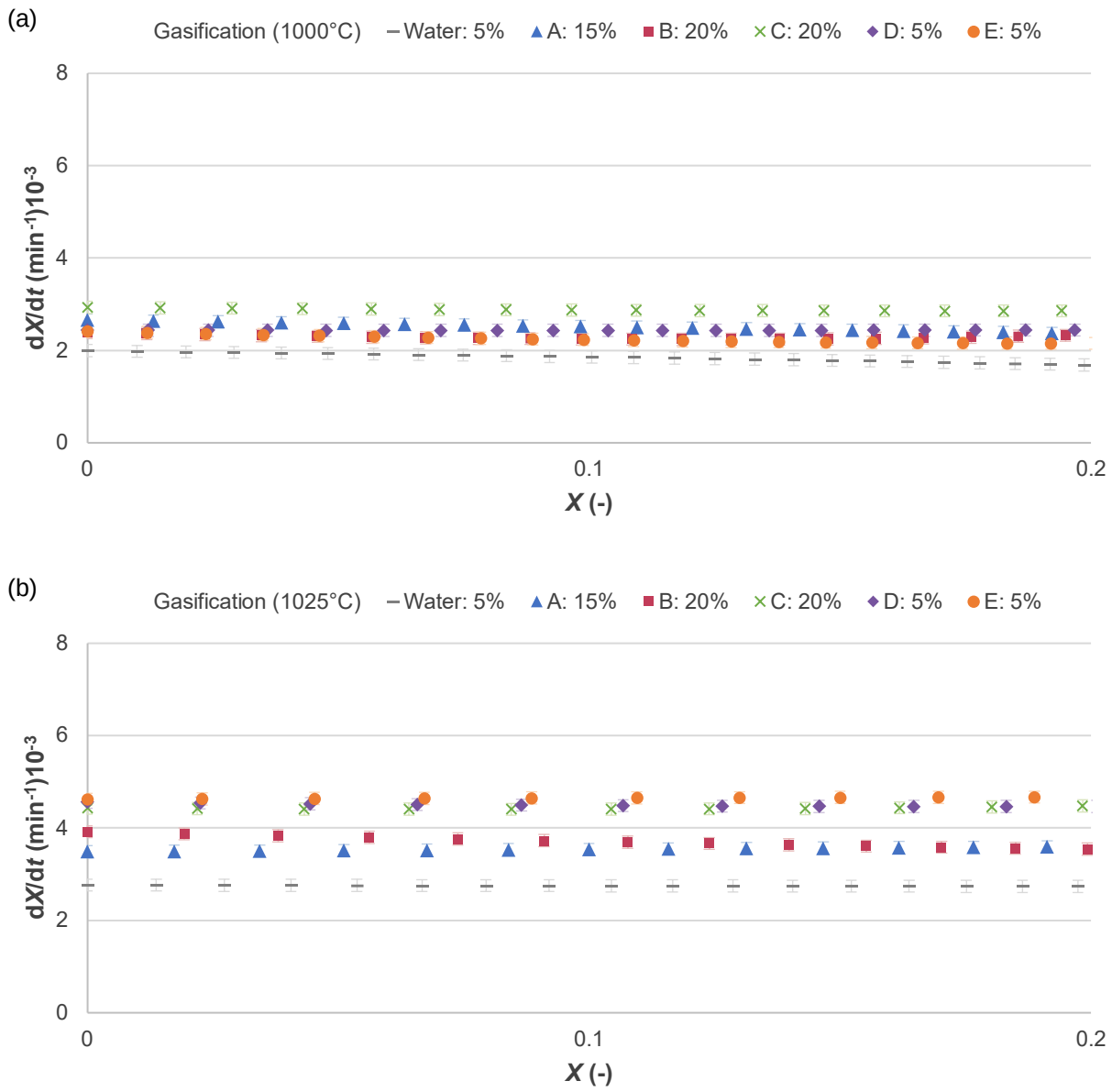

Figure 5-5: Graphs of the conversion rate versus conversion for the binderless and Binder A–E bound briquettes during gasification at (a) 1000°C and (b) 1025°C

5.6 Matching with industrial processes

A good binder should increase mechanical strength, increase water resistance, increase reactivity, be eco-friendly and be financially feasible (England, 2000; Mills, 1908; Waters, 1969). If the binder does not increase these properties, it should at least not decrease them. The results of the reactivity tests performed on the Binder A–E bound briquettes compared to the binderless briquettes indicate that the binders do not have a significant influence on the utilisation behaviour of the briquettes and are therefore mainly beneficial in terms of mechanical strength. This will be important in terms of transporting, handling and storing the briquettes. The negligible effect of Binders A–E during combustion and gasification therefore does not exempt them from use in

industrial processes and the properties of the coal will be the determining factor in matching them with suitable industrial processes (*i.e.* co-combustion or co-gasification).

According to Carpenter (2006), the co-combustion of briquettes may have a significant effect on the ignition, capacity, heat rate, availability and maintenance requirements of the plant. Pulverised coal combustion (PCC), stoker-fired boilers and circulating fluidised bed combustion (CFBC) boilers have been used to combust waste fuels (Fernando, 2007). The moisture content, volatile matter content, ash yield and calorific value requirements of the PCC and CFBC boilers are shown in Table 5-2.

Table 5-3: Properties of coal feedstock used in PCC and CFBC boilers

Property	**Unit**	**PCC[a-d]**	**CFBC[e-k]**
Moisture content (ar)	**%**	4–8, <12*	~12, <23–65*
Volatile matter content (db)	**%**	>20–30	10–55
Ash yield (db)	**%**	25–30, <35*	10–17, <25–65*
Calorific value (ar)	**MJ/kg**	>23*–25	20–25, >5

Sources: [a] De Korte and Jeffrey (2016), [b] Skorupska (1993), [c] Wu (2005), [d]Steyn and Minnitt (2010), [e]Hotta (2009), [f]Henderson (2003), [g]Fernando (2004), [h]Aziz and Dittus (2011), [i]Belaid (2017), [j]Wu (2006), and [k]Jin *et al.* (2003)

* Outer limits

The briquettes with lower mechanical strengths, *i.e.* binderless, Binder B and D bound, may be more suitable as feedstock for a PCC boiler. The agglomeration of the coal enables easier handling and transportation while the lower strength of the briquettes reduces the costs involved in pulverising the agglomerates. The moisture content (4.4–5.1%, adb), ash yield (26.1–31.3%, db) and volatile matter content (25.0–34.2%, db) of the briquettes are within the limit of the PPC boiler feedstock, but the CV (20.1–21.7 MJ/kg) is below the required value (Aziz & Dittus, 2011; de Korte & Jeffrey, 2016; Fernando, 2004). The ash yield is higher than the set maximum of CFBC boilers, but can be accommodated if the operating parameters are adjusted (Fernando, 2007).

Co-gasifying the briquettes in a Lurgi-gasifier is a good option due to its compatibility with low rank coal as a feedstock, as illustrated by the values in Table 5-4 (van Dyk *et al.*, 2001; Weiss & Turna, 2009). The properties of the briquettes are well suited for gasification. The absence of thermal degradation and swelling properties of the briquettes are also beneficial to the process as the production of fines and/ or clinkers lead to pressure drop fluctuations and unstable operations (Vamvuka, 1999; van Dyk *et al.*, 2001). The water-resistant Binder E bound briquettes may be especially suited to co-gasification due to the coal fed to the process being stored in heaps that are exposed to the elements, as well as wet sieving before use.

The briquettes are not well suited for use in the metallurgical industry due to their high ash yield, low volatile matter content and lack of swelling properties (Carpenter, 2004; Chatterjee, 2010).

Table 5-4: Properties of coal feedstock used in CTL gasifiers

Property	Unit	CTL
Moisture content (ar)	**%**	~5, <10–30*
Volatile matter content (db)	**%**	>21
Ash yield (adb)	**%**	<20–29, 35*
Calorific value (adb)	**MJ/kg**	~30, >20

Source: Vamvuka (1999), Van Dyk *et al.* (2006), Weiss & Turna (2009), Van Dyk *et al*. (2001), and Couch (2008),

* Outer limits

CHAPTER 6: CONCLUSION AND RECOMMENDATIONS

6.1 Overview

The conclusions that were made from the mechanical strength tests and reactivity experiments along with the resulting contribution to the knowledge of science and technology are discussed in this chapter. Recommendations for future studies are also listed.

6.2 Conclusions

The following conclusions were derived from the mechanical strength and reactivity results of the briquettes and are presented under the objectives stated in Chapter 1:

- Objective 1: Prepare and characterise the discard coal and waste materials (*i.e.* potential binders)

Highveld inertinite-rich, high-ash (30%, db) coal from a filter cake (-272 µm) was used to test the binding properties of industrial wastes.

Five industrial wastes were evaluated to determine their efficacy in the agglomeration of coal fines: (A) waterworks bio-sludge from a petrochemical industry, (B) acrylic acid containing a hydrocarbon by-product from a petrochemical industry, (C) pitch from a petrochemical industry, (D) wax emulsion from a petrochemical industry, and (E) recycled low-density polyethylene (LDPE) from a North-West plastic recycling company. These binders were selected for waste reduction due to possible advantageous properties they possess with regards to agglomeration and/or reactivity. The addition of the binders, however, mainly affected the agglomeration, *i.e*. strength and in some cases water resistance, of the briquettes.

- Objective 2: Assess the effect of different waste materials at various concentrations on the mechanical strength and water resistance of briquettes produced on laboratory-scale

The CS of the binderless briquettes (3.4 MPa) was higher than the minimum CS of bituminous ROM coal (2.1 MPa). Binders A–E increased the CS of the briquettes in the following order: C > E > B > A > D (descending). During the lab-scale production, 15% Binder C bound briquettes were the only briquettes that exceeded the CS of cylinder-shaped Highveld ROM coal (14 MPa) due to the binder's high viscosity.

Briquettes bound with 5–15% Binder E had an acceptable water resistance (WRI ≥ 95%).

- Objective 3: Quantify the effect of the waste materials on the mechanical strength of briquettes produced on pilot-scale

The CS, IRI, FR and AR were used to evaluate the strength of the briquettes. The optimal concentration for each binder, based on mechanical strength (CS, IRI, FR, AR), was determined as 15% Binder A (4.1 MPa; 68; 80%; 99.3%), 20% Binder B (2.3 MPa, 87, 71%, 99.5%), 20% Binder C (8.2 MPa, 1000, 100%, 99.2%), 5% Binder D (2.4 MPa, 21, 46%, 95.3%) and 5% Binder E (5.3 MPa, 97, 52%, 98.3%). Compared to the optimal binderless briquettes which were manufactured with 5% water (2.2 MPa, 22, 49%, 95.2%), the binders had a beneficial effect to the order of: C > E > A > B > D, with Binder D having almost no effect. Binders A–E, however, all had an increasing effect on the strength of the briquettes and can therefore be utilised to reduce the costs and pollution associated with disposing of the waste materials.

- Objective 4: Assess the effect of different waste materials on the water resistance of the pilot-scale briquettes

Briquettes bound with 20% Binder B, and 5–10% Binder E had an acceptable water resistance (WRI ≥ 95%). The Binder B bound briquettes were water resistant from an addition of 10% as the hydrophobic material was in sufficient concentration to coat the coal particles, preventing water from entering the briquettes. The briquettes bound with Binder E were water resistant from the lowest concentration due to the plastic melting and coating the particles to create a solid matrix between the coal particles.

- Objective 5: Conduct reactivity tests to determine the appropriate industrial processes where the briquettes could be utilised

The conversion rate of the combustion and gasification reactivity of the briquettes were unaffected by binder addition due to the decomposition of the binders below 500°C, during pyrolysis. The binders also did not affect the thermal (i.e. primary) fragmentation of the briquettes; however the composition of the char, tar and water yield may provide more insight into the behaviour of the binders during pyrolysis. The binderless as well as the Binder B and D bound briquettes may be suitable for use in PCC boilers due to their strength being high enough to enable transportation and low enough not to inhibit pulverising. Binders B, C and E bound briquettes may be more suited for use in a Lurgi-gasifier. None of the binders are recommended for use in blast furnaces due to the high ash yield, low volatile matter content and lack of swelling properties.

6.3 Contribution to the scientific field

The use of industrial wastes as binder in the briquetting of Highveld inertinite-rich coal fines is feasible. The effect of the binders was primarily observed with regards to the physical properties of the briquettes and the addition of industrial wastes to coal briquettes can consequently be used to reduce these wastes. This will also enable the use of coal fines which are an underutilised resource.

6.4 Recommendations

The following recommendations are made for future studies:

- Investigate the synergistic effects of the binders (*i.e.*, as compound binders) in different combinations to determine if the positive attributes can be combined for better quality briquettes. Other additives may also be investigated to minimise the hazardous gases that are released during end-use processes.
- Use Binder E (LDPE) to create extrudates with extrusion pelletising equipment to continually add heat during agglomeration thereby reducing the breakage that occurs due to the plastic swelling during post-agglomeration curing.
- Build an experimental rig that can move (*e.g.*, tumble) and heat the briquettes during thermal degradation testing to evaluate the thermal fragmentation and attrition of the briquettes since the heat weakens the briquettes, but that is not clear until force is applied to the briquettes.
- Do more in-depth analyses on the briquettes with regards to environmental impact, *e.g.* do a TG-MS analysis to evaluate the type of gases that are released during combustion/ gasification.
- Conduct a techno-economic feasibility study to determine the financial implications of using the briquettes in the proposed industries.

LIST OF REFERENCES

Adams, M.J., Mullier, M.A. & Seville, J.P.K. 1994. Agglomerate strength measurement using a uniaxial confined compression test. *Powder Technology*, 78(1):5-13. https://doi.org/10.1016/0032-5910(93)02777-8

Adeleke, A.A., Odusote, J.K., Lasode, O.A., Ikubanni, P.P., Malathi, M. & Paswan, D. 2019. Densification of coal fines and mildly torrefied biomass into composite fuel using different organic binders. *Heliyon*, 5(7):e02160. https://doi.org/10.1016/j.heliyon.2019.e02160

Altun, N.E., Hicyilmaz, C. & Bagci, A.S. 2003. Combustion characteristics of coal briquettes: 1. thermal features. *Energy Fuels*, 17(5):1266-1276. https://doi-org.nwulib.nwu.ac.za/10.1021/ef0202891

Andreikova, E.I., Dikovinkinaa, Y.A., Pervovaa, M.G. & Krasnikovaa, O.V. 2017. Pyrolysis of lignin in coal-tar pitch. *Solid Fuel Chemistry*, 51(1):6-16. https://doi.org/10.3103/S0361521917010025

Arnold, B.J. 2013. Coal formation. In: Osbourne, D.G., ed. *The coal handbook: towards cleaner production*, v. 1. pp. 31-52. https://doi.org/10.1533/9780857097309.1.31

ASTM (American Society for Testing and Materials). 2004. *Standard test method for major and minor elements in coal and coke ash by X-ray fluorescence*. West Conshohocken, PA. (ASTM D4326-04).

Aziz, T. & Dittus, M.H. 2011. Kuyasa mine-mouth coal-fired power project: evaluation of circulating fluidized-bed technology. In: Luckos, A. & Den Hoed, P., eds. *Conference proceedings*. Industrial Fluidization South Africa (IFSA), Johannesburg, South Africa. Johannesburg: Southern African Institute of Mining and Metallurgy. pp. 11-29.

Ban, T.E. 1981. *Traveling grate stoker for the combustion of difficultly ignited fuels*. (Patent: US 4263857A). https://patentimages.storage.googleapis.com/4f/56/56/bc67b7401b71a3/US4263857.pdf Date of access: 15 Aug. 2020.

Barišić, V., Zabetta, E.C., Eriksson, T., Hotta, A., Kokki, S., Nuortimo, K. & Palonen, J. 2009. CFB technology provides solutions for reducing CO_2 emissions. *Journal of the Southern African Institute of Mining and Metallurgy*, 109(2):107-119.

Beker, Ü.G. 1997. Briquetting of Afşin-Elbistan lignite of Turkey using different waste materials. *Fuel Processing Technology*, 51(1-2):137-144. https://doi.org/10.1016/S0378-3820(96)01081-8

Belaid, M. 2017. *Behaviour of selected South African coals in circulating fluidised bed (CFB) in comparison with Russian coal.* Johannesburg: University of the Witwatersrand. (Thesis – PhD). https://hdl.handle.net/10539/24855

Bell, D.A., Towler, B.F. & Fan, M. 2011. *Coal gasification and its applications*. Norwich: William Andrew, Inc.

BGR (Federal Institute for Geosciences and Natural Resources). 2019. *BGR energy study 2018: data and developments concerning German and global energy supplies*. https://www.bgr.bund.de/EN/Themen/Energie/Downloads/energiestudie_2018_en.pdf?__blob=publicationFile&v=3 Date of access: 20 July 2019.

Blesa, M.J., Miranda, J.L., Izquierdo, R.M. & Moliner, R. 2003. Curing temperature effect on mechanical strength of smokeless fuel briquettes prepared with molasses. *Fuel*, 82(8):943-947. https://doi.org/10.1016/S0016-2361(02)00416-7

Boerefijn, R., Ghadiri, M. & Salatino, P. 2007. Attrition in fluidised beds. In: Salman, A.D., Ghadiri, M. & Hounslow, M.J., eds. *Handbook of powder technology: particle breakage*, v. 12. Amsterdam: Elsevier Science. pp. 1019-1053. https://doi.org/10.1016/S0167-3785(07)12028-5

Borowski, G. & Hycnar, J.J. 2013. Utilization of fine coal waste as a fuel briquettes. *International Journal of Coal Preparation and Utilization*, 33(4):194-204. https://doi.org/10.1080/19392699.2013.787993

Botha, D.L. 2019. *Evaluation of binders in briquetting of coal fines for application in combustion processes.* Potchefstroom: North-West University. (Dissertation – MEng). http://hdl.handle.net/10394/33988

Bowen, B.H. & Irwin, M.W. 2008. *Coal characteristics*. [PowerPoint]. https://www.purdue.edu/discoverypark/energy/assets/pdfs/cctr/outreach/Basics8-CoalCharacteristics-Oct08.pdf Date of access: 18 July 2019.

BP 2019. *BP statistical review of world energy*. https://www.bp.com/content/dam/bp/business-sites/en/global/corporate/pdfs/energy-economics/statistical-review/bp-stats-review-2019-full-report.pdf Date of access: 20 July 2020.

Bunt, J.R. & Waanders, F.B. 2008. An understanding of lump coal physical property behaviour (density and particle size effects) impacting on a commercial-scale Sasol-Lurgi FBDB gasifier. *Fuel*, 87(13-14):2856-2865. https://doi.org/10.1016/j.fuel.2008.03.022

Bunt, J.R., Neomagus, H.W.J.P., Botha, A.A. & Waanders, F.B. 2015. Reactivity study of fine discard coal agglomerates. *Journal of Analytical and Applied Pyrolysis*, 113(1):723-728. https://doi.org/10.1016/j.jaap.2015.03.001

Cairncross, B. 2001. An overview of the Permian (Karoo) coal deposits of southern Africa. *Journal of African Earth Sciences*, 33(3-4):529-562. https://doi.org/10.1016/S0899-5362(01)00088-4

Carpenter, A. (IEA Clean Coal Centre). 2004. *CCC/88: use of coal in direct ironmaking processes*. https://www.iea-coal.org/report/use-of-coal-in-direct-ironmaking-processes-ccc-88/ Date of access: 16 June 2019.

Carpenter, A. (IEA Clean Coal Centre). 2006. *CCC/116: use of PCI in blast furnaces*. https://www.iea-coal.org/report/use-of-pci-in-blast-furnaces-ccc-116/ Date of access: 16 June 2019.

Carpenter, A. (IEA Clean Coal Centre). 2010. *CCC/166: injection of coal and waste plastics in blast furnaces*. https://www.iea-coal.org/report/injection-of-coal-and-waste-plastics-in-blast-furnaces-ccc-166/ Date of access: 16 June 2019.

Chaiklangmuang, S., Supa, S. & Kaewpet, P. 2008. Development of fuel briquettes from biomass-lignite. *Chiang Mai Journal of Science*, 35(1):43-50.

Chatterjee, A. 2010. *Sponge iron production by direct reduction of iron oxide*. New Delhi: PHI Learning Pvt. Ltd.

Chirone, R., Cammarota, A., D'Amore, M. & Massimilla, L. 1982. Fragmentation and attrition in the fluidized combustion of coal. In. *Conference proceedings*. 7th International Conference On Fluidized Bed Combustion, Philadelphia, Pennsylvania. Springfield: National Technical Information Service, U.S. Department of Commerce.

Clark, K., Meakins, R., Attalla, M. & Craig, K. (CSIRO Energy Technology). 1997. *Agglomeration and stabilisation of collie coals by binderless briquetting*. https://www.acarp.com.au/abstracts.aspx?repId=C3100 Date of access: 20 Oct. 2019.

CMSA (Chamber of Mines of South Africa). 2018. *National coal strategy for South Africa*. https://www.mineralscouncil.org.za/component/jdownloads/send/25-downloads/535-coal-strategy-2018 Date of access: 20 June 2019.

Coelho, M.C. & Harnby, N. 1978. The effect of humidity on the form of water retention in a powder. *Powder Technology*, 20(2):197-200. https://doi.org/10.1016/0032-5910(78)80048-5

Coetzee, G.H. 2011. *The influence of particle size on the steam gasification kinetics of coal.* Potchefstroom: North-West University. (Dissertation – MEng). http://hdl.handle.net/10394/8468

Coetzee, S., Neomagus, H.W.J.P., Bunt, J.R. & Everson, R.C. 2013. Improved reactivity of large coal particles by K_2CO_3 addition during steam gasification. *Fuel Processing Technology*, 114(1):75-80. https://doi.org/10.1016/j.fuproc.2013.03.041

Conkle, H.N. & Ragavan, J.K. 1992. Reconstitution of fine coal. *Coal Preparation*, 11(1-2):67-76. https://doi.org/10.1080/07349349208905208

Cook, A.C. 1975. Australian black coal: its occurrence, mining / preparation and use. In: Cook, A.C., ed. *Conference proceedings*. Symposium on Australian Black Coal: its Occurrence, Mining, Preparation and Use, Wollongong, Australia. Wollongong: Australasian Institute of Mining and Metallurgy, Illawarra Branch. pp. 150-171.

Couch, G.R. (IEA Clean Coal Centre). 1998. *CCC/O4: adding value to coal cleaning wastes*. https://www.iea-coal.org/report/adding-value-to-coal-cleaning-wastes-ccc-04/ Date of access: 13 June 2019.

Couch, G.R. (IEA Clean Coal Centre). 2002. *CCC/67: coal upgrading to reduce CO_2 emissions*. https://www.iea-coal.org/report/coal-upgrading-to-reduce-co2-emissions-ccc-67/ Date of access: 16 June 2019.

Couch, G.R. (IEA Clean Coal Centre). 2008. *CCC/132: coal to liquids*. https://www.iea-coal.org/report/coal-to-liquids-ccc-132/ Date of access: 16 July 2019.

Cozzani, V., Petarca, L. & Tognotti, L. 1995. Devolatilization and pyrolysis of refuse derived fuels: characterization and kinetic modelling by a thermogravimetric and calorimetric approach. *Fuel*, 74(6):903-912. https://doi.org/10.1016/0016-2361(94)00018-M

Crosby, N.T. & Patel, I. 1995. *General principles of good sampling practice*. Cambridge: Royal Society of Chemistry.

Dacombe, P., Pourkashanian, M., Williams, A. & Yap, L. 1999. Combustion-induced fragmentation behavior of isolated coal particles. *Fuel*, 78(15):1847-1857. https://doi.org/10.1016/S0016-2361(99)00076-9

Dakič, D., van der Honing, G. & Valk, M. 1989. Fragmentation and swelling of various coals during devolatilization in a fluidized bed. *Fuel*, 68(7):911-916. https://doi.org/10.1016/0016-2361(89)90129-4

de Assis, C.F.C., Oliveira, R.S., da Silva, G.L.R. & Assis, P.S. 2019. Characterization of coal briquettes using tar as a binding material for use in a coke oven. *REM - International Engineering Journal*, 72(1):113-118. https://doi.org/10.1590/0370-44672017720151

de Korte, G.J. 2016. Processing fine and ultra-fine coal. *Inside Mining*, 9(10):32-34. https://doi.org./10.10520/EJC196370

de Korte, G.J. & Jeffrey, L. 2016. *South African coal quality for independent power producers*. Paper presented at the Fossil Fuel Foundation's (FFF) independent power generation (IPP) one-day conference, Rosebank, Johannesburg, 17 March. http://www.fossilfuel.co.za/conferences/2016/IPP/de-Korte-Johan-and-Jeffrey-Lesley.pdf Date of access: 14 May 2019.

Dec, R.T. 2005. Processing of industrial wastes in the roller press for recycle or safe disposal. *Powder Handling and Processing*, 17(3):156-162.

Dehont, F. 2006. *Coal briquetting technology*. https://e8335568-00aa-4e25-85be-32e8bca96419.filesusr.com/ugd/b19918_3b9ef89fab2746ac986f16f4019fe773.pdf Date of access: 17 June 2019.

Department of Energy (South Africa). 2018. *South African coal sector report*. http://www.fossilfuel.co.za/initiatives/2013/SACRM-Value-Chain-Overview.pdf Date of access: 15 Aug. 2019

Department of Environmental Affairs (South Africa). 2013. National Environmental Management: Waste Act, 2008 (Act no. 59 of 2008): list of waste activities that have, or are likely to have, a detrimental effect on the environment. (Notice 921). *Government Gazette*, 37083, 29 Nov.

Department of Environmental Affairs (South Africa). 2018. *South Africa state of waste report 2nd draft*. https://remade.co.za/wp-content/uploads/2020/01/South-Africa-State-of-Waste-Report.pdf

Department of Minerals and Energy (South Africa). 2001. *National inventory discard and duff coal: summary report*. http://www.energy.gov.za/Coal/coal_discard_report.pdf Date of access: 16 June 2019.

Dohm, E., Luttrell, G., Bratton, R., Ripepi, N. & Taulbee, D.N. 2012. Evaluation of methods used to quantify the durability of coal-biomass briquettes. In. *Conference proceedings*. 29th Annual International Pittsburgh Coal Conference (PCC 2012), vol. 1, Pittsburgh, USA. NY: Curran Associates, Inc. pp. 148-157.

Dong, L., Wang, Z., Zhang, Y., Lu, J., Zhou, E., Duan, C. & Cao, X. 2019. Study on pyrolysis characteristics of coal and combustion gas release in inert environment. *Journal of Chemistry*, 2019(3):1-9. https://doi.org/10.1155/2019/1032529

du Toit, G.J.D. 2013. *The influence of CO_2 on the steam gasification rate of a typical South African coal.* Potchefstroom: North-West University. (Dissertation – MEng). http://hdl.handle.net/10394/9649

Einhorn, H.J. & Hogarth, R.M. 1975. Unit weighting schemes for decision making. *Organizational Behavior and Human Performance*, 13(2):171-192. https://doi.org/10.1016/0030-5073(75)90044-6

Ellison, G. & Stanmore, B.R. 1981a. High strength binderless brown coal briquettes part I: production and properties. *Fuel Processing Technology*, 4(4):277-289. https://doi.org/10.1016/0378-3820(81)90004-7

Ellison, G. & Stanmore, B.R. 1981b. High strength binderless brown coal briquettes part II: an investigation into bonding. *Fuel Processing Technology*, 4(4):291-304. https://doi.org/10.1016/0378-3820(81)90005-9

Encyclopedia Britannica. 2016. Coulomb force. In: Gregersen, E., Lotha, G. & Rodriguez, E., eds. *Britannica*. https://www.britannica.com/science/Coulomb-force Date of access: 10 Jan. 2021.

Engelleitner, W.H. 2001. *Binders: how they work and how to select one*. https://www.powderbulk.com/wp-content/uploads/pdf/pbe_20010201_31.pdf Date of access: 12 May 2020.

England, T. 1993. *The development of binderless, smokeless briquettes from bituminous colliery waste.* Johannesburg: University of the Witwatersrand. (Dissertation – MSc). http://hdl.handle.net/10539/22763

England, T. (Coaltech 2020). 2000. *Task 4.4.1: phase 1 a review of past and present work both locally and internationally*. https://coaltech.co.za/wp-content/uploads/2019/10/Project-4.4.1-a-Coal-Agglomeration-Review-of-past-and-present-work-both-locally-and-internationally-2000.pdf Date of access: 18 June 2019.

Ennis, B.J., Li, J., Tardos, G.I. & Pfeffer, R. 1990. The influence of viscosity on the strength of an axially strained pendular liquid bridge. *Chemical Engineering Science*, 45(10):3071-3088. https://doi.org/10.1016/0009-2509(90)80054-I

Ennis, J.M. & Ennis, D.M. 2012. A comparison of three commonly used methods for treating no preference votes. *Journal of Sensory Studies*, 27(2):123-129. https://doi.org/10.1111/j.1745-459X.2012.00374.x

Falcon, R.M.S. 2013. Coal petrography. In: Osbourne, D.G., ed. *The coal handbook: towards cleaner production*, v. 1. pp. 53-79. https://doi.org/10.1533/9780857097309.1.53

Falcon, R.M.S. 2016. *Coal resources of South Africa and their unique qualities*. Paper presented at the Fossil Fuel Foundation's (FFF) independent power generation (IPP) one-day conference, Rosebank, Johannesburg, 17 March. http://www.fossilfuel.co.za/conferences/2016/IPP/Falcon-Rosemary.pdf Date of access: 16 Aug. 2019.

Falcon, R.M.S. & Ham, A.J. 1988. The characteristics of Southern African coals. *Journal of the Southern African Institute of Mining and Metallurgy*, 88(5):145-161. https://journals.co.za/doi/10.10520/AJA0038223X_1835

Fernando, R. (IEA Clean Coal Centre). 2001. *CCC/55: the use of petroleum coke in coal-fired plant*. https://www.iea-coal.org/report/the-use-of-petroleum-coke-in-coal-fired-plant-ccc-55/ Date of access: 16 June 2019.

Fernando, R. (IEA Clean Coal Centre). 2004. *CCC/90: current design and construction of coal-fired power plant*. https://www.iea-coal.org/report/current-design-and-construction-of-coal-fired-power-plant-ccc-90/ Date of access: 16 June 2019.

Fernando, R. (IEA Clean Coal Centre). 2007. *CCC/126: cofiring of coal and waste fuels*. https://www.iea-coal.org/report/cofiring-of-coal-and-waste-fuels-ccc-126/ Date of access: 16 June 2019.

Fernando, R. (IEA Clean Coal Centre). 2008. *CCC/140: coal gasification*. https://www.iea-coal.org/report/coal-gasification-ccc-140/ Date of access: 16 June 2019.

FFF (Fossil Fuel Foundation). 2011. *Overview of the South African coal value chain*. http://www.fossilfuel.co.za/initiatives/2013/SACRM-Value-Chain-Overview.pdf

FFF (Fossil Fuel Foundation). 2013. *The South African coal roadmap*. http://www.fossilfuel.co.za/initiatives/2013/SACRM-Roadmap.pdf Date of access: 17 Aug. 2019.

Folgueras, M.B., Díaz, R.M., Xiberta, J. & Prieto, I. 2003. Thermogravimetric analysis of the co-combustion of coal and sewage sludge. *Fuel Processing Technology*, 82(15-17):2051-2055. https://doi.org/10.1016/S0016-2361(03)00161-3

Franke, M. & Rey, A. 2006. Pelleting quality. *World Grain*, May, p. 78-79

Gajewski, W. & Kosowska, M. 2005. A study of the fragmentation of coal particles during fluidized-bed combustion. In: Washington, G. & Jefferson, T., eds. Industrial Fluidization South Africa (IFSA 2005). Johannesburg: South African Institute of Mining and Metallurgy. pp. 1-11.

Gao, H. & Li, J. 2019. Thermogravimetric analysis of the co-combustion of coal and polyvinyl chloride. *PLoS ONE*, 14(10):1-35. https://doi.org/10.1371/journal.pone.0224401

Green, D.W. & Southard, M.Z. 2019. *Perry's chemical engineers' handbook*. 9th. NY: McGraw-Hill Education. https://www-accessengineeringlibrary-com.nwulib.nwu.ac.za/content/book/9780071834087/toc-chapter/chapter21/section/section83 Date of access: 12 Oct. 2020.

GreenCape 2019. *Waste: 2019 market intelligence report*. https://www.greencape.co.za/assets/Uploads/WASTE-MARKET-INTELLIGENCE-REPORT-WEB.pdf Date of access: 14 May 2020.

Gregory, H.R. 1960. A new process for briquetting coal without binders. *Journal of the Institute of Fuel*, 33(1):447-461.

Gregory, H.R., Jones, R.D.C. & Phillips, J.W. 1959. Compaction of briquettes. *Nature*, 184(4680):120-121. https://doi.org/10.1038/184120b0

Gug, J., Cacciola, D. & Sobkowicz, M.J. 2015. Processing and properties of a solid energy fuel from municipal solid waste (MSW) and recycled plastics. *Waste Management*, 35(1):283-292. https://doi.org/10.1016/j.wasman.2014.09.031

Gunnink, B. & Zhuoxiong, L. 1994. Compaction of binderless coal for coal log pipelines. *Fuel Processing Technology*, 37(3):237-254. https://doi.org/10.1016/0378-3820(94)90018-3

Gwenzi, W., Ncube, R.S. & Rukuni, T. 2020. Development, properties and potential applications of high-energy fuel briquettes incorporating coal dust, biowastes and post-consumer plastics. *SN Applied Sciences*, 2(6), https://doi.org/10.1007/s42452-020-2799-8

Habib, U., Habib, M. & Khan, A.U. 2014. Factors influencing the performance of coal briquettes. *Walailak Journal of Science and Technology*, 11(1):1-5. https://doi.org/10.2004/wjst.v11i1.417

Han, Y., Tahmasebi, A., Yu, J., Li, X. & Meesri, C. 2013. An experimental study on binderless briquetting of low-rank coals. *Chemical Engineering and Technology*, 36(5):749-756. https://doi.org/10.1002/ceat.201300067

Hancox, P.J. & Götz, A.E. 2014. South Africa's coalfields: a 2014 perspective. *International Journal of Coal Geology*, 132(1):170-254. https://doi.org/10.1016/j.coal.2014.06.019

Hand, P.E. (Coaltech 2020). 2000. *Task 4.8.1: dewatering and drying of fine coal to a saleable product*. http://www.wrc.org.za/wp-content/uploads/mdocs/SP%2084%20Dewatering%20and%20drying%20of%20fine%20coal%20to%20a%20saleable%20product%20-%202000.pdf Date of access: 18 July 2019.

Hapgood, K. & Rhodes, M. 2008. Size enlargement. In: Rhodes, M., ed. *Introduction to particle technology*. 2nd. Chichester: Wiley. pp. 337-358. https://doi.org/10.1002/9780470727102.ch13

Hardman, D.R. & Lind, G. (Coaltech 2020). 2003. *Task 2.1: generation of fine coal in-section* https://coaltech.co.za/wp-content/uploads/2019/10/Task-2.1-The-generation-of-fine-coal-in-section-2003.pdf Date of access: 18 July 2019.

Henderson, C. (IEA Clean Coal Centre). 2003. *CCC/74: clean coal technologies*. https://www.iea-coal.org/report/clean-coal-technologies-ccc-74/ Date of access: 13 March 2020.

Henderson, C. (IEA Clean Coal Centre). 2014. *CCC/242: increasing the flexibility of coal-fired power plants*. https://www.iea-coal.org/report/increasing-the-flexibility-of-coal-fired-power-plants-ccc-242/ Date of access: 13 March 2020.

Himbane, P.B., Ndiaye, L.G., Napoli, A. & Kobor, D. 2018. Physicochemical and mechanical properties of biomass coal briquettes produced by artisanal method. *African Journal of Environmental Science and Technology*, 12(12):480-486. https://doi.org/10.5897/AJEST2018.2568

Holley, C.A. 1983. Binders and binder systems for agglomeration. In: Koerner, R.M. & McDougall, J.A., eds. *Conference proceedings*. 18th Biennial Conference of The Institute for Briquetting and Agglomeration (IBA), Colorado Springs, Colorado. Erie: IBA. pp. 41-49.

Holley, C.A. & Antonetti, J.M. 1977. Agglomeration of coal fines. In: Messman, H.C. & Tibbetts, T.E., eds. *Conference proceedings*. 15th Biennial Conference of The Institute for Briquetting and Agglomeration (IBA), Montreal, Quebec. Laramie: IBA. pp. 1-12.

Holuszko, M.E. & Laskowski, J.S. 2004. Use of pelletization to assess the effect of particle–particle interactions on coal handleability. *Coal Preparation*, 24(3-4):179-194. https://doi.org/10.1080/07349340490498565

Hotta, A. 2009. Foster Wheeler's solutions for large scale CFB boiler technology: features and operational performance of Łagisza 460 MWe CFB boiler. In: G., Y., H., Z., C., Z. & Z., L., eds. *Conference proceedings*. 20th International Conference on Fluidized Bed Combustion, Xi'an, China. Heidelberg: Springer. pp. 59-70.

Hu, H., Zhou, Q., Zhu, S., Meyer, B., Krzack, S. & Chen, G. 2004. Product distribution and sulfur behavior in coal pyrolysis. *Fuel Processing Technology*, 85(8-10):849-861. https://doi.org/10.1016/j.fuproc.2003.11.030

ISO (International Organization for Standardization). 1998. *Representation of results of particle size analysis – part 1: graphical representation*. Geneva, Switzerland: ANSI. (ISO 9276-1:1998).

ISO (International Organization for Standardization). 2001. *Hard coal and coke – mechanical sampling – part 4: coal – preparation of test samples*. Geneva, Switzerland: ANSI. (ISO 13909-4:2001).

ISO (International Organization for Standardization). 2003. *Hard coal – determination of the crucible swelling number*. Geneva, Switzerland: ANSI. (ISO 501:2003).

ISO (International Organization for Standardization). 2005. *Classification of coals*. Geneva, Switzerland: ANSI. (ISO 11760:2005).

ISO (International Organization for Standardization). 2006. *Solid mineral fuels – determination of sulfur by IR spectrometry*. Geneva, Switzerland: ANSI. (ISO 19579:2006).

ISO (International Organization for Standardization). 2007. *Brown coals and lignites – determination of the yields of tar, water, gas and coke residue by low temperature distillation*. Geneva, Switzerland: ANSI. (ISO 647: 1974).

ISO (International Organization for Standardization). 2008. *Hard coal – determination of total moisture*. Geneva, Switzerland: ANSI. (ISO 589:2008).

ISO (International Organization for Standardization). 2009a. *Particle size analysis – laser diffraction methods*. Geneva, Switzerland: ANSI. (ISO 13320:2009).

ISO (International Organization for Standardization). 2009b. *Solid mineral fuels – determination of gross calorific value by the bomb calorimetric method and calculation of net calorific value* Geneva, Switzerland: ANSI. (ISO 1928:2009).

ISO (International Organization for Standardization). 2010a. *Solid mineral fuels – determination of ash*. Geneva, Switzerland: ANSI. (ISO 1171:2010).

ISO (International Organization for Standardization). 2010b. *Hard coal and coke – determination of volatile matter*. Geneva, Switzerland: ANSI. (ISO 562:2010).

Iveson, S.M. & Litster, J.D. 1998. Liquid-bound granule impact deformation and coefficient of restitution. *Powder Technology*, 99(3):234-242. https://doi.org/10.1016/S0032-5910(98)00115-6

Iveson, S.M. & Page, N.W. 2001. Tensile bond strength development between liquid-bound pellets during compression. *Powder Technology*, 117(1-2):113-122. https://doi.org/10.1016/S0032-5910(01)00319-9

Iveson, S.M., Beathe, J.A. & Page, N.W. 2002. The dynamic strength of partially saturated powder compacts: the effect of liquid properties. *Powder Technology*, 127(2):149-161. https://doi.org/10.1016/S0032-5910(02)00118-3

Iveson, S.M., Litster, J.D., Hapgood, K. & Ennis, B.J. 2001. Nucleation, growth and breakage phenomena in agitated wet granulation processes: a review. *Powder Technology*, 117(1-2):3-39. https://doi.org/10.1016/S0032-5910(01)00313-8

Jeffrey, L., Henry, G. & McGill, J. 2015. *Introduction to South African coal mining and exploration*. https://researchspace.csir.co.za/dspace/bitstream/handle/10204/8153/McGill_2015.pdf?sequence=1&isAllowed=y Date of access: 23 Sept. 2019.

Jeffrey, L.S. 2005. Characterization of the coal resources of South Africa. *The Journal of the South African Institute of Mining and Metallurgy*, 105(2):95-102.

Jin, Z., Hu, Y. & Liu, Y. 2003. Design study of coal-fired circulating fluidized bed boiler. In. *Conference proceedings*. 5th International Symposium on Coal Combustion, Nanjing, China. Nanjing: Southeast University Press. pp. 329-333.

Jones, R.D.C. 1963. Briquetting. In: Lowry, H.H., ed. *Chemistry of Coal Utilisation: supplementary volume*. New York: Wiley. pp. 675-753.

Jordaan, J. 1986. Highveld coalfield. In: Anhaeusser, C.R. & Maske, S., eds. *Mineral Deposits of southern Africa*, v. 2. Johannesburg: GSSA. pp. 1985-1994.

Kaliyan, N. & Morey, V.R. 2009. Factors affecting strength and durability of densified biomass products. *Biomass & Bioenergy*, 33(3):337-359. https://doi.org/10.1016/j.biombioe.2008.08.005

Kaliyan, N. & Morey, V.R. 2010. Natural binders and solid bridge type binding mechanisms in briquettes and pellets made from corn stover and switchgrass. *Bioresource Technology*, 101(3):1082-1090. https://doi.org/10.1016/j.biortech.2009.08.064

Karra, V.K. & Fuerstenau, D.W. 1977. The effect of humidity on the trace mixing kinetics in fine powders. *Powder Technology*, 16(1):97-105. https://doi.org/10.1016/0032-5910(77)85027-4

Keningley, S.T., Knight, P.C. & Marson, A.D. 1997. An investigation into the effects of binder viscosity on agglomeration behaviour. *Powder Technology*, 91(2):95-103. https://doi.org/10.1016/S0032-5910(96)03230-5.

Kidena, K., Katsuyama, M., Murata, S., Nomura, M. & Chikada, T. 2002. Study on plasticity of maceral concentrations in terms of their structural features. *Energy Fuels*, 16(5):1231-1238. https://doi.org/10.1021/ef020029j

Komarek, R.K. 1967. Selecting binders and lubricants for agglomeration processes. *Chemical Engineering*, 4 Dec., p. 154-155

Komarek, R.K. 1991. Binderless briquetting of peat, lignite, sub-bituminous and bituminous coals in roll press. In: Roth, D.L., ed. 22nd Biennial Conference of the Institute for Briquetting and Agglomeration (IBA), San Antonio, Texas. Laramie: IBA. pp. 233-242.

Koornneef, J., Junginger, M. & Faaij, A. 2007. Development of fluidized bed combustion – an overview of trends, performance and cost. *Progress in Energy and Combustion Science*, 33(1):19-55. https://doi.org/10.1016/j.pecs.2006.07.001

Ladner, W.R. 1988. The products of coal pyrolysis: properties, conversion and reactivity. *Fuel Processing Technology*, 20(1):207-222. https://doi.org/10.1016/0378-3820(88)90021-5

Laj, C. & Barnikel, F. 2016. *Type, distribution and use of coal in South Africa*. Paper presented at the 35th International Geological Congress, Cape Town, West Cape, 28 Aug. https://cdn.egu.eu/media/filer_public/ab/bf/abbffe4a-ec58-44a6-aac7-b9527aae0782/9_-_malumbazo.pdf.

Leckner, B. & Lind, F. 2020. Combustion of municipal solid waste in fluidized bed or on grate – a comparison. *Waste Management*, 109(1):94-108. https://doi.org/10.1016/j.wasman.2020.04.050

Leokaoke, N.T., Bunt, J.R., Neomagus, H.W.J.P., Waanders, F.B. & Strydom, C.A. 2019. CO_2 reactivity of briquettes derived from discard inertinite-rich Highveld coal using lignosulphonate and resin as binders. *Journal of the Southern African Institute of Mining and Metallurgy*, 119(10):847-854. https://dx.doi.org/10.17159/2411-9717/720/2019

Leokaoke, N.T., Bunt, J.R., Neomagus, H.W.J.P., Waanders, F.B., Strydom, C.A. & Mthombo, T.S. 2018. Manufacturing and testing of briquettes from inertinite-rich low-grade coal fines using various binders. *The Journal of the Southern African Institute of Mining and Metallurgy*, 118(1):83-88. http://dx.doi.org/10.17159/2411-9717/2018/v118n1a10

Lewitt, M. (IEA Clean Coal Centre). 2011. *CCC/185: opportunities for fine coal utilisation*. https://www.iea-coal.org/report/opportunities-for-fine-coal-utilisation-ccc-185/ Date of access: 20 June 2020.

Li, Y. & Liu, H. 2000. High-pressure densification of wood residues to form an upgraded fuel. *Biomass and Bioenergy*, 19(3):177-186. https://doi.org/10.1016/S0961-9534(00)00026-X

Lindley, J.A. & Vossoughi, M. 1989. Physical properties of biomass briquets. *Transactions of the ASAE*, 32(2):361-366. https://doi.org/10.13031/2013.31010

Liu, G., Benyon, P., Benfell, K.E., Bryant, G.W., Tate, A.G., Boyd, R.K., ... Wall, T.F. 2000. The porous structure of bituminous coal chars and its influence on combustion and gasification under chemically controlled conditions. *Fuel*, 79(6):617-626. https://doi.org/10.1016/S0016-2361(99)00185-4

Lloyd, P.J. 2000. The potential of coal wastes in South Africa. *The South African Institute of Mining and Metallurgy*, 1(1):69-72. http://hdl.handle.net/11189/6391

Lloyd, P.J. 2002. *Coal mining and the environment*. http://www.erc.uct.ac.za/sites/default/files/image_tool/images/119/Papers-pre2004/02Lloyd_Coal_environment.pdf Date of access: 18 Aug. 2019.

Lu, Y. 1989. *A study of the properties of coal agglomerates and their effect on bulk density.* Wollongong: University of Wollongong. (Thesis – MSc). https://ro.uow.edu.au/theses/2584 Date of access: 22 Sept. 2019.

Mahinpey, N. & Gomez, A. 2016. Review of gasification fundamentals and new findings: reactors, feedstock, and kinetic studies. *Chemical Engineering Science*, 148(1):14-31. https://doi.org/10.1016/j.ces.2016.03.037

Mamaila, M. 2020. CFBC boiler technology viable for South Africa. *Engineering News*, 21 Aug. https://www.engineeringnews.co.za/article/cfbc-boiler-technology-viable-for-s-africa-2020-08-21/rep_id:4136 Date of access: 3 Nov. 2020.

Mangena, S.J. 2001. *The amenability of some South African bituminous coals to binderless briquetting.* Pretoria: Technikon Pretoria. (Dissertation – MTech).

Mangena, S.J. & du Cann, V.M. 2007. Binderless briquetting of some selected South African prime coking, blend coking and weathered bituminous coals and the effect of coal properties on binderless briquetting. *International Journal of Coal Geology*, 71(2-3):303-312. https://doi.org/10.1016/j.coal.2006.11.001

Mangena, S.J., de Korte, G.J., McCrindle, R.I. & Morgan, D.L. 2004. The amenability of some Witbank bituminous ultra fine coals to binderless briquetting. *Fuel Processing Technology*, 85(15):1647-1662. https://doi.org/10.1016/j.fuproc.2003.12.011

Maree, Z., Strydom, C.A. & Bunt, J.R. 2020. Chemical and physical characterization of spent coffee ground biochar treated by a wet oxidation method for the production of a coke substitute. *Waste Management*, 113(1):422-429. https://doi.org/10.1016/j.wasman.2020.06.025

Mark, C. & Barton, T.M. 1996. A new look at the uniaxial compressive strength of coal In: Aubertin, M., Hassani, F. & Mitri, H., eds. *Conference proceedings*. Rock Mechanics: Tools and Techniques- Proceedings of the 2nd North American Rock Mechanics Symposium, NARMS'96, Montreal, Quebec. Rotterdam: Taylor & Francis. pp. 405-411.

Massaro, M.M., Son, S.F. & Groven, L.J. 2014. Mechanical, pyrolysis, and combustion characterization of briquetted coal fines with municipal solid waste plastic (MSW) binders. *Fuel*, 115(1):62-69. http://dx.doi.org/10.1016/j.fuel.2013.06.043

Matjie, R.H., Ward, C.R. & Li, Z. 2012. Mineralogical transformations in coal feedstocks during combustion, based on packed-bed combustor tests – part 1: bulk coal and ash studies. *Coal Combustion and Gasification Products*, 4(1):45-54. https://doi.org/10.4177/CCGP-D-12-00003.1

Mazzone, D.N., Tardos, G.I. & Pfeffer, R. 1987. The behavior of liquid bridges between two relatively moving particles. *Powder Technology*, 51(1):71-83. https://doi.org/10.1016/0032-5910(87)80041-4

Mehta, R.H. & Parekh, B.K. 1996. Pelletization studies of ultra-fine clean coal. *Mining, Metallurgy & Exploration*, 13(1):41-44. https://doi.org/10.1007/BF03402716

Merriam-Webster Inc. 2019. *Merriam-Webster dictionary*. https://www.merriam-webster.com/dictionary/coal Date of access: 18 Nov. 2019.

Messman, H.C. 1977. Binders for briquetting and agglomeration. In: Messman, H.C. & Tibbetts, T.E., eds. *Conference proceedings*. 15th Biennial Conference of The Institute for Briquetting and Agglomeration (IBA), Montreal, Quebec. Erie: IBA. pp. 173-178.

Meyer, J.A. 2020. *The effect of microalgae as a binder on the characteristics of agglomerated coal fines.* Potchefstroom: North-West University. (Dissertation – MSc).

Miettinen, K. 2008. Introduction to multiobjective optimization: noninteractive approaches. In: Branke, J., Deb, K., Miettinen, K. & Słowiński, R., eds. *Multiobjective optimization – lecture notes in computer science*, v. 5252. Berlin: Springer. pp. 1-26. https://doi.org/10.1007/978-3-540-88908-3_1

Miller, M.R., Fields, G.L., Fisher, R.W. & Wheelock, T.D. 1979. Coal briquetting without a binder. In. *Conference proceedings*. 16th Biennial Conference of The Institute for Briquetting and Agglomeration (IBA), San Diego, California. Erie: IBA. p 325.

Mills, J.E. 1908. *Binders for coal briquets*. https://pubs.usgs.gov/bul/0343/report.pdf Date of access: 13 July 2019.

Mishra, A., Gautam, S. & Sharma, T. 2018. Effect of operating parameters on coal gasification. *International Journal of Coal Science & Technology*, 5(1):113–125. https://doi.org/10.1007/s40789-018-0196-3

Mitchual, S.J., Frimpong-Mensah, K. & Darkwa, N.A. 2013. Effect of species, particle size and compacting pressure on relaxed density and compressive strength of fuel briquettes. *International Journal of Energy and Environmental Engineering*, 4(30):1-6. https://doi.org/10.1186/2251-6832-4-30

Mjonono, D., Harrison, S.T.L. & Kotsiopoulos, A. (IMWA). 2018. *Development of co-disposal methods for fine coal waste and coal waste rock to facilitate the prevention of acid mine drainage*. https://www.imwa.info/docs/imwa_2018/IMWA2018_Mjonono_541.pdf Date of access: 13 Sept. 2020.

Mochida, Y. & Honda, H. 1963. Hardness of briquetted coal. In. *Conference proceedings*. Symposium on Low Temperature Carbonisation of Non-caking Coals and Lignite and Briquetting of Coal Fines, vol. 1, Hyderabad, India. New Delhi: CSIR. pp. 1-22.

Moodley, L. 2007. *The evaluation of the fluidised bed combustion performance of South African coals in the presence of sorbents.* Durban: University of KwaZulu-Natal. (Dissertation – MEng). http://hdl.handle.net/10413/2220

Motaung, S.R., Mangena, S.J., de Korte, G.J., McCrindle, R.I. & van Heerden, J.H.P. 2007. Effects of coal composition and flotation reagents on the water resistance of binderless briquettes. *Coal Preparation*, 27(4):230-248. https://doi.org/10.1080/07349340701672102

Muzenda, E. 2014. *Potential uses of South African coal fines: a review*. Paper presented at the 3rd International Conference on Mechanical, Electronics and Mechatronics Engineering (ICMEME'2014), Abu Dhabi, 19-20 March. https://ujcontent.uj.ac.za/vital/access/services/Download/uj:4784/CONTENT1?view=true Date of access: 19 Aug. 2019.

Nwabue, F.I., Unah, U. & Itumoh, E.J. 2017. Production and characterization of smokeless bio-coal briquettes incorporating plastic waste materials. *Environmental Technology & Innovation*, 8(1):233-245. http://dx.doi.org/10.1016/j.eti.2017.02.008

O'Keefe, J.M.K., Bechtel, A., Christanis, K., Dai, S., DiMichele, W.A., Eble, C.F., ... Hower, J.C. 2013. On the fundamental difference between coal rank and coal type. *International Journal of Coal Geology*, 118(1):58-87. https://doi.org/10.1016/j.coal.2013.08.007

Olugbade, T.O. & Ojo, O.T. 2021. Binderless briquetting technology for lignite briquettes: a review. *Energy, Ecology & Environment*, 6(1):69-79. https://doi.org/10.1007/s40974-020-00165-3

Osbourne, D.G. & Gupta, S.K. 2013. Industrial uses of coal. In: Osbourne, D.G., ed. *The coal handbook: towards cleaner production*, v. 1. pp. 3-30. https://doi.org/10.1533/9780857097309.1.3

Otero, M., Calvo, L.F., Gil, M.V., García, A.I. & Morán, A. 2008. Co-combustion of different sewage sludge and coal: a non-isothermal thermogravimetric kinetic analysis. *Bioresource Technology*, 99(14):6311-6319. https://doi.org/10.1016/j.biortech.2007.12.011

Özer, M., Basha, O.M. & Morsi, B. 2017. Coal-agglomeration processes: a review. *International Journal of Coal Preparation and Utilization*, 27(2):131-167. https://doi.org/10.1080/19392699.2016.1142443

Patil, D., Taulbee, D.N., Parekh, B.K. & Honaker, R.Q. 2009. Briquetting of coal fines and sawdust: effect of particle-size distribution. *International Journal of Coal Preparation and Utilization*, 29(5):251-264. https://doi.org/10.1080/19392690903294423

Piersol, R.J. 1933. *Briquetting Illinois coals without a binder by compression and impact: a progress report of a laboratory investigation*. https://www.ideals.illinois.edu/bitstream/handle/2142/43905/briquettingillin55731pier.pdf?sequence=2&isAllowed=y Date of access: 15 March 2019.

Pietsch, W. 1997. Size enlargement by agglomeration. In: Fayed, M.E. & Otten, L., eds. *Handbook of powder science & technology*. Switzerland: Springer. pp. 202-377. https://doi.org/10.1007/978-1-4615-6373-0

Pietsch, W. 2004. *Agglomeration processes: phenomena, technologies, equipment*. Weinheim Wiley-VCH. https://doi.org/10.1002/9783527619801

Pretorius, G.N., Bunt, J.R., Gräbner, M., Neomagus, H.W.J.P., Waanders, F.B., Everson, R.C. & Strydom, C.A. 2017. Evaluation and prediction of slow pyrolysis products derived from coals of different rank. *Journal of Analytical and Applied Pyrolysis*, 128(1):156-167. https://doi.org/10.1016/j.jaap.2017.10.014

Rahman, A.N.E., Aziz Masood, M., Prasad, C.S.N. & Venkatesham, M. 1989. Influence of size and shape on the strength of briquettes. *Fuel Processing Technology*, 23(3):185-195. https://doi.org/10.1016/0378-3820(89)90018-0

Rambuda, M. 2015. *Gasification and combustion kinetics of typical South African coal chars.* Potchefstroom: North-West University. (Dissertation – MEng). http://hdl.handle.net/10394/15519

Reddick, J.F., Von Blottnitz, H. & Kothuis, B. 2007. A cleaner production assessment of the ultra-fine coal waste generated in South Africa. *The Journal of The Southern African Institute of Mining and Metallurgy*, 107(12):811. http://hdl.handle.net/11427/24673

Richards, S.R. 1990. Physical testing of fuel briquettes. *Fuel Processing Technology*, 25(2):89-100. https://doi.org/10.1016/0378-3820(90)90098-D

Rife, H.M. & Walker, A.H. 1953. *Polymerization of acrylic acid in aqueous solution*. (Patent: US US2789099A). https://patentimages.storage.googleapis.com/3f/96/49/395073ac5ce58d/US2789099.pdf Date of access: 13 May 2020.

Roets, L., Bunt, J.R., Neomagus, H.W.J.P. & van Niekerk, D. 2014. An evaluation of a new automated duplicate-sample Fischer Assay setup according to ISO/ASTM standards and analysis of the tar fraction. *Journal of Analytical and Applied Pyrolysis*, 106(1):190-196. https://doi.org/10.1016/j.jaap.2014.01.016

Roets, L., Strydom, C.A., Bunt, J.R., Neomagus, H.W.J.P. & van Niekerk, D. 2015. The effect of acid washing on the pyrolysis products derived from a vitrinite-rich bituminous coal. *Journal of Analytical and Applied Pyrolysis*, 116(1):142-151. https://doi.org/10.1016/j.jaap.2015.09.016

Rubio, B., Izquierdo, M.T. & Segura, E. 1999. Effect of binder addition on the mechanical and physicochemical properties of low rank coal char briquettes. *Carbon*, 37(11):1833-1841. https://doi.org/10.1016/S0008-6223(99)00057-3

Sakawa, M., Sakurai, Y. & Hara, Y. 1982. Influence of coal characteristics on CO_2 gasification. *Fuel*, 61(8):717-720. https://doi.org/10.1016/0016-2361(82)90245-9

Sasol 2018. *Integrated report: value through focus and discipline*. http://www.integratedreport.sasol.com/index.php Date of access: 13 May 2019.

Sastry, K.V.S. 1995. *Pelletization of fine coals*. https://www.osti.gov/servlets/purl/171245

Schreuder, N. 2017. CFBC the preferred coal combustion technology. *Mining Weekly*, 22 Sept. https://www.miningweekly.com/article/cfbc-the-preferred-coal-combustion-technology-says-falcon-2017-09-22 Date of access: 30 July 2020.

SEAISI (South East Asia Iron and Steel Institute). 2016. *The making of iron and steel*. https://www.seaisi.org/mainFE/pdf/The%20Making%20of%20Iron%20&%20Steel.pdf Date of access: 20 Apr. 2020.

Senneca, O., Urciuolo, M., Chirone, R. & Cumbo, D. 2011. An experimental study of fragmentation of coals during fast pyrolysis at high temperature and pressure. *Fuel*, 90(9):2931-2938. https://doi.org/10.1016/j.fuel.2011.04.012

Simons, S.J.R. 2007. Liquid bridges in granules. In: Salman, A.D., Hounslow, M.J. & Seville, J.P.K., eds. *Handbook of powder technology: granulation*, v. 11. Amsterdam: Elsevier Science. pp. 1257-1316. https://doi.org/10.1016/S0167-3785(07)80062-5

Skinner, J. & Brown, M. 2011. The inefficiencies and deficiencies of waste coal. *Vermont Journal of Environmental Law*, 13(2):229-253. https://doi-org.nwulib.nwu.ac.za/10.2307/vermjenvilaw.13.2.229

Skorupska, N.M. (IEA Clean Coal Centre). 1993. *IEACR/52: coal specifications – impact on power station performance*. https://www.iea-coal.org/report/coal-specifications-impact-on-power-station-performance-ieacr-52/ Date of access: 16 June 2019.

Smoot, D.L. & Smith, P.J. 1985. *Coal combustion and gasification*. NY: Springer (The plenum chemical engineering series).

Sørum, L., Grønli, M.G. & Hustad, J.E. 2001. Pyrolysis characteristics and kinetics of municipal solid wastes. *Fuel*, 80(9):1217-1227. https://doi.org/10.1016/S0016-2361(00)00218-0

Spears, D.D. 2000. Role of clay minerals in UK coal combustion. *Applied Clay Science*, 16(1-2):87-95. https://doi.org/10.1016/S0169-1317(99)00048-4

Speight, J.G. 2005. *Handbook of coal analysis*. 166. Hoboken: Wiley & Sons. (Chemical analysis: a series of monographs on analytical chemistry and its applications).

Speight, J.G. 2008. *Synthetic fuels handbook: properties, process, and performance*. Available from Access Engineering: https://www.accessengineeringlibrary.com/content/book/9780071490238 Date of access: 20 May 2019.

Speight, J.G. 2012. *The chemistry and technology of coal*. 3rd ed. Boca Raton: CRC Press.

Steyn, M. & Minnitt, R.C.A. 2010. Thermal coal products in South Africa. *Journal of the Southern African Institute of Mining and Metallurgy*, 110(10):593-599. http://ref.scielo.org/7rxrcm

Straka, P., Buchtele, J. & Kovářová, J. 1998. Co-pyrolysis of waste polymers with coal. *Macromolecular Symposia*, 135(1):19-23. https://doi.org/10.1002/masy.19981350105

Strydom, C.A., Mthombo, T.S., Bunt, J.R. & Neomagus, H.W.J.P. 2018. Some physical and chemical characteristics of calcium lignosulphonate-bound coal fines. *The Journal of The Southern African Institute of Mining and Metallurgy*, 118(12):1277-1283. http://dx.doi.org/10.17159/2411-9717/2018/v118n12a6

Stubington, J.F. & Linjewile, T.M. 1989. The effects of fragmentation on devolatilization of large coal particles. *Fuel*, 68(2):155-160. https://doi.org/10.1016/0016-2361(89)90316-5

Swanepoel, L. 2017. *A process for the agglomeration of coal slurry including ultrafines*. (Patent: ZA 134566). https://patents.google.com/patent/WO2017134566A1/pt-PT Date of access: 15 May 2019.

Taulbee, D., Neathery, J., Patil, D.P., Sowder, N. & O'Daniel, B. 2010. Combustion of briquettes and fuels pellets prepared from blends of biomass and fine coal. In: Honaker, R.Q., ed. *Conference proceedings*. International Coal Preparation Congress Lexington, Kentucky. Littleton: SME. pp. 161-170.

Taulbee, D.N., Hodgen, R. & Patil, D. 2013. Drying and agglomeration of high-moisture coals and coal fines. *IBA Proceedings*, 33(1):63-81. https://doi.org/10.13140/2.1.4483.3924.

Tembe, E.T., Otache, P.O. & Ekhuemelo, D.O. 2014. Density, shatter index, and combustion properties of briquettes produced from groundnut shells, rice husks and saw dust of Daniellia oliveri. *Journal of Applied Bioscience*, 82(1):7372-7378. https://doi.org/10.4314/jab.v82i1.7

Uwaoma, R.C., Strydom, C.A., Matjie, R.H., Bunt, J.R., Okolo, G.N. & Brand, D.J. 2019. Pyrolysis of tetralin liquefaction derived residues from lighter density fractions of waste coals taken from waste coal disposal sites in South Africa. *Energy Fuels*, 33(9):9074-9086. https://doi.org/10.1021/acs.energyfuels.9b01823

Vamvuka, D. 1999. Gasification of coal. *Energy Exploration & Exploitation*, 17(6):515-581. http://www.jstor.com/stable/43754156

van der Merwe, G.W. 2011. *The influence of particle size and density on the combustion of Highveld coal.* Potchefstroom: North-West University. (Dissertation – MEng). http://hdl.handle.net/10394/11099

van Dyk, J.C. 2001. Development of an alternative laboratory method to determine thermal fragmentation of coal sources during pyrolysis in the gasification process. *Fuel*, 80(2):245-249. https://doi.org/10.1016/S0016-2361(00)00089-2

van Dyk, J.C., Keyser, M.J. & van Zyl, J.W. 2001. *Suitability of feedstocks for the Sasol-Lurgi fixed bed dry bottom gasification process*. Paper presented at the Gasification Technologies Conference, San Francisco, California, 7-10 Oct. https://www.globalsyngas.org/uploads/eventLibrary/GTC01063.pdf Date of access: 9 June 2019.

van Dyk, J.C., Keyser, M.J. & Coertzen, M. 2006. Syngas production from South African coal sources using Sasol–Lurgi gasifiers. *International Journal of Coal Geology*, 65(3-4):243-253. https://doi.org/doi:10.1016/j.coal.2005.05.007

Venter, P. & Naude, N. 2015. Evaluation of some optimum moisture and binder conditions for coal fines briquetting. *The Journal of the South African Institute of Mining and Metallurgy*, 115(4):329-333.

Wallouch, R.W., Murty, H.N. & Heintz, E.A. 1972. Pyrolysis of coal tar pitch binders. *Carbon*, 10(6):729-735. https://doi.org/10.1016/0008-6223(72)90080-2

Waters, P.L. 1969. Binders for fuel briquettes: a critical survey. *Division of Mineral Chemistry, Technical Communication*, 51(1):1-69.

WCA (World Coal Association). 2019a. *Fact sheet: steel and raw materials*. https://www.worldsteel.org/en/dam/jcr:16ad9bcd-dbf5-449f-b42c-b220952767bf/fact_raw%2520materials_2019.pdf Date of access: 20 May 2020.

WCA (World Coal Association). 2019b. *IEA coal market report 2019 – a wake-up call for our global community*. https://www.worldcoal.org/file_validate.php?file=WCA%20response%20to%20IEA%20Coal%20Market%20Report%202019.pdf Date of access: 10 Jan. 2020.

WCA (World Coal Association,). 2019c. *Uses of coal*. https://www.worldcoal.org/coal/uses-coal Date of access: 11 Nov. 2019.

Weiss, M. & Turna, O. 2009. A new name, but a well proven technology: back to Lurgi. In. *Conference proceedings*. Gasification Technologies Conference Colorado Springs, USA Red Hook: Curran Associates, Inc.

Whyle, S. 2016. Biofuels tested for boiler efficiency. *Engineering News*. https://www.engineeringnews.co.za/article/biofuels-tested-in-the-hunt-for-combustion-efficiency-2016-06-03 Date of access: 6 June 2019.

Woodruff, E.B., Lammers, H.B. & Lammers, T.F. 2017. *Steam Plant Operation*. 10th ed. Available from Access Engineering: https://www-accessengineeringlibrary-com.nwulib.nwu.ac.za/content/book/9781259641336/chapter/chapter4 Date of access: 15 Oct. 2019.

Wu, Z. (IEA Clean Coal Centre). 2003. *CCC/76: understanding fluidised bed combustion*. https://www.iea-coal.org/report/understanding-fluidised-bed-combustion-ccc-76/ Date of access: 15 March 2020.

Wu, Z. (IEA Clean Coal Centre). 2005. *CCC/95: fundamentals of pulverised coal combustion*. https://www.iea-coal.org/report/fundamentals-of-pulverised-coal-combustion-ccc-95/ Date of access: 16 June 2019.

Wu, Z. (IEA Clean Coal Centre). 2006. *CCC/110: developments in fluidised bed combustion technology*. https://www.iea-coal.org/report/developments-in-fluidised-bed-combustion-technology-ccc-110/ Date of access: 15 March 2020.

Xu, W. & Tomita, A. 1987. Effect of temperature on the flash pyrolysis of various coals. *Fuel*, 66(5):632-636. https://doi.org/10.1016/0016-2361(87)90271-7

Young, B.C. 1999. Adding value with agglomerated waste materials. In: Roth, D.L., ed. *Conference proceedings*. 26th Biennial Conference of The Institute for Briquetting and Agglomeration (IBA), San Diego, California. Erie: IBA. pp. 207-218.

Young, B.C. 2015. *Using binders to briquette carbonaceous materials and steel wastes*. https://www.powderbulk.com/wp-content/uploads/pdf/pbe_20150601_0018.pdf Date of access: 17 April 2019.

Zhang, G., Sun, Y. & Xu, Y. 2018. Review of briquette binders and briquetting mechanism. *Renewable & Sustainable Energy Reviews*, 82(1):477-487. https://doi-org.nwulib.nwu.ac.za/10.1016/j.rser.2017.09.072

Zhang, H., Cen, K., Yan, J. & Ni, M. 2002. The fragmentation of coal particles during the coal combustion in a fluidized bed. *Fuel*, 81(14):1835-1840. https://doi.org/10.1016/S0016-2361(02)00111-4

Zhang, L., Huang, J., Fang, Y. & Wang, Y. 2006. Gasification reactivity and kinetics of typical Chinese anthracite chars with steam and CO_2. *Energy Fuels*, 20(3):1201-1210. https://doi.org/10.1021/ef050343o

Zhu, Q. (IEA Clean Coal Centre). 2013. *CCC/219: developments in circulating fluidised bed combustion*. https://www.iea-coal.org/report/developments-in-circulating-fluidised-bed-combustion-ccc-219/ Date of access: 15 May 2020.

APPENDIX A: SUMMARY OF THE MATERIAL SAFETY DATA SHEETS FOR THE WASTE BINDERS

Table A-1: Physical and chemical properties of Binders A–E adapted from the material safety data sheets (MSDS)

Property	**Value**				
Binder:	**A**	**B**	**C**	**D**	**E**
State of matter	Liquid (20°C)	Liquid (20°C)	Liquid (≥60°C)	Liquid (20°C)	Solid (20°C)
Colour	Brownish	Dark brown	Dark brown	Off-white	Black
Odour	Pungent	Acrylic-like	Pungent	Odourless	Odourless
pH	7–8	–	–	8–10	–
Boiling; melting point	–; 0°C	102.5°C; –	179–219°C; –	96°C; –	–; 105–130°C
Flash point	–	59°C	81°C	–	341°C
Density	0.96–1.13 g/cm^3 (25°C) Bulk: 958.97 kg/m^3 (22°C)	75%: 1.072 g/cm^3 (20°C) 25%: 0.884 g/cm^3 (>50°C)	1.224 g/cm^3	1.0 g/cm^3 (25°C)	0.90–0.96 g/cm^3 (20°C)
Water solubility	Dispersible	Insoluble, gel formation	–	Soluble	Insoluble
Dynamic viscosity	–	–	500 mPa.s (100°C)	–	–

A: waterworks bio-sludge, B: acrylic acid containing a hydrocarbon by-product (25:75 ratio of two different by-products), C: pitch, D: wax emulsion, E: recycled low-density polyethylene (LDPE)

APPENDIX B: MOISTURE EVAPORATION/ADSORPTION OF LAB-SCALE BRIQUETTES

The weight change of the briquettes containing a liquid binder was recorded over a period of 21 days and converted to a percentage of the initial weight of the briquettes. This was done to evaluate the evaporation/adsorption of moisture and aid in the discussion of the binding mechanisms present within the briquettes. The change in weight was small ($< 0.1 \pm 0.01$ g) therefore these values only act as a guide to describe the changes in CS over time and not as a definitive explanation. The briquettes were manufactured for the Phase 1 lab-scale analysis where the effect of maximum moisture addition (17%) on the CS (MPa) and WRI (%) of the briquettes bound with Binders A-E was tested. Figure B-1 is a graph showing the weight change of the briquettes manufactured using Binders A–D (5–15% addition). Binder E is excluded from this discussion because it is a solid and therefore behaves different to the liquid binders.

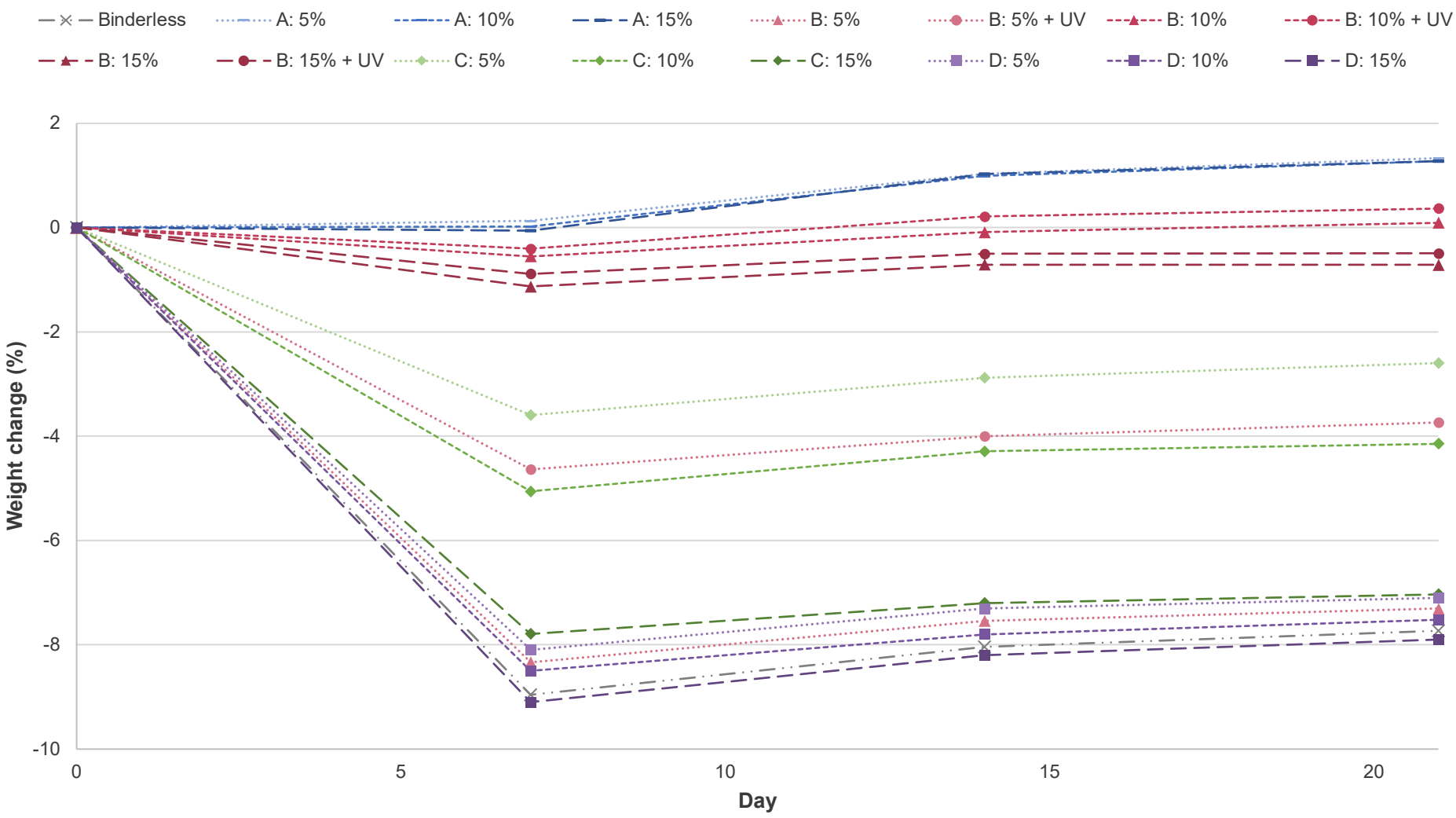

Figure B-1: Weight change (%) over 21 days of the Phase 1 lab-scale briquettes that were manufactured with Binders A–D (5–15%) at maximum moisture addition (17%)

APPENDIX C: DROP SHATTER TEST RESULTS FOR THE PILOT-SCALE BRIQUETTES

The mechanical strength results obtained from the Richards (1990) drop shatter test, *i.e.* the impact resistance index, IRI (-), and friability index, FR (%), are tabulated and discussed in this appendix.

C.1 Impact resistance index

The IRI is a measure of the briquette's ability to withstand impact forces, *e.g.* hitting a surface during transportation, handling or loading (Dohm *et al.*, 2012). The Richards (1990) method was used where the number of drops before the briquette broke, N_{drops}, and number of pieces it broke into, N_{pieces}, were inserted into Equation 2-4. The minimum IRI is 50 and the briquettes were dropped a maximum of 10 times (Lindley & Vossoughi, 1989; Richards, 1990).

$$\mathrm{IRI} = \frac{N_{\mathrm{drops}}}{N_{\mathrm{pieces}}} \times 100 \qquad (2\text{-}4)$$

The IRI is directly proportional to N_{drops} and inversely proportional to N_{pieces}. This is due to a briquette being stronger if it can withstand more drops or if it breaks into larger, *i.e.* useable, pieces when it does break. Figure C-1 shows the effect of N_{pieces} on the IRI for up to 10 drops, which indicates that even if a briquette can withstand many drops, it will still have a low IRI if it shatters.

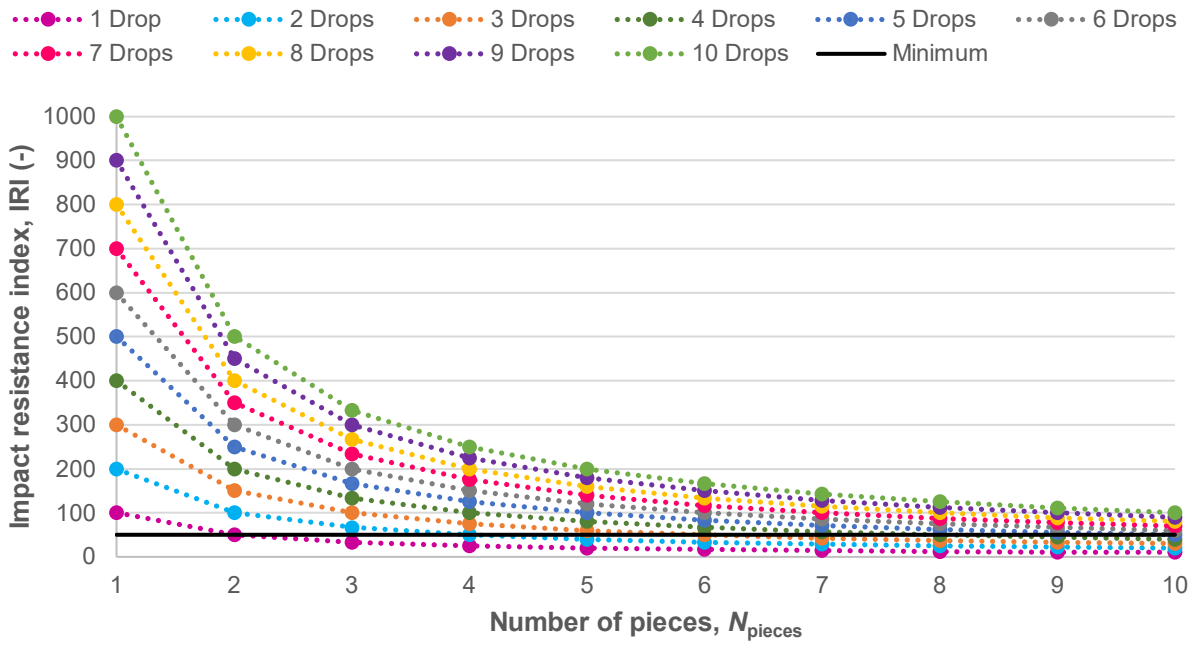

Figure C-1: Example of the impact resistance index dependence on the number of pieces the briquette breaks into, $N_{pieces} < 10$, and number of drops before it breaks, $N_{drops} < 10$

The IRI results, over 21 days, of the briquettes produced with water and Binders A–E are shown in Table C-1. The highlighted cells contain the values that are above the minimum of 50 when the error values are accounted for. The average percentage standard deviation is below 40%, as reported by Richards (1990). There is no clear trend in IRI based on binder concentration or curing time so the average IRI over the 21-day period was used to determine which binders and concentrations where higher than the minimum IRI and is discussed in more detail in Chapter 4.

Table C-1: Impact resistance index results for binderless and Binders A–E bound pilot-scale briquettes, over a 21-day period

Binder		Day 0	Day 7	Day 14	Day 21	Average
Water	**2.5%**	15 ± 3	23 ± 5	19 ± 5	16 ± 7	**18 ± 5**
	10%	14 ± 2	18 ± 4	36 ± 13	19 ± 3	**22 ± 6**
	15%	11 ± 2	17 ± 5	31 ± 2	23 ± 6	**20 ± 4**
A	**5.0%**	30 ± 5	24 ± 5	38 ± 10	19 ± 6	**28 ± 6**
	10%	40 ± 9	69 ± 14	44 ± 5	50 ± 0	**51 ± 7**
	15%	45 ± 6	83 ± 14	50 ± 8	92 ± 25	**68 ± 13**
B	**5.0%**	33 ± 5	22 ± 6	50 ± 2	30 ± 4	**34 ± 4**
	10%	60 ± 11	72 ± 12	61 ± 16	72 ± 12	**66 ± 13**
	15%	40 ± 7	43 ± 6	42 ± 7	72 ± 12	**49 ± 8**
	20%	75 ± 9	82 ± 8	128 ± 12	61 ± 16	**87 ± 11**
C	**5.0%**	31 ± 9	42 ± 7	42 ± 7	34 ± 7	**37 ± 8**
	10%	127 ± 38	258 ± 41	72 ± 12	138 ± 28	**149 ± 30**
	15%	1000 ± 0	1000 ± 0	1000 ± 0	1000 ± 0	**1000 ± 0**
	20%	1000 ± 0	1000 ± 0	1000 ± 0	1000 ± 0	**1000 ± 0**
D	**2.5%**	14 ± 3	14 ± 1	15 ± 3	10 ± 3	**13 ± 2**
	5.0%	9 ± 2	13 ± 3	50 ± 21	11 ± 2	**21 ± 7**
E	**5%**	100 ± 24	102 ± 11	92 ± 30	95 ± 21	**97 ± 21**
	10%	228 ± 91	132 ± 48	77 ± 16	80 ± 36	**129 ± 48**

Binder A bound briquettes ≥ 50, Binder B bound briquettes ≥ 50, Binder C bound briquettes ≥ 50, Binder E bound briquettes ≥ 50

C.2 Friability index

The friability index, FR (%), is a measure of a briquette's durability, *i.e.* ability to withstand attrition forces caused by rubbing against surfaces/other briquettes (Dohm *et al.*, 2012). The FR can be calculated by weighing the briquette, m_0, before the drop shatter test and weighing the largest piece after the briquette breaks, m_f. The values can then be inserted in Equation 2-7.

$$\mathrm{FR} = \frac{m_\mathrm{f}}{m_0} \times 100 \tag{2-7}$$

The FR is directly proportional to m_f, as illustrated in Figure C-2. The minimum acceptable FR is 80% and the m_f should therefore be larger than 80% of the m_0, leading to less than 20% of the briquette being small pieces/fines (Kaliyan & Morey, 2009). The FR will be low (~ 50%) if the briquette breaks in half, which is more likely due to the seam in the pillow-shaped briquettes, and very low (< 30%) if the briquette shatters.

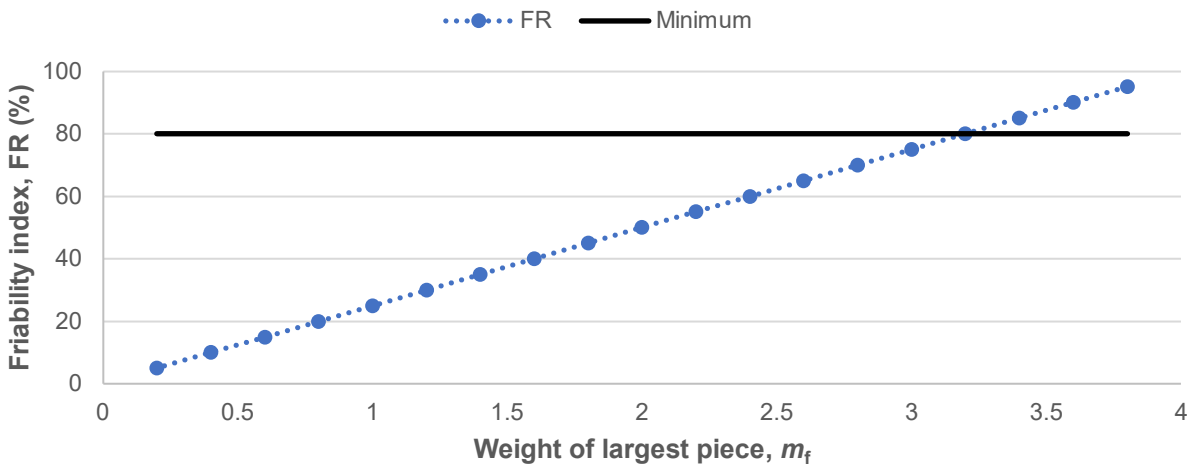

Figure C-2: Example of the friability index dependence on the weight of the largest piece of briquette, m_f, after it breaks for a briquette with an initial weight, m_0, of 4 g

The FR results, over 21 days, of the briquettes produced with water and Binders A–E are shown in Table C-2. The cells that contain values higher than the minimum FR of 80% when the error values are accounted for, are highlighted. Binder C bound briquettes (15–20%) were the only briquettes that met the minimum FR requirement. As seen with the IRI results, there is no clear trend associated with the curing time or binder concentrations, and the average FR for the briquettes were therefore considered in Chapter 4.

Table C-2: Friability index results for binderless and Binders A–E bound pilot-scale briquettes, over a 21-day period

Binder		Day 0	Day 7	Day 14	Day 21	Average
Water	**2.5%**	33 ± 5	68 ± 1	44 ± 6	36 ± 17	**45 ± 7**
	10%	47 ± 15	42 ± 5	47 ± 8	60 ± 11	**49 ± 10**
	15%	37 ± 13	41 ± 21	53 ± 8	66 ± 18	**49 ± 15**
A	**5.0%**	65 ± 26	70 ± 14	81 ± 13	53 ± 28	**67 ± 20**
	10%	50 ± 4	53 ± 15	85 ± 7	58 ± 20	**61 ± 11**
	15%	81 ± 5	87 ± 6	72 ± 19	81 ± 9	**80 ± 11**
B	**5.0%**	45 ± 16	43 ± 22	80 ± 18	64 ± 11	**58 ± 17**
	10%	75 ± 7	73 ± 19	84 ± 3	76 ± 11	**77 ± 11**
	15%	65 ± 4	73 ± 28	83 ± 17	86 ± 12	**77 ± 19**
	20%	60 ± 8	75 ± 8	84 ± 13	66 ± 21	**71 ± 14**
C	**5.0%**	46 ± 5	60 ± 18	84 ± 10	62 ± 17	**63 ± 13**
	10%	58 ± 13	73 ± 25	65 ± 24	87 ± 10	**71 ± 18**
	15%	100 ± 0	100 ± 0	100 ± 0	100 ± 0	**100 ± 0**
	20%	100 ± 0	100 ± 0	100 ± 0	100 ± 0	**100 ± 0**
D	**2.5%**	51 ± 25	43 ± 13	64 ± 14	47 ± 25	**51 ± 19**
	5.0%	14 ± 7	48 ± 15	84 ± 12	39 ± 10	**46 ± 11**
E	**5.0%**	51 ± 2	49 ± 1	48 ± 1	60 ± 3	**52 ± 2**
	10%	56 ± 12	70 ± 19	49 ± 3	63 ± 10	**60 ± 11**

Binder C bound briquettes ≥ 80%

C.3 Limitations of the drop shatter test

A limitation of this test, which was also observed by Li and Liu (2000), is the fact that the fines generated when the briquette breaks is not considered since it is difficult to count, and therefore quantify, the smaller pieces. The way the briquette hits the floor also plays a role in its breakage; especially pillow shaped briquettes that have seams which may act as weak points that cause the briquette to break in half. The briquettes also bounce an indeterminate number of times when they hit the floor, and this added impact is unaccounted for in the IRI calculation. The uncontrolled variables caused by these limitations can therefore be the cause of the large errors that were observed, and a more controlled test should consequently be considered for future studies.

APPENDIX D: WATER RESISTANCE TEST RESULTS FOR THE PILOT-SCALE BRIQUETTES

The water resistance test results are shown in this appendix. Most of the briquettes were not water resistant, however the effect of the binders on the water resistance of the briquettes could still be visually assessed to describe their performance. The briquettes were classified as intact, mostly intact, mostly degraded, or degraded and the time (1, 5, 10, 20, 30 min) when the briquettes were degraded was recorded (Taulbee *et al.*, 2013). If the briquettes were still fully intact after 30 min they were determined to be water resistant and the wet compressive strength, CS_{wet} (MPa), was determined (Richards, 1990). The results will be discussed in Section 4.3.4.

D.1 Effect of additional water on briquette water resistance

The images for the water resistance test of the binderless briquettes with 2.5, 5 and 10% water addition are shown in Table D-1. The briquettes were completely degraded at 5 min and therefore not water resistant.

Table D-1: Water resistance test images of the pilot-scale binderless briquettes with 2.5, 5 and 10% moisture addition

View	Time immersed in water				
	Before	Immediately	1 min	5 min	5 min + tilt
Water – 2.5%					
Top					
Side					

View	Time immersed in water				
	Before	Immediately	1 min	5 min	5 min + tilt
Water – 5.0%					
Top					
Side					
Water – 10.0%					
Top					
Side					

D.2 Effect of Binder A on briquette water resistance

The images for the water resistance test of the briquettes with 5, 10 and 15% Binder A addition are shown in Table D-2. The briquettes were mostly intact after 10 min, but the light pressure that was added caused them to completely degrade. The 15% Binder A bound briquettes show less degradation, and it can therefore be concluded that Binder B has a positive effect on the water resistance of the briquettes.

Table D-2: Water resistance test images of the pilot-scale binderless briquettes bound with 5, 10 and 15% Binder A

View	Time immersed in water					
	Before	Immediately	1 min	5 min	10 min	10 min + press
Binder A – 5%						
Top						
Side						
Binder A – 10%						
Top						
Side		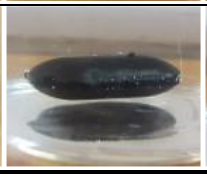				
Binder A – 15%						
Top						
Side			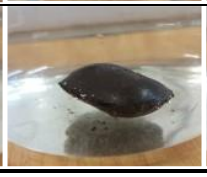		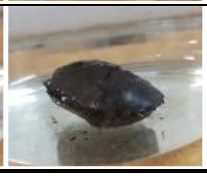	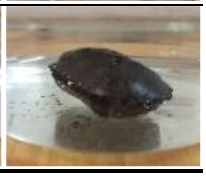

D.3 Effect of Binder B on briquette water resistance

The images for the water resistance test of the briquettes with 5, 10, 15 and 20% Binder B addition are shown in Table D-3. The 5% Binder B bound briquette was mostly intact but showed degradation at 10 min and is consequently considered not water resistant. The 10, 15 and 20% Binder B bound briquettes were completely intact after 30 min and can be classified as water resistant. The CS_{wet} of the briquettes was determined.

Table D-3: Water resistance test images of the pilot-scale binderless briquettes bound with 5, 10, 15 and 20% Binder B

View	Time immersed in water					
	Before	Immediately	1 min	5 min	10 min	10 min + press
Binder B – 5%						
Top						
Side						
	Before	Immediately	1 min	30 min	30 min + press	After
Binder B – 10%						
Top						
Side						
Binder B – 15%						
Top	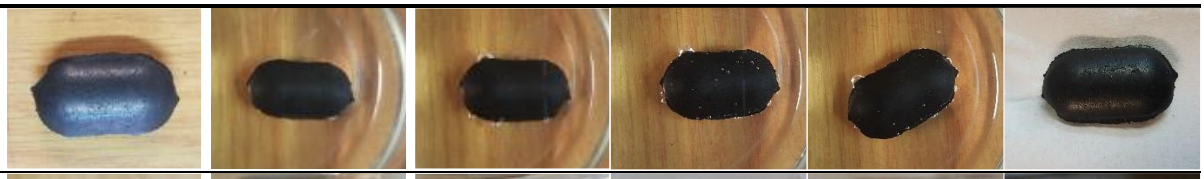					
Side						

	Before	Immediately	1 min	30 min	30 min + press	After
Binder B – 20%						
Top				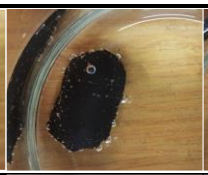	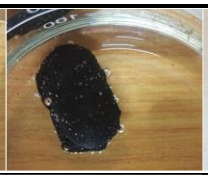	
Side						

D.4 Effect of Binder C on briquette water resistance

The images for the water resistance test of the briquettes with 5, 10, 15 and 20% Binder C addition are shown in Table D-4. The 5, 10 and 15% Binder C bound briquettes all degraded before 5 min and are therefore not water resistant. The 20% Binder C briquette was mostly intact after 30 min but was deemed not water resistant due to the slight degradation that was observed.

Table D-4: Water resistance test images of the pilot-scale binderless briquettes bound with 5, 10, 15 and 20% Binder C

View	**Time immersed in water**				
	Before	Immediately	1 min	5 min	5 min + tilt
Binder C – 5%					
Top					
Side					

View	Time immersed in water				
	Before	Immediately	1 min	5 min	5 min + tilt
Binder C – 10%					
Top					
Side					
Binder C – 15%					
Top					
Side					

	Before	Immediately	1 min	5 min	30 min	30 min + press
Binder C – 20%						
Top						
Side						

D.5 Effect of Binder D on briquette water resistance

The images for the water resistance test of the briquettes with 2.5 and 5.0% Binder D addition are shown in Table D-5. Both the 2.5 and 5.0% Binder D bound briquettes completely degraded before 5 min and are therefore not water resistant.

Table D-5: Water resistance test images of the pilot-scale binderless briquettes bound with 2.5 and 5.0% Binder D

View	Time immersed in water				
	Before	Immediately	1 min	5 min	5 min + tilt
Binder D – 2.5%					
Top					
Side					
Binder D – 5.0%					
Top					
Side					

D.6 Effect of Binder E on briquette water resistance

The images for the water resistance test of the briquettes with 5 and 10% Binder E addition are shown in Table D-6. Both the 5 and 10% Binder E bound briquettes were completely intact after 30 min and the CS_{wet} was determined.

Table D-6: Water resistance test images of the pilot-scale binderless briquettes bound with 5 and 10% Binder E

View	Time immersed in water					
	Before	Immediately	1 min	30 min	30 min + press	After
Binder E – 5%						
Top						
Side						
Binder E – 10%						
Top						
Side						

APPENDIX E: OPTIMISATION OF THE PILOT-SCALE BINDER CONCENTRATIONS

The optimisation of the binder concentrations was done with an a posteriori weighing method (Einhorn & Hogarth, 1975; Miettinen, 2008). The mechanical strength, water resistance, handling, cost and hazard of the binders were used to compare their qualities. A summary of the mechanical strength (CS, IRI, FR, AR) and water resistance (WRI, CS_{wet}) of the binderless and Binder A–E bound briquettes is provided in Table E-1.

Table E-1: Summary of the mechanical strength and water resistance results for the pilot-scale briquettes

Binder		CS (MPa)	IRI (-)	FR (%)	AR (%)	WRI (%)	CS_{wet} (MPa)
Type	**Concentration (wt%)**						
Water	**2.5**	1.8	18	45	94	0	–
	5	2.2	22	49	95	0	–
	10	2.3	20	49	97	0	–
A	**5**	2.7	28	67	98	0	–
	10	3.5	51	61	99	0	–
	15	4.1	68	80	99	0	–
B	**5**	2.5	34	58	98	0	–
	10	2.8	66	77	99	89	0.44
	15	2.7	49	77	99	92	0.49
	20	2.3	87	71	99	97	0.59
C	**5**	2.6	37	63	98	0	–
	10	5.5	149	71	99	0	–
	15	8.0	1000	100	99	0	–
	20	8.2	1000	100	99	0	–
D	**2.5**	1.6	13	51	96	0	–
	5	2.4	21	46	95	0	–
E	**5**	5.3	97	52	98	96	1.30
	10	2.2	129	60	97	97	1.45

The CS, WRI and durability (AR, FR) of the briquettes are distinct quality measures and cannot be used interchangeably because the stress component that has the largest impact on the briquette strength is not known (Kaliyan & Morey, 2009). The average of the FR and AR was

used to avoid inflating the importance of the values because both quantify the durability of the briquettes. The values were transformed to a 0–1 scale to remove the effect of their differing units (Einhorn & Hogarth, 1975; Miettinen, 2008). The scalarised values are presented in Table E-2. The CS, IRI, durability and WRI were calculated as a fraction of the maximum value obtained from the tests for each property. The handling, cost and hazard values were assigned to the briquettes based on their binder concentrations and was calculated as the difference of the concentration (fraction) from the maximum (1.00). The handling and hazard values of the binders that were harmful or necessitated more preparation therefore decreased with binder concentration, and the cost of the binders had a positive effect because the aim of the study entails the reuse of wastes, *i.e* the assumption is made that it is more cost effective to use the hazardous wastes than to dispose of them (Young, 1999).

Table E-2: Mechanical strength results, water resistance index, handling, binder cost and hazardous nature of the briquettes as fractions for the optimisation of the binder concentrations

Binder		CS	IRI	Durability	WRI	Handling	Cost	Hazard
Maximum		**1.00**	**1.00**	**1.00**	**1.00**	**1.00**	**1.00**	**1.00**
Water	**2.5%**	0.22	0.02	0.69	0.00	1.00	1.00	1.00
	5%	0.27	0.02	0.72	0.00	1.00	1.00	1.00
	10%	0.28	0.02	0.73	0.00	1.00	1.00	1.00
A	**5%**	0.33	0.03	0.83	0.00	0.95	0.85	0.95
	10%	0.43	0.05	0.80	0.00	0.90	0.90	0.90
	15%	0.51	0.07	0.90	0.00	0.85	0.95	0.85
B	**5%**	0.30	0.03	0.78	0.00	1.00	0.85	0.95
	10%	0.35	0.07	0.88	0.89	1.00	0.90	0.90
	15%	0.33	0.05	0.88	0.92	1.00	0.95	0.85
	20%	0.28	0.09	0.85	0.97	1.00	1.00	0.80
C	**5%**	0.32	0.04	0.80	0.00	0.95	0.85	0.95
	10%	0.67	0.15	0.85	0.00	0.90	0.90	0.90
	15%	0.98	1.00	0.99	0.00	0.85	0.95	0.85
	20%	1.00	1.00	1.00	0.00	0.80	1.00	0.80
D	**2.5%**	0.19	0.01	0.74	0.00	1.00	0.83	1.00
	5%	0.29	0.02	0.71	0.00	1.00	0.85	1.00
E	**5%**	0.64	0.10	0.75	0.96	0.95	0.85	0.95
	10%	0.27	0.13	0.78	0.97	0.90	0.90	0.90

The weights of the variables were considered to be equal because the specific effect of each variable is beyond the scope of this study (Einhorn & Hogarth, 1975; Ennis & Ennis, 2012). The weight of each variable was therefore assigned as 0.143 and the results are shown in Table E-3. The values were used to compare the properties for each binder independently and no effort was made to correlate these values between different binders.

Table E-3: Optimisation of the binder concentrations based on mechanical strength results, water resistance index, handling, binder cost and hazardous nature of the briquettes as weighted fractions

Binder		CS	IRI	Durability	WRI	Handling	Cost	Hazard	Total
Maximum		**0.143**	**0.143**	**0.143**	**0.143**	**0.143**	**0.143**	**0.143**	**1.00**
Water	**2.5%**	0.032	0.003	0.099	0.000	0.143	0.111	0.143	**0.53**
	5%	0.039	0.003	0.103	0.000	0.143	0.107	0.143	**0.54**
	10%	0.040	0.003	0.105	0.000	0.143	0.100	0.143	**0.53**
A	**5%**	0.047	0.004	0.118	0.000	0.136	0.122	0.136	**0.56**
	10%	0.061	0.007	0.114	0.000	0.129	0.129	0.129	**0.57**
	15%	0.072	0.010	0.128	0.000	0.122	0.136	0.122	**0.59**
B	**5%**	0.043	0.005	0.112	0.000	0.143	0.122	0.136	**0.56**
	10%	0.049	0.009	0.126	0.127	0.143	0.129	0.129	**0.71**
	15%	0.047	0.007	0.126	0.132	0.143	0.136	0.122	**0.71**
	20%	0.040	0.012	0.122	0.139	0.143	0.143	0.114	**0.71**
C	**5%**	0.046	0.005	0.115	0.000	0.136	0.122	0.136	**0.56**
	10%	0.096	0.021	0.122	0.000	0.129	0.129	0.129	**0.63**
	15%	0.140	0.143	0.142	0.000	0.122	0.136	0.122	**0.80**
	20%	0.143	0.143	0.142	0.000	0.114	0.143	0.114	**0.80**
D	**2.5%**	0.027	0.002	0.105	0.000	0.143	0.118	0.143	**0.54**
	5%	0.041	0.003	0.101	0.000	0.143	0.122	0.143	**0.55**
E	**5%**	0.092	0.014	0.107	0.137	0.136	0.122	0.136	**0.74**
	10%	0.038	0.018	0.112	0.139	0.129	0.129	0.129	**0.69**

Optimal binderless moisture concentration, Optimal Binder A concentration, Optimal Binder B concentration, Optimal Binder C concentration, Optimal Binder D concentration, Optimal Binder E concentration

The optimal binderless briquettes were produced with 5% water addition and the optimal binder bound briquettes contained 15% Binder A, 20% Binder B, 20% Binder C, 5% Binder D, and 5% Binder E.

APPENDIX F: THERMAL FRAGMENTATION TEST

The fragmentation test was performed to determine the effect of binder addition on the primary fragmentation of the coal which is caused by the release of volatiles and thermal stresses (Chirone *et al.*, 1982; van Dyk, 2001). Some cracking on the surface of the briquette was observed, Figure 5-2, but no measurable fragmentation, *i.e.* breakage, occurred. After applying manual force to break the briquettes in half, Figure F-1, it can be observed that the binders influenced the attrition, *i.e.* formation of fines, of the briquettes (Boerefijn *et al.*, 2007; Chirone *et al.*, 1982). The fragmentation test should therefore be conducted with more samples at a time and/or additional mechanical movement, *e.g.* tumbler, during heating.

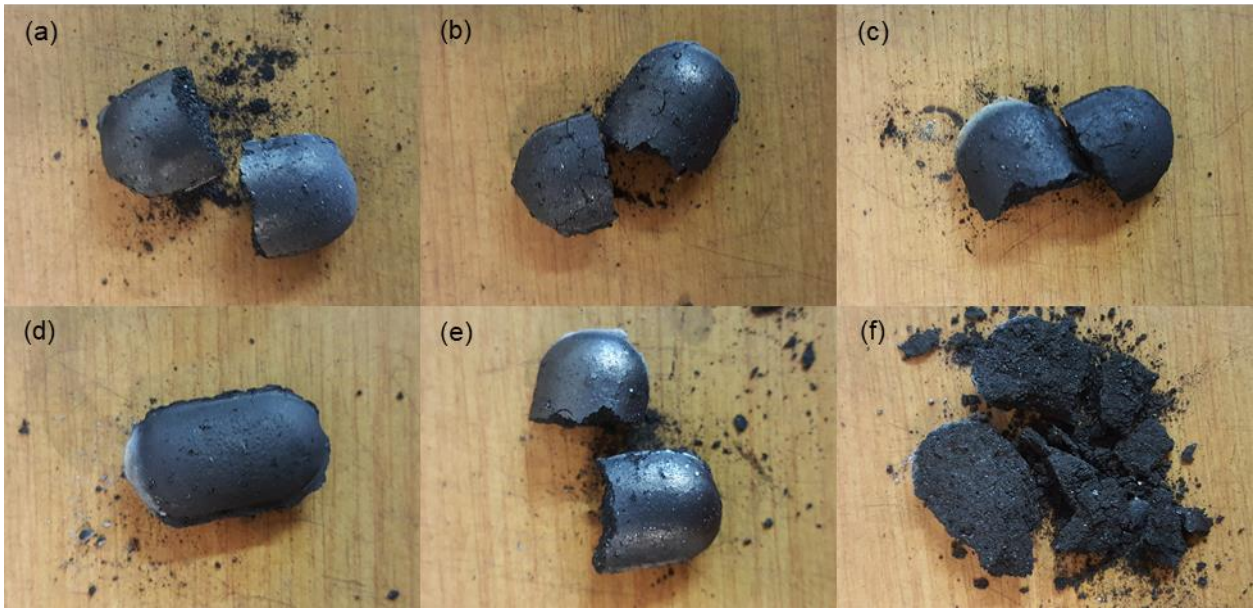

Figure F-1: Thermal fragmentation post-test images of the optimal concentration briquettes with (a) 5% moisture, (b) 15% Binder A, (c) 20% Binder B, (d) 20% Binder C, (e) 5% Binder D, and (f) 5% Binder E that were manually broken in half

APPENDIX G: FREE SWELLING INDEX RESULTS

The free swelling index, FSI, from the standard test and the calculated values were determined and discussed in this appendix. The limitations of the test method are also presented.

G.1 FSI from the standard method

The results obtained from the standard procedure to determine the free swelling index (FSI) of coal, described in ISO 501 (2003), is shown in Figure G-1. Fines from the binderless and Binder A–E bound briquettes (after crushing) did not exhibit any swelling during the test and therefore all had an FSI of 0. The coal that was used in this study is a low-rank coal and consequently does not qualify to be used as a coking coal (Speight, 2008). The binders also did not exhibit any swelling properties which may be due to their low melting/boiling points (< 219°C), Appendix A.

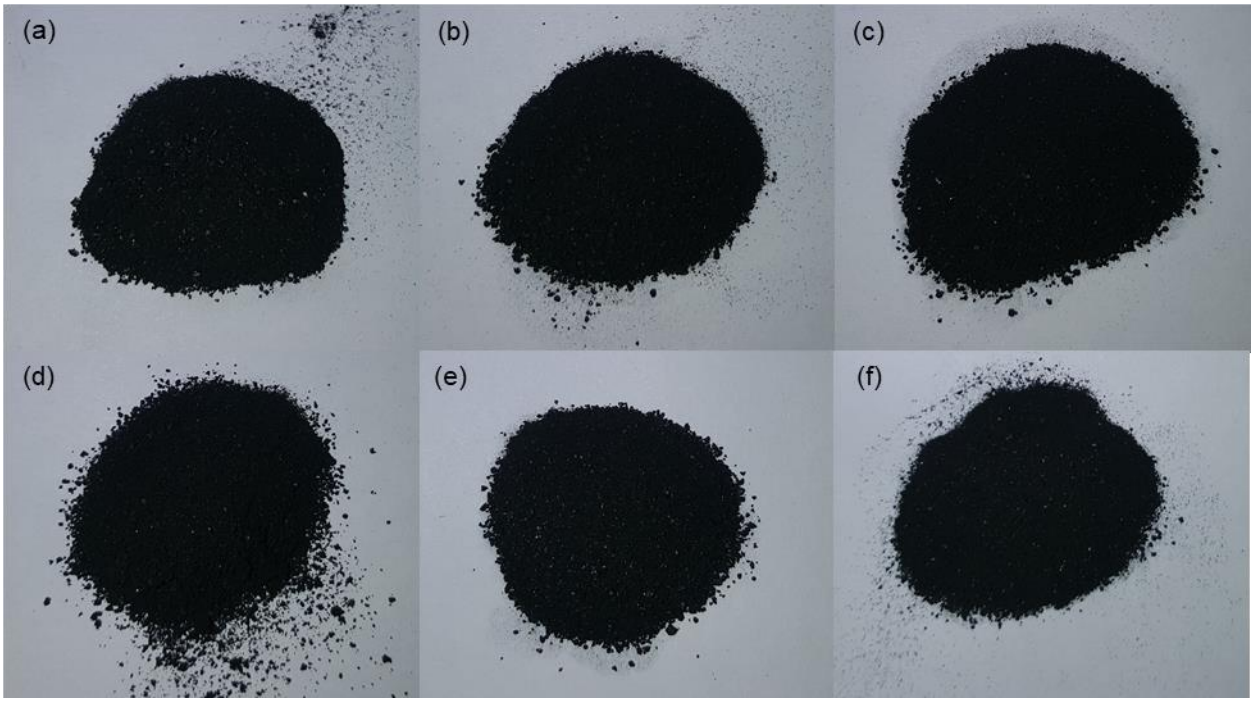

Figure G-1: Images of the optimal concentration briquettes with (a) 5% moisture, (b) 15% Binder A, (c) 20% Binder B, (d) 20% Binder C, (e) 5% Binder D, and (f) 5% Binder E after the free swelling index test

G.2 FSI from the calculated method

The method proposed by Dakič *et al.* (1989) was used to calculate the FSI of the briquettes through dividing the volatile matter content by the inherent moisture, as provided in Table 5-1, to obtain the pore resistance number (PRN) for use in Equation 2-12. The three film binders, *i.e.* water, Binder A and Binder D, had the lowest FSI of 0.2. This is due to the binders consisting mainly of water which is inversely proportional to the PRN. Binders B (0.6), C (0.4), and D (0.3) had a small increase in FSI which is due to the higher volatile matter content of the binders which

is directly proportional to the PRN (Dakič *et al.*, 1989). Compared to the binderless briquette FSI (5% water addition), the binders do not inhibit the FSI and consequently should not negatively affect the performance of coking coals.

Table G-1: Free swelling index calculated with the pore resistance number of the optimal briquettes

Binder	PRN (-)	FSI (-)
Water: 5%	4.7	0.2
A: 15%	5.1	0.2
B: 20%	9.0	0.6
C: 20%	7.4	0.4
D: 5%	5.0	0.2
E: 5%	5.8	0.3

G.3 Limits of the FSI determination

The standard method of determining the FSI of coal requires the test sample to be crushed (-212 µm) beforehand. This may break the binder bonds between the coal particles and an accurate representation of the briquettes' swelling behaviour due to binder addition is therefore not provided. The thermal fragmentation test may provide more insight into the effect of the binders on coal pyrolysis since it is determined with whole briquettes.

APPENDIX H: COMBUSTION RESULTS

The isothermal combustion results for the optimal briquettes are shown in this Appendix. Figure H-1 shows the mass loss (g) of the briquette over time (min). The combustion experiments were run until no more mass loss could be observed. The ash yield from the combustion tests at 900°C differed by ± 3% from the proximate analysis results.

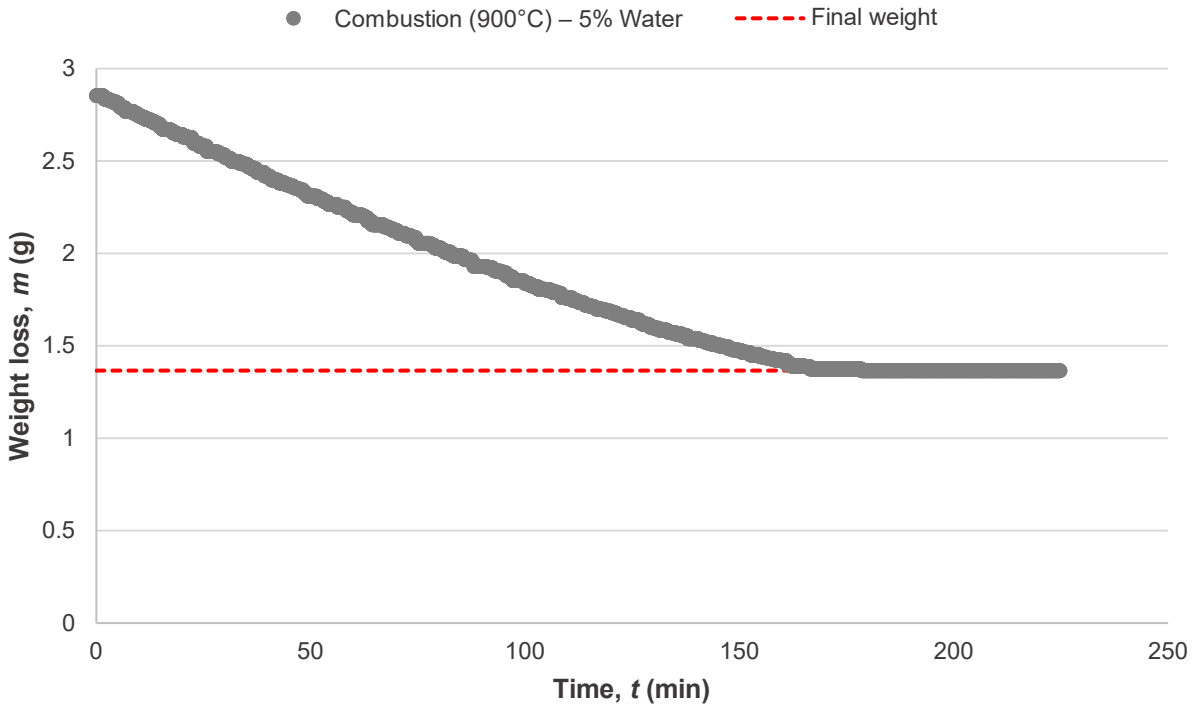

Figure H-1: Graph of the weight loss, *m* (g), over time, *t* (min), for the isothermal combustion of the binderless briquette with 5% moisture addition at 900°C

After combustion the briquettes were removed and broken to ensure that complete burnout occurred, as shown in Figure H-2 (van der Merwe, 2011).

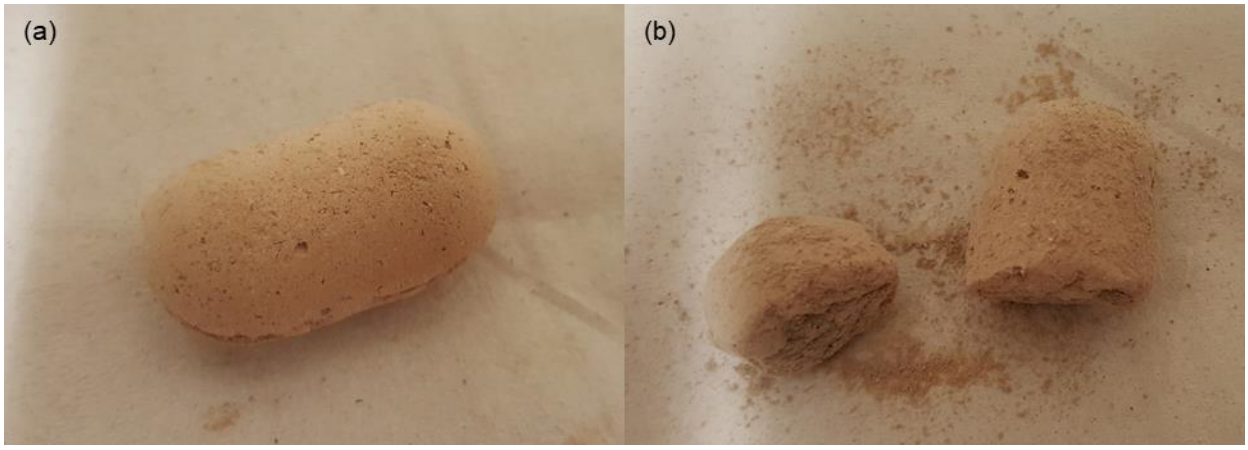

Figure H-2: Images of the binderless briquette with 5% moisture addition (a) after isothermal combustion at 900°C and (b) after force was applied

The conversion, X (-), versus time, t (min), of the optimal briquettes during combustion testing at 850°C are shown in Figure H-3.

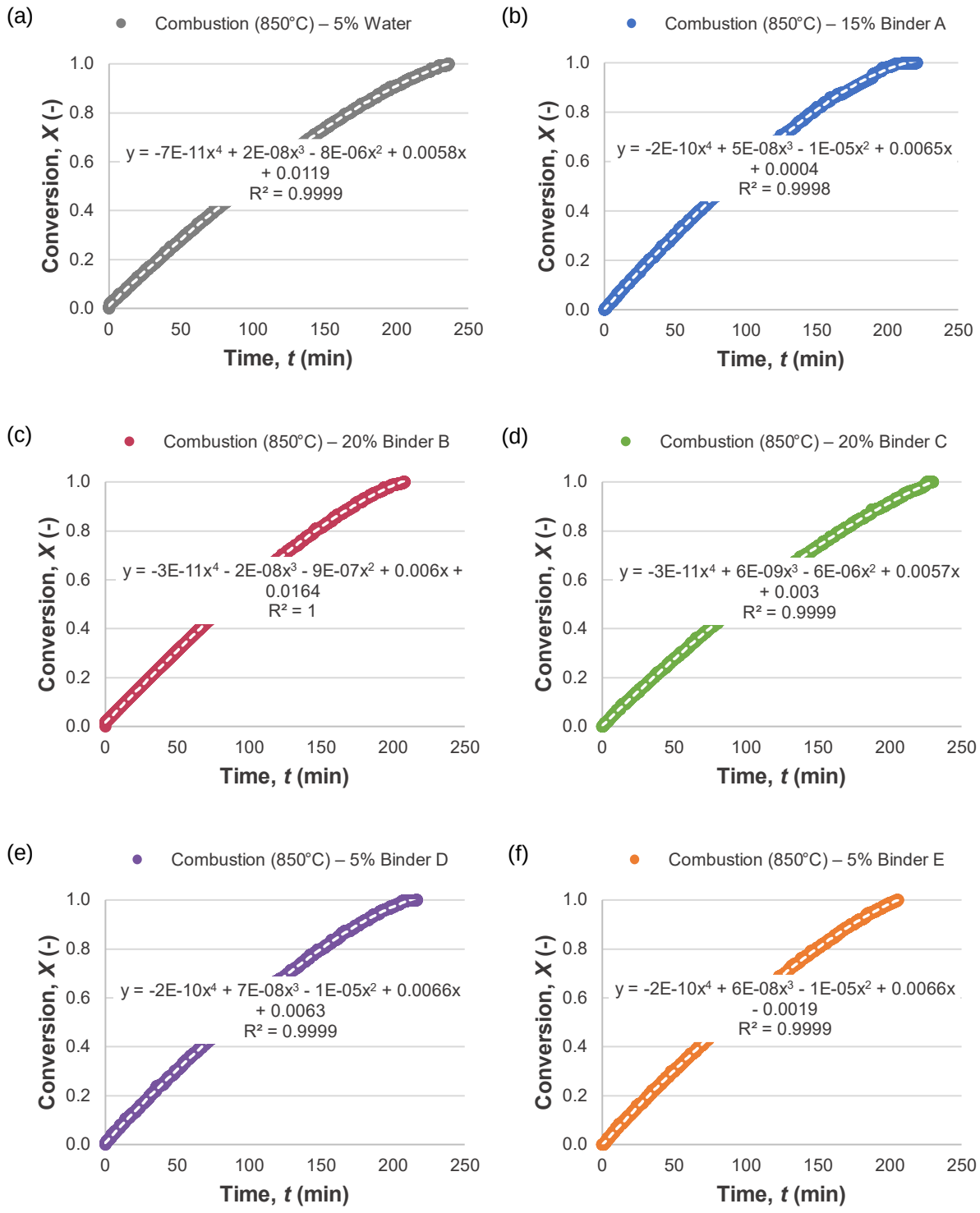

Figure H-3: Combustion (850°C) graphs of the fractional conversion over time for the (a) binderless and optimal briquettes bound with binder (b) A, (c) B, (d) C, (e) D, and (f) E

The conversion, X (-), versus time, t (min), of the optimal briquettes during combustion testing at 875°C are shown in Figure H-4.

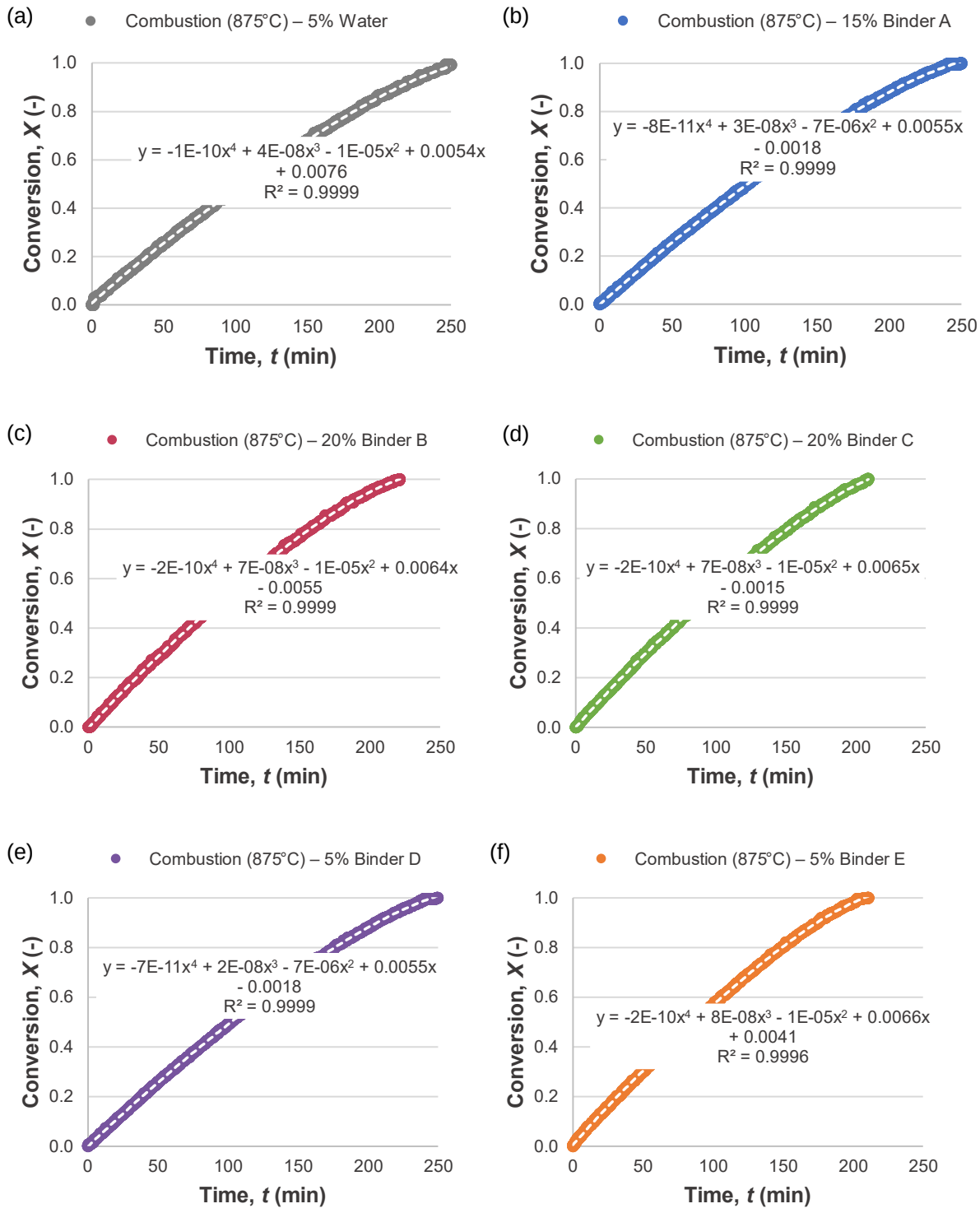

Figure H-4: Combustion (875°C) graphs of the fractional conversion over time for the (a) binderless and optimal briquettes bound with binder (b) A, (c) B, (d) C, (e) D, and (f) E

The conversion, X (-), versus time, t (min), of the optimal briquettes during combustion testing at 900°C are shown in Figure H-5.

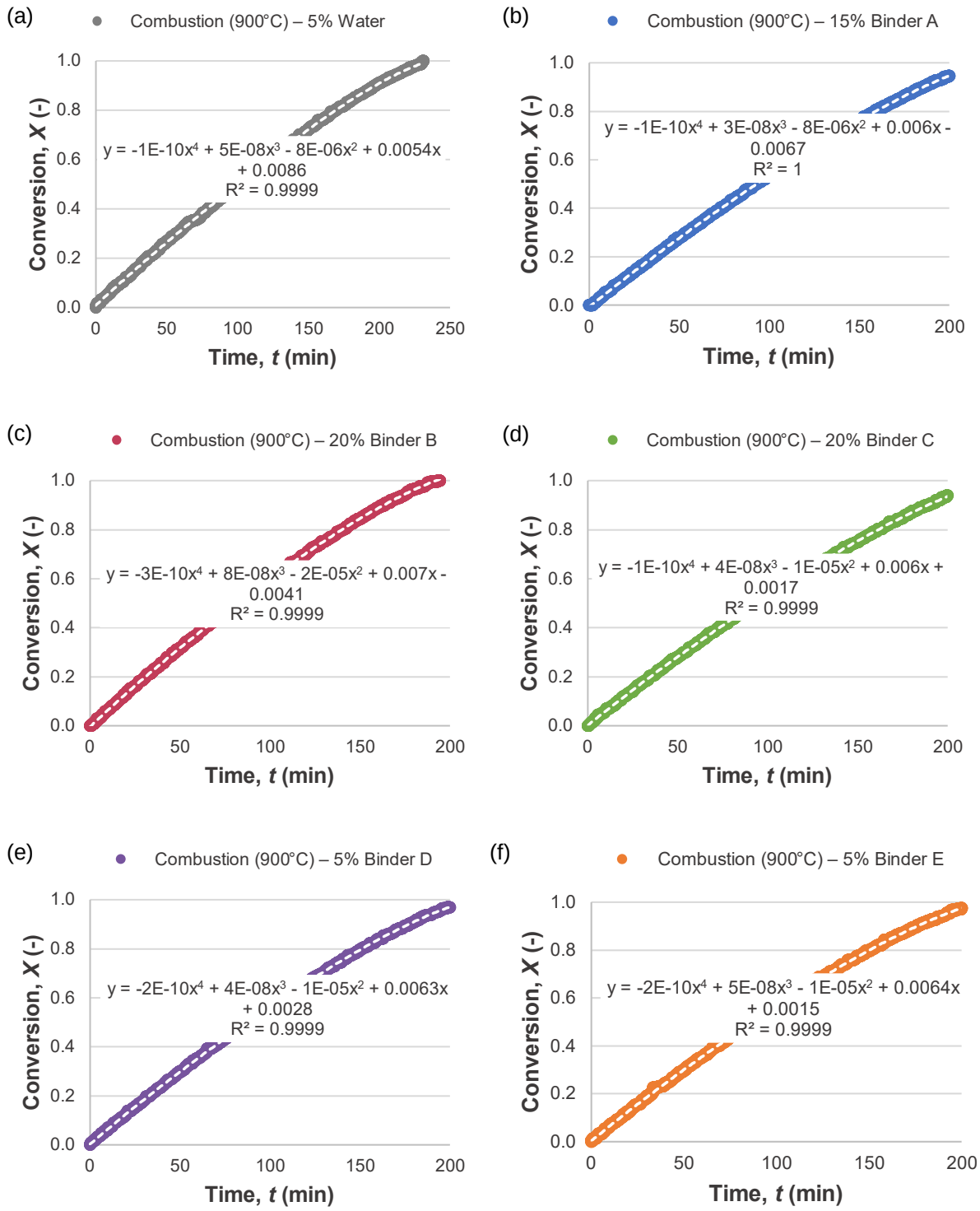

Figure H-5: Combustion (900°C) graphs of the fractional conversion over time for the (a) binderless and optimal briquettes bound with binder (b) A, (c) B, (d) C, (e) D, and (f) E

APPENDIX I: REPEATIBILITY OF EXPERIMENTS

The repeatability of the coal characterisation and briquette reactivity is described in this appendix.

I.1 Particle size distribution

The particle size distribution (PSD) results of the coal from three runs are shown in Figure I-1. There was almost no variation between the values which indicates that the test is repeatable and the average of the three runs was used as the PSD of the coal fines in Chapter 3.

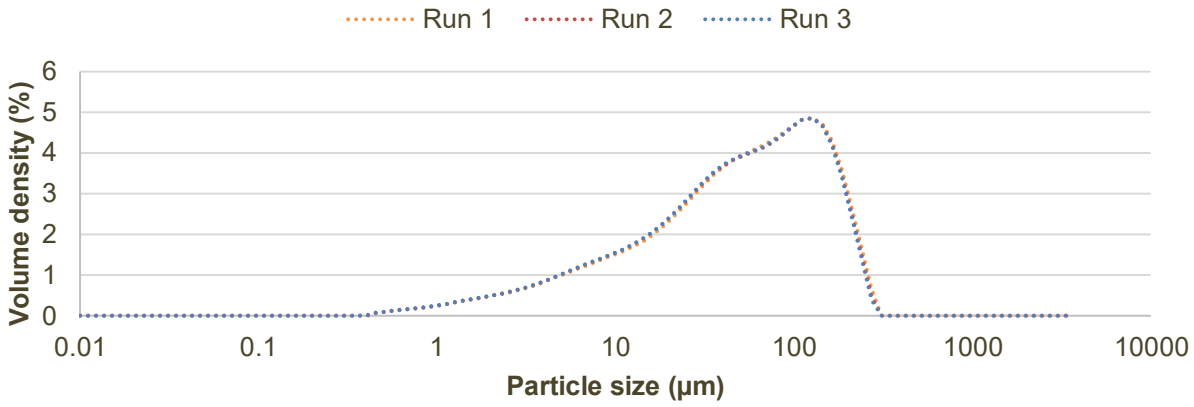

Figure I-1: Particle size distribution, PSD, results of the coal fines (-1 mm) for three runs

I.2 Comparison of char yields

The char yields of the proximate analysis, Fischer assay and pyrolysis of the optimal pilot-scale briquettes are shown in Table I-1. The values have a standard error of less than 1% which indicates that the test results are reproducible and accurate.

Table I-1: Comparison of the char yields obtained from the proximate analysis, Fischer assay and pyrolysis experiments of the optimal pilot-scale briquettes

Binder		Proximate analysis (%, db)	Fischer assay (%, db)	Pyrolysis (%)
Type	**Concentration (wt%)**			
Water	**5**	71.2	71.0	71.6
A	**15**	69.0	71.0	69.7
B	**20**	65.0	66.6	66.1
C	**20**	62.9	63.5	63.1
D	**5**	71.2	71.5	71.0
E	**5**	67.2	68.3	69.0

I.3 Combustion repeats

Conversion rate, d*X*/d*t* (min^{-1}), versus conversion, *X* (-), for the combustion (900°C) results of two runs with a 20% Binder C bound briquette are shown in Figure I-2. The data points on the graph have an error margin of ±0.3 min^{-1} for a 95% confidence level up to ~50% conversion, and the results can consequently be used to evaluate the reactivity of the briquettes.

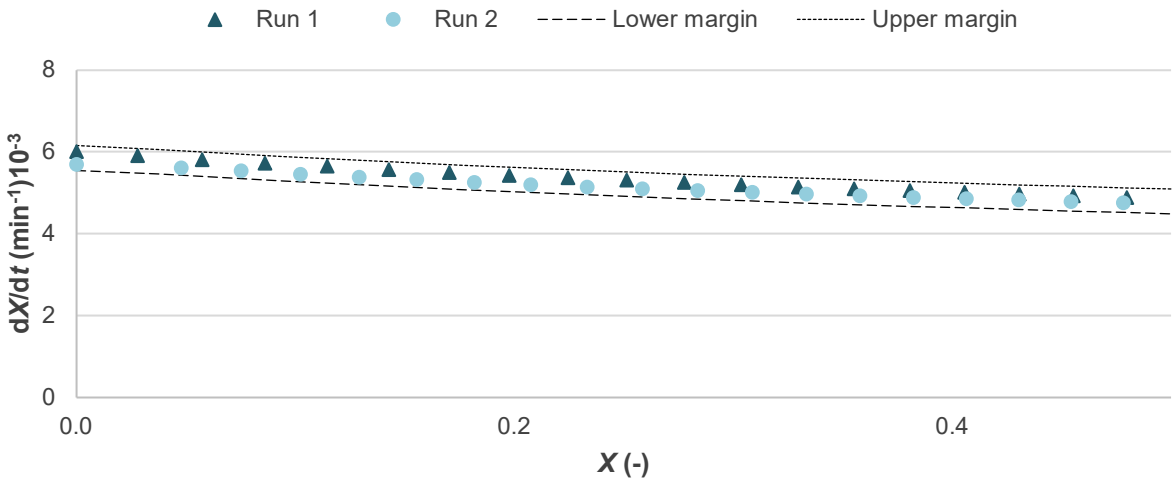

Figure I-2: Repeatability of the combustion results for 20% Binder C bound briquettes at 900°C

I.4 Gasification repeats

Conversion rate, d*X*/d*t* (min^{-1}), versus conversion, *X* (-), for the gasification (1000°C) results of two runs with a binderless briquette (5% water) are shown in Figure I-3. The data points on the graph have an error margin of ±0.1 min^{-1} for a 95% confidence level up to ~20% conversion, and the results can consequently be used to evaluate the reactivity of the briquettes.

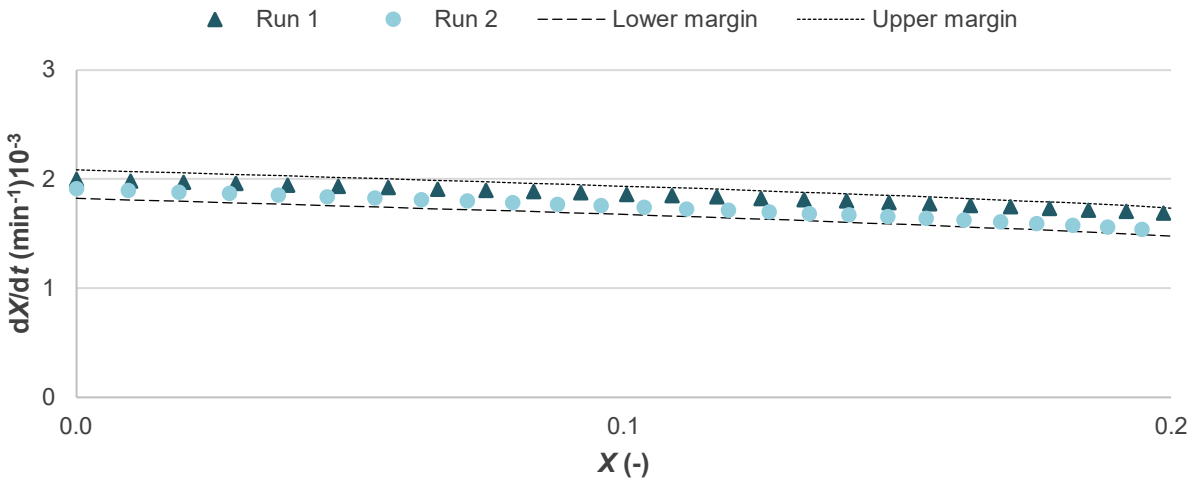

Figure I-3: Repeatability of the gasification results for binderless briquettes at 1000°C